Monte Carlo Simulation of Ultra-Supercritical Pulverized Coal-Fired Power Plant: Efficiency Improvement

A Thesis

Submitted to the Faculty of Graduate Studies and Research

In Partial Fulfillment of the Requirements

for the Degree of

Master of Applied Science

in Industrial Systems Engineering

University of Regina

by

Yaowaluk Thongprasat

Regina, Saskatchewan

September, 2013

Copyright 2013: Y. Thongprasat

UNIVERSITY OF REGINA

FACULTY OF GRADUATE STUDIES AND RESEARCH

SUPERVISORY AND EXAMINING COMMITTEE

Yaowaluk Thongprasat, candidate for the degree of Master of Applied Science in Industrial Systems Engineering**,** has presented a thesis titled, ***Monte Carlo Simulation of Ultra Supercritical Pulverized Coal-Fired Power Plant: Efficiency Improvement,*** in an oral examination held on August 29, 2013. The following committee members have found the thesis acceptable in form and content, and that the candidate demonstrated satisfactory knowledge of the subject material.

External Examiner:	Dr. Daoyong Yang, Petroleum Systems Engineering
Supervisor:	Dr. Adisorn Aroonwilas, Industrial Systems Engineering
Committee Member:	Dr. Liming Dai, Industrial Systems Engineering
Committee Member:	Dr. Amornvadee Veawab, Environmental Systems Engineering
Chair of Defense:	Prof. Robert Truszkowski, Department of Visual Arts

Abstract

Coal is the predominant energy source for the world's electricity generation due to its abundance and low cost compared to other types of fuel. Coal-fired power plants are the primary source of anthropogenic emissions of carbon dioxide (CO_2). A reduction of CO_2 emissions is required to efficiently operate coal-fired power plants. Efficiency improvement will not only help reduce CO_2 emissions, but also produce more electricity with less coal consumption. This can be achieved by either adjusting process operating conditions or replacing existing power plants with new technologies. Ultra-supercritical pulverized coal-fired (USC-PC) power plants are one of the available technology options that would allow a power station to operate more efficiently at high pressure and temperature. Such advanced USC-PC technology offers reliable performance with high efficiency and less coal consumption.

This thesis is aimed at investigating the behaviour of operating and design parameters that could lead to efficiency improvement for ultra-supercritical pulverized coal-fired power generation. This research aim was achieved by initially developing a process-based computer model of an ultra-supercritical pulverized coal-fired power plant to perform a simulation. The model was built in a Microsoft® Excel spreadsheet based on the fundamental knowledge of coal combustion, heat transfer, materials and energy balances, and thermodynamics of the steam power cycle. Verification of the developed process-based model was achieved by comparing simulation results with published literatures. Rank coefficient and Monte Carlo approaches using Crystal Ball® software were selected to perform simulations of the developed model for sensitivity analysis and parametric studies.

It was found that free moisture content in coal, temperature of preheated air, temperatures of main steam and 1st reheated steam, excess air, boiler and turbine efficiency, pressure drop across the boiler, and steam pressure at different stages throughout the series of turbines are the most influential parameters in the net efficiency of stream power plants. This study also presents a correlation empirical equation of net efficiency of operating and process parameters obtained from the parametric study. Optimization studies and an added consideration of carbon capture storage (CCS) are suggested as future work in order to achieve the highest efficiency for USC-PC power plant.

Acknowledgements

It is my pleasure to thank many people who assisted in completing this thesis. The thesis would not have been completed without them. I would like to express my sincere gratitude to my supervisor, Dr. Adisorn Aroonwilas, who always provided me valuable advice, encouragement, help, and support. I really am grateful for the opportunity he provided to pursue my education, bringing me into a new area of research. I am also grateful for the financial support provided towards the completion of this thesis.

I would like to thank Natural Sciences and Engineering Research Council of Canada (NSERC) and the Faculty of Graduate Studies and Research (FGSR) at the University of Regina for their financial support provided during my studies.

I would also like to thank Jantira Hengmeechai for her encouragement, valuable friendship, help, and support. Most importantly, I would like to thank my parents and sister for their love and support in everything, especially through the challenges I encountered during my studies.

Table of Contents

List of Tables

List of Figures

List of Appendices

Acronyms and Abbreviations

DTI	Department of Trade and Industry (United Kingdom)
EIA	Environmental Investigation Agency
FWHs	feedwater heaters
FBC	fluidized bed combustor power plant
G	generator
GA	Genetic Algorithm
GHGs	greenhouse gases
HHV	high heating value
HP	high pressure turbine
IEA	International Energy Agency
IP	intermediate pressure turbine
IGCC	integrated gasification combined cycle power plant
LHV	low heating value
LP	low pressure turbine
MWh	megawatt-hour
NN	Neural Network
PC	pulverized coal-fired power plant
PFB	pressurized fluidized bed power plant
RH	reheater
SH	superheater
TWh	terawatt-hour

U.S.DOE	United State Department of Energy
USC	ultra-supercritical
VHP	very high pressure turbine

Nomenclature

A	percent ash content in coal by weight, %
C	percent carbon content in coal by weight, %
$C_{p,i}$	heat capacity of combustion product *I*, kJ/kmol K
E_a	percent excess air, %
F_m	percent free moisture content in coal, %
h_i	specific enthalpy of stream *i*, kJ/kg
$\Delta\dot{H}_i$	enthalpy change of combustion product *i*, kJ/s
H	percent hydrogen content in coal by weight, %
HHV	high heating value, kJ/kg coal
L	latent heat of vapourization , kJ/kg vapour
$\dot{m}_i$	mass flow rate of combustion product *i*, kg/s
N	percent nitrogen content in coal by weight, %
O	percent oxygen content in coal by weight, %
P	pressure, MPa
P_{drop_boiler}	percent pressure drop across boiler, %
P_{drop_FWHs}	percent pressure drop across FWHs, %
P_w	power output, kJ/s
q_h	HHV-based combustion heat, kJ/kg coal
q_l	LHV-based combustion heat, kJ/kg coal
$\dot{Q}_{boiler}$	heat input into boiler, kJ/s
$\dot{Q}_{econ}$	heat transfer rate for economizer, kJ/s

$\dot{Q}_{evap}$	heat transfer rate for evapourator, kJ/s
$\dot{Q}_{furnace}$	furnace heat, kJ/s
$\dot{Q}_h$	rate of HHV-based combustion heat, kJ/s
$\dot{Q}_l$	rate of LHV-based combustion heat, kJ/s
$\dot{Q}_{preheater}$	heat transfer rate at air preheater, kJ/s
$\dot{Q_{RH,i}}$	heat transfer rate for reheater *i*, kJ/s
$\dot{Q_{SH,i}}$	heat transfer rate for superheater *i*, kJ/s
R^2	coefficient of multiple determination
s_i	specific entropy of stream *i*, kJ/kg
S	percent sulfur content in coal by weight, %
T	temperature, K
T_{air}	preheated air temperature, °C
T_m	temperature of main steam, °C
T_{r1}	1st reheating temperature, °C
W	mass of water vapour in coal, kg vapour/kg coal
$\dot{W}_{VHP,i}$	power produced from section *i* of very high pressure turbine, kJ/s
$\dot{W}_{HP,i}$	power produced from section *i* of high pressure turbine, kJ/s
$\dot{W}_{IP,i}$	power produced from section *i* of intermediate pressure turbine, kJ/s
$\dot{W}_{LP,i}$	power produced from section *i* of low pressure turbine, kJ/s
$\dot{W}_{output}$	net power output of overall system, kJ/s
$\dot{W}_P$	pumping power input, kJ/s

$\dot{W}_{P,i}$	power input for pump i, kJ/s
$\dot{W}_{P,actual}$	actual pumping power, kJ/s
$\dot{W}_{P,isen}$	isentropic pumping power, kJ/s
$\dot{W}_{P,total}$	total pumping power, kJ/s
$\dot{W}_{T}$	turbine power, kJ/s
$\dot{W}_{T,actual}$	actual turbine power, kJ/s
$\dot{W}_{T,isen}$	isentropic turbine power, kJ/s
$\dot{W}_{T,total}$	total turbine power, kJ/s

Greek letter

$\eta_{furnace}$	furnace efficiency, %
η_{boiler}	boiler efficiency, %
η_{net}	net efficiency, %
η_{besed}	reference efficiency, %
η_{P}	pump efficiency, %
η_{T}	turbine efficiency, %
η_{th}	thermal efficiency of steam cycle, %

Chapter 1

Introduction

1.1 Electricity Generation by Coal

Coal is a fossil fuel that is the predominant energy source supplying world electricity generation due to its abundance and low cost compared to other types of fuel. In 2006, coal-fired power generation produced 7,400 TWh (Terawatt hours) of electricity, and global production is projected to reach 9,500 TWh in 2015 (EIA, 2009). It is considered the largest fuel share of the world's total electricity generation, and will remain an important energy source in future at least in the next 20 years. According to the Energy Information Administration (EIA), in 2009, coal accounted for 41% of world energy resources in 2006 and is expected to increase to 43% in 2030.

The demand for coal for electricity production across the globe has rapidly increased in recent years, particularly in Asia. However, as reported by the International Energy Agency (IEA) in 2011, the developing countries that rely on coal for power generation and industrial sectors, such as China and India, are constructing more advanced ultra-supercritical pulverized coal-fired (USC-PC) power plants. The growing demand of coal for coal-fired power plants is indicative of the increasing trends in coal consumption.

1.2 Coal-Fired Power Generation and Environmental Concern

These increases in coal consumption for coal-fired power generation significantly raise public concern regarding negative impacts on human health and the environment due to the emission of carbon dioxide (CO_2). Coal-fired power generation is a major factor contributing to global CO_2 emissions. More than 70% of the emissions of CO_2 are currently produced from coal power generation (IEA, 2011). CO_2 is a greenhouse gas (GHG) released during the combustion process when fossil fuels are burned. It is a primary factor contributing to climate change since GHGs prevent heat from leaving the earth's atmosphere resulting in global warming. Currently, organizations and research efforts have been devoted to studying and developing techniques to reduce the GHG emissions from both existing and new (future) coal-fired power plants.

1.3 Reduction of GHG Emission for Coal-fired Power Plant

It is widely recognized that there are two approaches to reducing of CO_2 emissions: (i) improvement in net efficiency of steam power generation, and (ii) integration of carbon capture storage (CCS) into power plant operations (DTI, 2006; U.S.DOE, 2009). First, efficiency improvement can be obtained from an increase in power cycle efficiency by producing more electricity with less coal consumption supplied for combustion, which would reduce CO_2 emissions. This approach can be done either by adjusting operating conditions of existing power plants or adopting available technologies to replace the existing configuration of power plants. Second, integrating a CO_2 capture

unit into power plants offers a reduced rate of CO_2 emission. However, the CO_2 capture option is energy intensive, consuming a large amount of heat energy for operation (Folger, 2010). From an economical point of view, the challenge of CCS technology is the increased cost of electricity even though it offers great environmental benefits. As a consequence, the approach of net efficiency improvement is a viable solution that was selected for study in this thesis.

1.4 Coal-Fired Power Generation Technologies

Currently, the technologies for coal-fired power generation are widely available for commercial and demonstration purposes. Four well-known technologies are pulverized coal-fired (PC) power plants, circulating fluidized bed (CFB) power plants, pressurized fluidized bed (PFB) power plants, and integrated gasification combined cycle (IGCC) power plants. This thesis focuses particularly on the PC technology for pulverized coal-fired power plants operating at ultra-supercritical condition. The PC power plant is the conventional power generation technology based on a simple Rankin steam cycle. Coal is combusted in a furnace at temperatures ranging from 1650-1900°C, producing high quality steam (high pressure) for driving a series of turbines (Woodruff et al., 2005). Typically, the efficiency of pulverized coal-fired power plants depends on the operating conditions. PC plants can be sub-categorized into three types in accordance with their operating conditions: subcritical plants, supercritical plants, and ultra-supercritical plants. A conventional coal-fired power plant operating under subcritical

conditions offers efficiencies up to 37% (US.DOE, 1999). However, high efficiency in PC plants can be achieved by raising the steam pressure and temperature of the steam cycle. Table 1.1 shows the operating conditions and corresponding performance according to the types of PC power plants under their current operating capabilities. Subcritical PC power plants operate under a critical point which is at temperatures below 374°C and pressures below 22 MPa. Supercritical and ultra-supercritical PC power plants operate above the critical point. According to Table 1.1, subcritical PC plants, supercritical PC plants, and ultra-supercritical PC power plants offer efficiencies of 37%, 40%, and 41%, respectively.

The technology of ultra-supercritical pulverized coal-fired power plants allows the power station to not only operate at higher temperature and pressure but also maintain reliable performance. This advanced technology offers high efficiency and requires less consumption of coal, which leads to fewer pollutants emitted to the atmosphere. It should be noted that this advanced technology is still relatively new. This advanced technology also limits to available advanced materials that can withstand high pressure and temperature. There are many research projects attempting to improve this advanced technology, but these only focus on the effect of one or a pair of operating conditions (e.g., temperature and pressure), advanced materials improvement, or new design of components (e.g., boiler, furnace, and turbine) (see Table 2.4). This thesis aims at investigating the behaviour of operating and process parameters to improve the net efficiency of ultra-supercritical pulverized coal-fired power generation.

Table 1.1: Operating conditions and performance for subcritical, supercritical and ultra-supercritical coal-fired power plants (US.DOE, 1999).

Type of Plant	Typical operating conditions		Example		Net Plant Efficiency (% HHV)
	Pressure (MPa)	Temperature (° C)	Steam Pressure (MPa)	Steam Temperature (° C)	
Subcritical (conventional pulverized coal plant with emission control systems to meet current air quality standards)	< 22	< 550	16.5	Main steam: 537.8 Reheating steam: 537.8	37.6 %
Supercritical (single reheat configuration with emissions control systems to meet air quality standards expected in 2005)	22-24	> 550	24.1	Main steam: 565.6 Reheating steam: 565.6	39.9 %
Ultra-Supercritical (double reheat configuration with emissions control systems to meet air quality standards expected in 2010)	25-35	> 550	31.0	Main steam: 593.3 1st reheating steam: 593.3 2nd reheating steam: 593.3	41.4 %

(Designed data based on a 400 MW pulverized coal-fired power plants)

1.5 Research Objective

The purpose of this research is to investigate the effects of various operating and design parameters on the net efficiency of an ultra-supercritical pulverized coal-fired power plant. The key operating parameters that control the power plant performance are identified and examined in terms of how plant performance responds to various design and operating conditions. This study provides the development of an Excel-based coal-fired power generation model that combines various elements of fundamental knowledge including electricity generation, coal combustion, material and energy balances, and the thermodynamics of a steam power cycle. The approaches of Monte Carlo simulation and rank coefficient were selected to perform a simulation of the developed model for a sensitivity analysis and parametric study.

The specific objectives of this study are listed as follows:

1. To develop a pulverized coal-fired power plant model used for the simulation under ultra-supercritical operating conditions.
2. To construct thermodynamic properties equations for convenient use during a simulation.
3. To investigate the performance of the power plant such as its thermal efficiency and the net plant efficiency of the steam power cycle.
4. To develop empirical equations for the ultra-supercritical pulverized coal-fired (USC-PC) plant.

1.6 Thesis Outline

This thesis is divided into five chapters. Chapter 1 provided an introduction to the thesis. Chapter 2 includes basic principles and a literature review of the steam power cycle, coal combustion with chemical reactions, and limitations of previous studies. Details of the development of a process-based computer model including process components and empirical equations for thermodynamic properties of working fluid are given in Chapter 3. Chapter 4 presents the model verification and a discussion of the simulation results. Chapter 5 provides conclusions from the research and suggestions for future work.

Chapter 2

Basic Principles and Literature Review

This chapter provides background on the steam power cycle, thermodynamics associated with the steam cycle, the principles of coal combustion and the associated chemical reactions, as well as the pulverized coal-fired technology available today. A review of process design and operation of power plants as well as technology limitations is also given.

2.1 Basic Principles

2.1.1 Coal Combustion

There is a variety of fuels used for generating electricity, including coal, oil, and natural gas. Among these, coal is commonly used due to its abundance. Coal varies in chemical composition of which the characteristics depend upon location as shown in Table 2.1. The composition of coal does have a great impact on the energy released during combustion. The Institute of Gas Technology developed an empirical equation for assessing heat of combustion (in kJ/kg of coal) on a dry basis. It is commonly referred to as the High Heating Value-HHV, (q_h), and is given as follows (Perry et al., 2008):

$$q_h = 2.326[146.58C + 568.78H + 29.4S - 6.58A - 51.53(O + N)] \quad (2.1)$$

where *C, H, S, A, O,* and *N* are weight percentages (on a dry basis) of carbon, hydrogen, sulfur, ash, oxygen, and nitrogen, respectively.

Table 2.1: Types of coal and chemical compositions (U.S.DOE, 1999; Geers and O'Brien, 2002; Sanpasertpanich, 2007).

Content (percent by weight)	Bituminous coal			Subbituminous coal		Lignite	
	Pittsburg #8	**Illinois #6**	**Upper Freeport MV**	**Spring Creek**	**Decker**	**North Dakota**	**Hallaville**
Moisture (wt %)	5.2	11.2-17.6	2.2	24.1	23.4	33.3	37.7
HHV [a] (kJ/kg coal)	30856	28818	30854	28285	29033	25043	26949
Component on dry basis							
C (wt %)	74.0	69.0	74.9	70.3	72.0	63.3	66.3
H (wt %)	5.1	4.9	4.7	5.0	5.0	4.5	4.9
O (wt %)	7.9	10.0	4.97	17.69	16.41	19.0	16.2
N (wt %)	1.6	1.0	1.27	0.96	0.95	1.0	1.0
S (wt %)	2.3	4.3	0.76	0.35	0.44	1.1	1.2
A (ash) (wt %)	9.1	10.8	13.4	5.7	5.2	11.1	10.4

[a] The HHV is equal to $2.36[146.58C + 568.78H + 29.4S - 6.58A - 51.53(O+N)]$ (Perry et al., 1997).

Under practical conditions, coal contains a certain amount of moisture that consumes a portion of energy for vapourization during combustion. This leads to a reduction in heat energy available for steam generation. Such reduced heating value is referred to as the Low Heating Value-LHV, (q_l), and it can be approximated by (Sanpasertpanich, 2007):

$$q_l = q_h - L \cdot W \tag{2.2}$$

$$\dot{Q}_L = \dot{Q}_H - L \cdot W \tag{2.3}$$

where q_l is Low Heating Value (in kJ/kg), L represents the latent heat of water vapour (in kJ/kg water)and W denotes mass of water vapour in flue gas per mass of coal burned (in kg/hr)

Combustion is associated with chemical reactions of combustible elements in fuel with oxygen in air, releasing energy in the form of heat as the product of this process. For the pulverized coal-fired power generation, the combustion process takes place at a furnace where supplied coal mixes together with air at an elevated temperature. During the combustion process, coal components such as carbon, sulfur, and nitrogen are converted into gaseous products. This heat released from the combustion is used to change the phase of working fluid from liquid water to superheated steam at high pressure. This produced steam is then used to drive a series of turbines. Finally, electricity is generated as a product of this entire process (Singer, 1991).

In typical power plants, the combustion of coal takes place in the presence of air containing about 79% N_2 and 21% O_2. This O_2 participates in the combustion process according to the following equations (Woodruff et al., 2005):

$$C + O_2 \rightarrow CO_2 \quad (2.4)$$

$$4H + O_2 \rightarrow 2H_2O \quad (2.5)$$

$$S + O_2 \rightarrow SO_2 \quad (2.6)$$

$$N + O_2 \rightarrow NO_2 \quad (2.7)$$

These equations are used for determining the amount of air required for the complete combustion as well as determining the composition of the flue gas derived from the combustion.

2.1.2 Steam Power Cycle

Coal-fired power generation is an example of the use of steam cycle to transfer its heat from coal combustion to produce high pressure and temperature steam at a boiler and, then, convert mechanical energy to electricity at a turbine system. The exhaust steam from the turbines is then condensed into liquid form (referred to as condensate) in a low-pressure condenser. The liquid water is then pumped back to the boiler to complete the cycle. The basic steam cycle is commonly known as the "**Rankine Cycle"**. It was first introduced in 1859 by W. J. M Rankine, a Scottish engineering professor who modified the concept of the Carnot cycle (Singer, 1991; Smith et al., 1996). This simple steam cycle consists of a boiler, a steam turbine, a condenser, and a pump as demonstrated in Figure 2.1A.

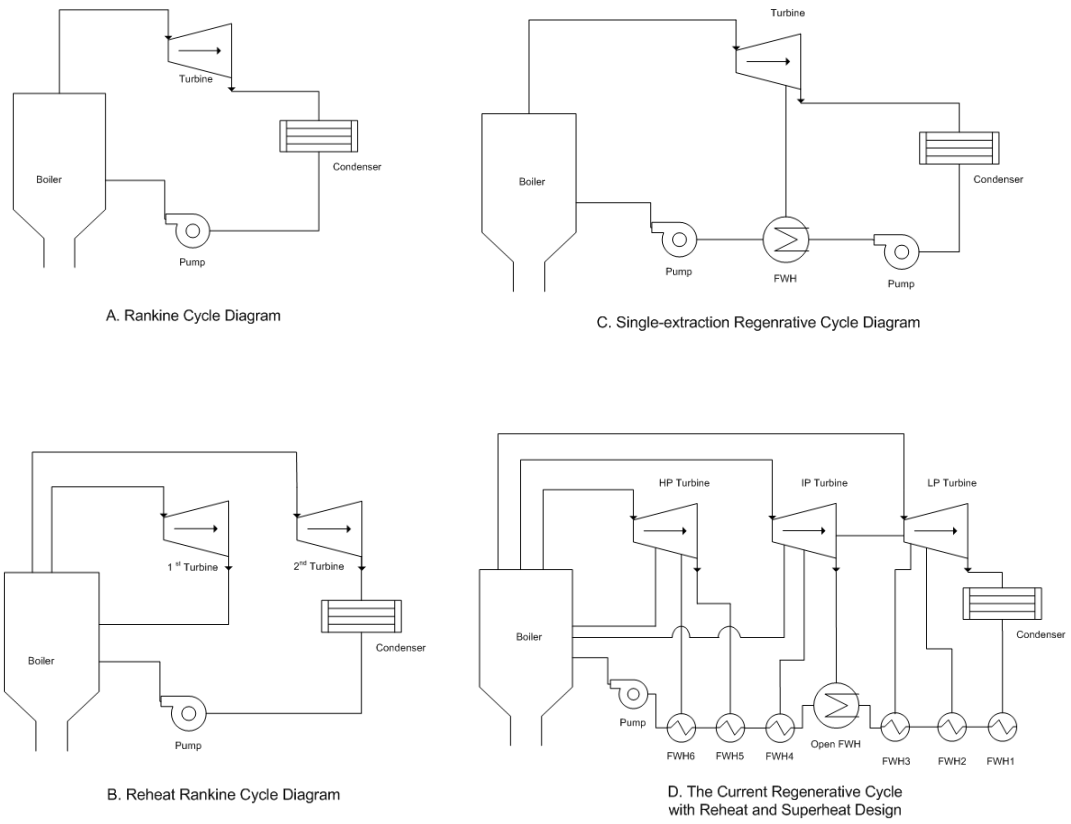

Figure 2.1: Schematic of the thermodynamic steam cycle of power plant evolution (Woodruff et al., 2005; Singer, 1991; Smith et al., 1996; Boyce, 2012).

According to Figure 2.1A., the steam cycle starts with liquid water entering the boiler where the combustion of fuel takes place, and it releases heat, producing superheated steam at high pressure and high temperature. Then, the high quality steam from the boiler enters a turbine, converting its energy to mechanical work for generating electricity. The low pressure steam from the turbine is subsequently condensed at the condenser. To complete the steam cycle, a pump is employed to send the condensate back to the boiler. It should be noted that the thermal efficiency of this basic cycle is rather small, resulting in an inefficient use of fuel. An improved version of the Rankine Cycle was later achieved by reheating steam from the turbine. This process is called the "**Reheat Rankine Cycle**". To achieve this reheat cycle, the high quality steam from the high-pressure turbine is returned to the boiler to regain its temperature at constant pressure. After the reheating process, the reheated steam is routed to the lower pressure turbine and then the expansion process is completed in the low-pressure condenser as shown in Figure 2.1B. In the early 1920s, a modified cycle, which is known as the "**Regenerative Rankine Cycle**", has become widely used in modern steam power stations. The idea of this concept is to integrate operating components called feedwater heaters working in a series to raise the temperature of working fluid (or condensate) from the condenser before entering the boiler. A flow diagram of a simple Regenerative Rankine cycle is shown in Figure 2.1C. The complexity of a Reheat-regenerative Ranking cycle, which is currently used in commercial plants, is shown in Figure 2.1D. It involves extracting or bleeding steam from the turbine system at different points. This extracting of steam is used to transfer heat to the liquid water at the feedwater heater.

Thus, the temperature of liquid water before entering the boiler is elevated resulting in an increase of thermal efficiency of the steam cycle.

Thermal efficiency is a performance measurement of steam cycles that reflects the degree of power output derived from the heat input into the system. The thermal efficiency (η_{th}) can be defined as:

$$\eta_{th} = \frac{\dot{W}_{output}}{\dot{Q}_{in}} \tag{2.8}$$

where $\dot{W}_{output}$ is net power output and $\dot{Q}_{in}$ is heat energy supplied to the boiler.

Another term commonly used to describe the performance of a power plant is the "net efficiency" (η_{net}). This term demonstrates the relationship between power output and the consumption of coal. The general equations can be written as follows:

HHV-based efficiency

$$\eta_{net,HHV} = \frac{\dot{W}_{output}}{\dot{m}_{coal} \cdot q_h} \tag{2.9}$$

LHV-based efficiency

$$\eta_{net,LHV} = \frac{\dot{W}_{output}}{\dot{m}_{coal} \cdot q_L} \tag{2.10}$$

2.2 Design and Operation of Power Plants

After the successful development of the reheat-regenerative Rankine cycle, large-scale pulverized coal-fired power plants were constructed and operated. In the 1960s, the traditional pulverized coal fired (PC) power plant usually operated under subcritical

operating conditions or at pressures below the critical point of water. A process flow diagram of a subcritical plant is given in Figure 2.2. The conventional subcritical-PC plant, which operates at 17 MPa/ 538°C/ 538°C single reheat offers a net efficiency of about 37.6% (U.S.DOE., 1999). At present, global warming is gaining attention due to an increase in electricity demand resulting in pollutant emission. Hence, an improvement of the conventional subcritical-PC has been translated into new technologies offering an increase in plant efficiency and a reduction in coal consumption. The improved technologies rely on the development of advanced materials used for boilers and steam turbines that allow power plants to operate at higher temperatures and pressures. The advanced power plants can be classified into two different classes: supercritical-PC, shown in Figure 2.3, and ultra-supercritical-PC (see Figure 2.4). Supercritical-PC plants operating at 24 MPa/ 566°C/ 566°C single reheat offer a net efficiency of about 39.9% while ultra-supercritical-PC operating at 31 MPa/ 593°C/ 593°C/ 593°C double reheat offer a net efficiency of about 41.1% (U.S.DOE., 1999).

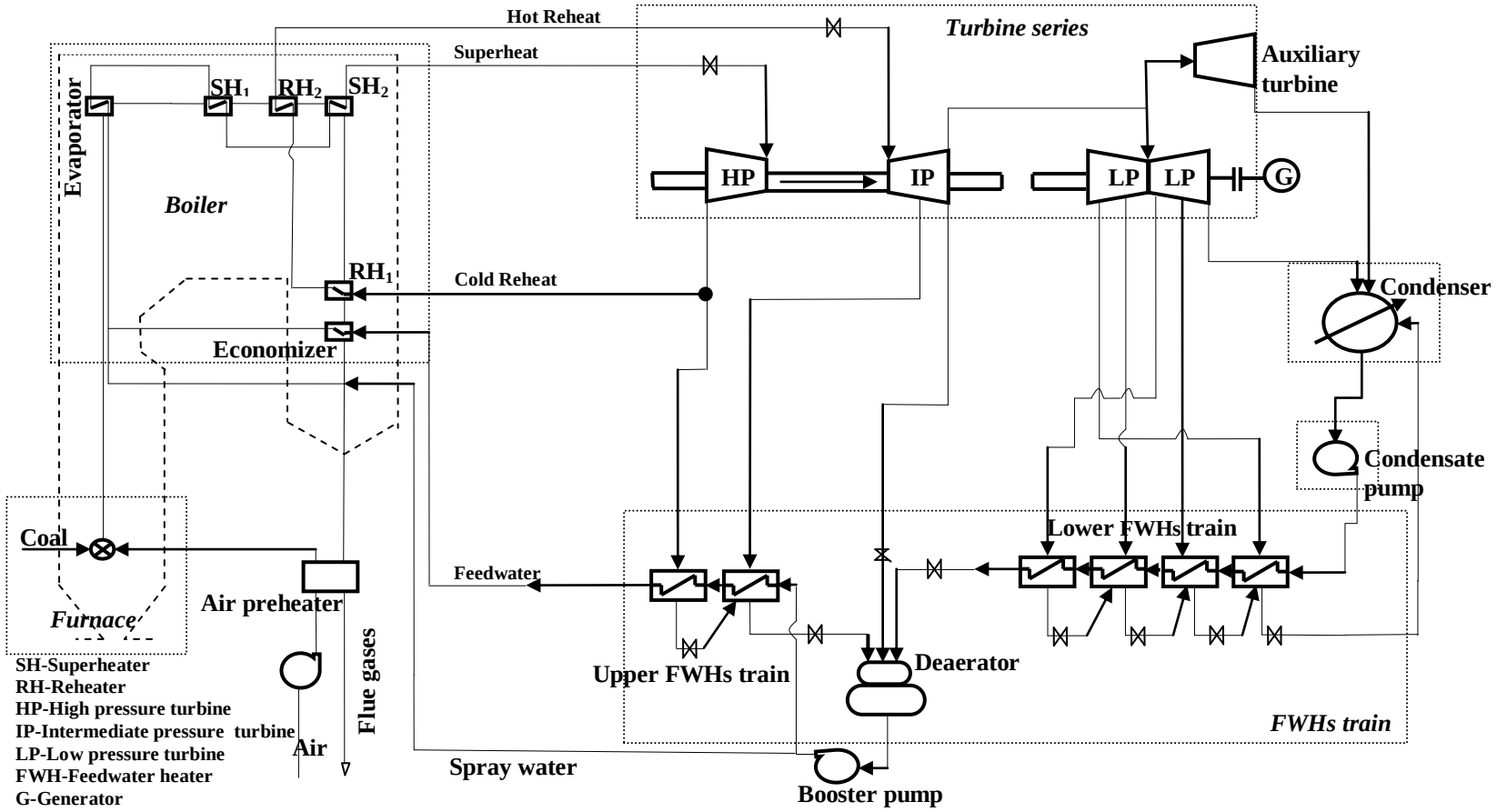

Figure 2.2: The schematic of a subcritical pulverized coal-fired power plant (Modified from Singer, 1991; Drbal et al., 1996; U.S.DOE, 1999 and Sanpasertparnich, 2007).

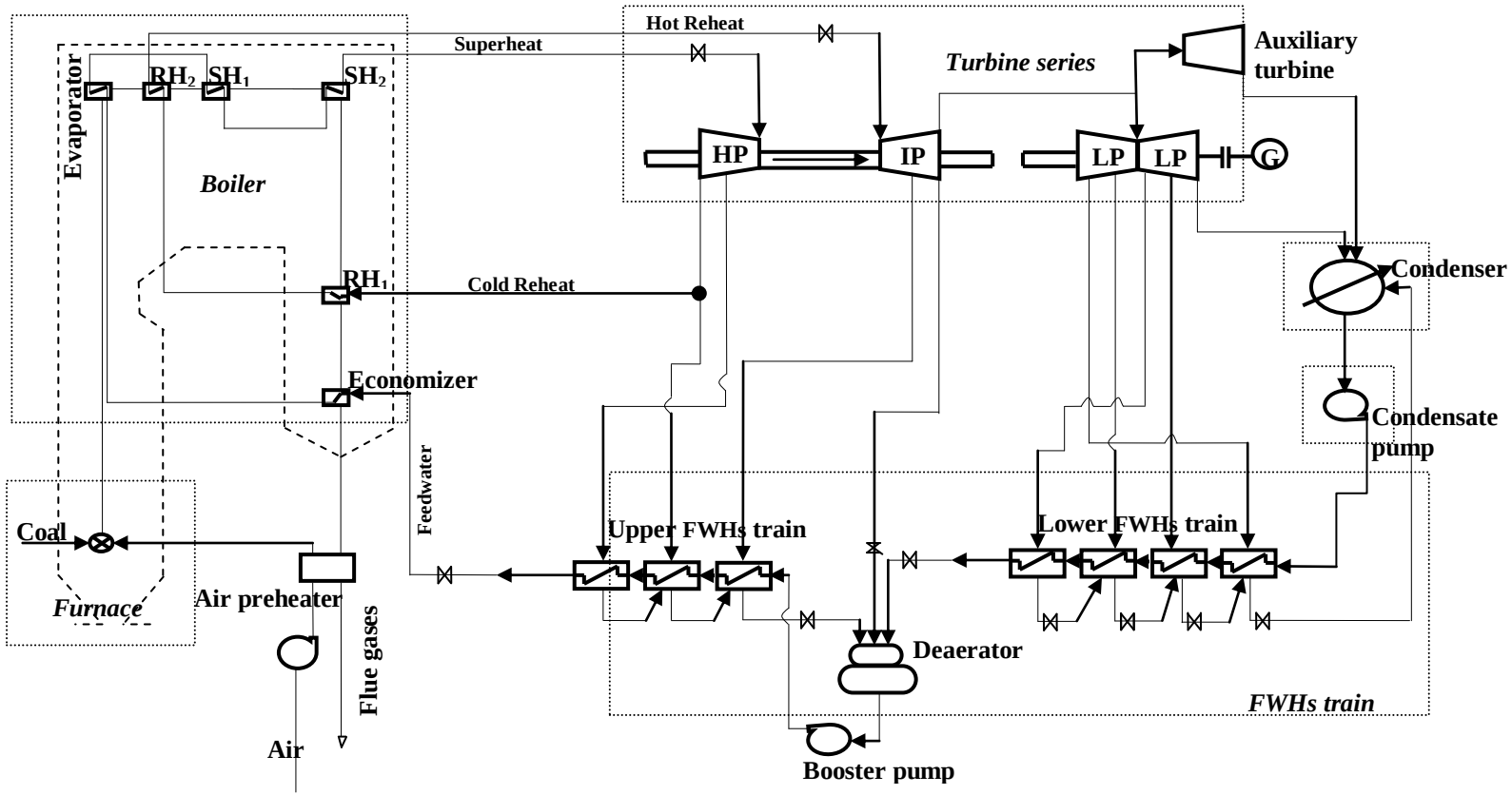

Figure 2.3: The schematic of a supercritical pulverized coal-fired power plant (Modified from Singer, 1991; Drbal et al., 1996; U.S.DOE, 1999 and Sanpasertparnich, 2007).

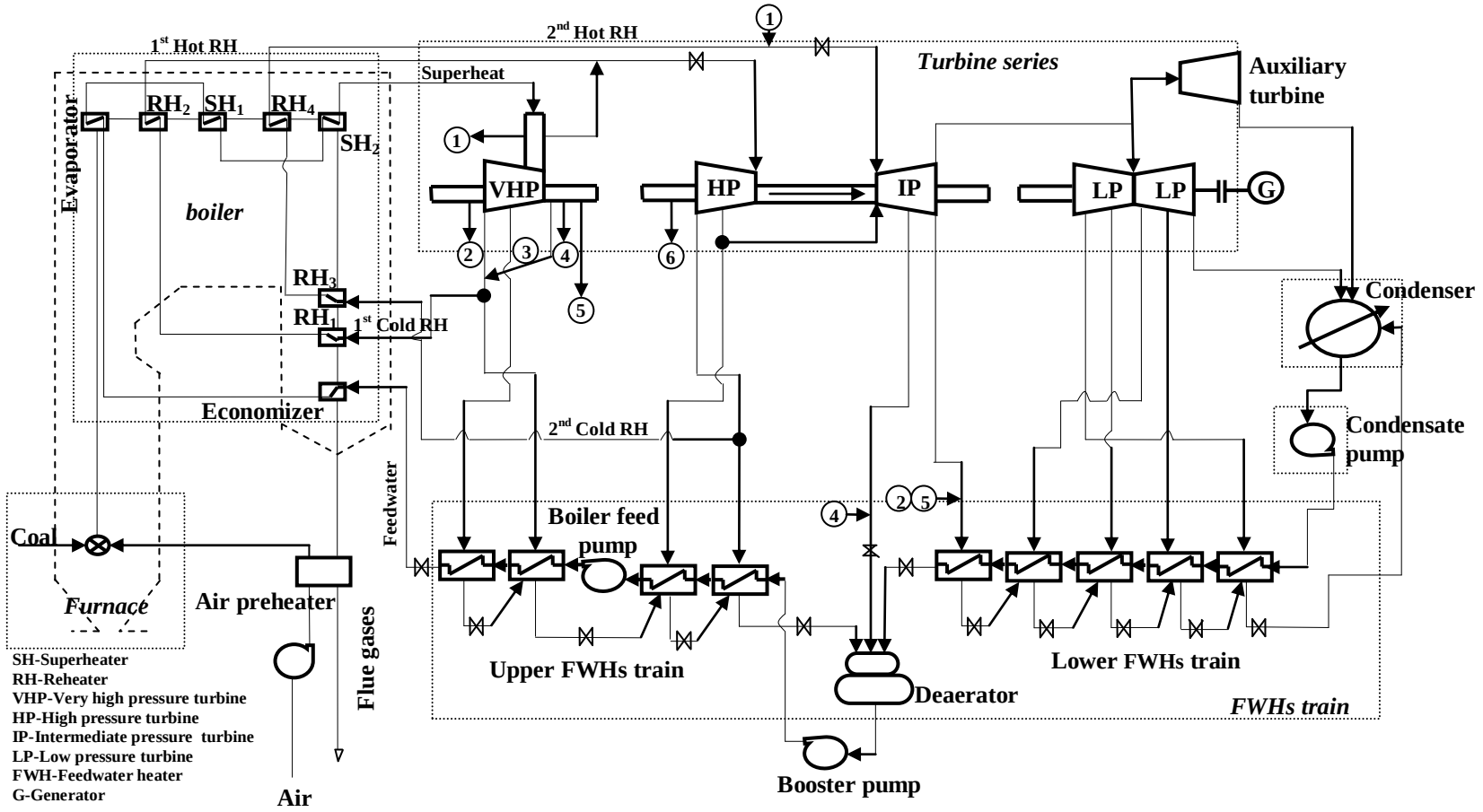

Figure 2.4: The schematic of an ultra-supercritical pulverized coal-fired power plant (Modified from Singer, 1991; Drbal et al., 1996; U.S.DOE, 1999 and Sanpasertparnich, 2007).

This study focuses on a 400 MW ultra-supercritical pulverized coal-fired power plant as depicted in Figure 2.4. This cycle consists of a once-through boiler, a series of turbines, a vacuum condenser, a boiler feed pump, a deaerator, a set of closed feedwater heaters (FWHs), and an air preheater. High pressure and temperature of superheated steam is generated in the once-through boiler by receiving heat from the coal combustion. The combustion of coal produces hot flue gas while heat transfer takes place through a series of heat exchangers in the boiler including superheaters (SHs), reheaters (RHs), an evapourator and an economizer. The superheated steam at the boiler is then routed to the turbine series where small portions of steam are extracted to heat the FWHs. The exhausted steam from the very-high-pressure (VHP) turbine is reheated in the boiler at constant pressure. This reheated steam is called the 1^{st} reheating steam. Similarly, the exhausted steam from the high-pressure (HP) turbine is sent back to the boiler for the 2^{nd} reheating. The reheated steam at this point in then routed to the intermediate-pressure (IP) turbine and finally to the low-pressure (LP) turbine. The low pressure steam from the LP turbine is then condensed into saturated liquid at the condenser. To complete the steam cycle, the saturated liquid or condensate is pumped to the boiler, passing through a train of FWHs.

The typical operating conditions of this ultra-supercritical power plant are 30.7-33.6 MPa of main steam pressure, 566-650°C main steam temperature, 566-600°C at 1^{st} reheating temperature, 566-600°C at 2^{nd} reheating temperature, 15-20% excess air for coal combustion, 5-8 kPa back pressure, and 250-350°C preheated air temperature (Singer, 1991; Drbal et al., 1996; Perry et al., 1997; U.S.DOE., 1999; Woodruff, 2005;

Sanpasertpanich, 2007; Cao et al., 2007; Wright et al. 2005; Feng, 2008; Asthana and Panigrahi, 2008). The number of FWHs required for a steam cycle depends upon the operating conditions of coal-fired power plant. According to Table 2.2, as the operating conditions increase, so does the amount of FWHs operating in the steam cycle. The ultra-supercritical power plant does require a total of ten FWHs while a total of only seven FWHs is needed for a conventional subcritical power plant.

The technology of ultra-supercritical pulverized coal-fired power plant with a capacity of 400 MW not only proposes an improvement of net efficiency by 1.4% but also offers a reduction of CO_2 emissions by 20.7 tonne/ hr as presented in Table 2.2

2.3 Simulation Tool

It was necessary to identify the strengths and drawbacks of various simulation techniques before selecting the best ones to apply to this study. Table 2.3 shows several of the most popular techniques suitable for chemical process simulation, including Genetic Algorithm, Neural Network, Monte Carlo, and a combination of factorial design and response surface methodology.

Genetic Algorithm (GA) and Neural Network (NN) are compatible with collection of data set input parameters in which a relationship between them cannot be clearly defined as simple equations. GA is a probabilistic optimization method based on the mechanics of biological evolution (Mukhopadhyay et al., 2009). GA mimics an

Table 2.2: Typical operating conditions of a coal-fired power plant (U.S.DOE, 1999).

Description	**subcritical PC**	**Supercritical PC**	**Ultra-supercritical PC**
Net efficiency (% HHV)	37.6	39.9	41.3
Unit size (MW)	400	400	400
Operating conditions			
Pressure (MPa)	17	24	31
Main steam temperature (°C)	538	566	593
1^{st} Reheating temperature (°C)	538	566	593
2^{nd} Reheating temperature (°C)	-	-	593
Operating components			
Turbines	HP/IP/LP	HP/IP/LP	VHP/HP/IP/LP
The number of feed water heaters (FWHs)	6 closed FWHs+1 deaerator	7 closed FWHs+1 deaerator	9 closed FWHs+1 deaerator
Emission rate			
SO_2 (lb/MW)	3.13	1.47	1.42
NO_x (lb/MW)	4.09	1.35	1.35
Particulate matters (lbMW)	0.272	0.08	0.08
CO_2 (lb/MW)	1,846	1,740	1,679
Comparison			
Coal feed (tonne/hr)	140.28	133.86	128.22
CO_2 emission (tonne/hr)	514.36	490.82	470.14

Table 2.3: The comparison of the optimization techniques used in literatures (Balabin et al., 2009; Biegler et al., 2002; Lee et al., 2007; Mukhopadhyay, 2009; Roman et al., 2007; Sanpasertparnich, 2007; Srinivas and Deb, 1994; Yao, 1999).

Technique	Advantage	Disadvantage
1. Genetic Algorithm	• suitable for complex models	• complex mathematics involved • time consuming
2. Neural Network	• mathematical model not required • minimizes error and offers optimal results • flexible and adaptable for any type of application • able to solve complex systems • able to deal with a large number of parameters	• high computational cost • requires combination with GA to optimize parameters • massive processing unit and storage memory of the computer required • difficult to detect fault performance
3. Monte Carlo Simulation (the adaptation of simulated annealing)	• easy to understand the real system • suitable for uncertain and complicated models • compatible with Excel-based model	• generates only one solution at a time • requires construction of a theoretical model
4. A combination of factorial design and response surface methodology	• suitable for experimental data • straightforward method	• computational cost when dealing with the complexity • time consuming

evolutionary process by generating possible candidate solutions. This algorithm relies on common techniques inspired by the process of natural evolution such as inheritance, mutation, selection, and crossover (Mukhopadhyay et al., 2009; Srinivas and Deb, 1994). The drawback of this algorithm is its expensive operating cost, and it also requires complicated knowledge of computing and optimization (Srinivas and Deb, 1994).

Neural Network is a knowledge-based approach mimicing the biological neural system in the human brain (Yao, 1999). Neural Network interacts with observed data sets to formulate a mathematical model through a learning process to carry out the output (Lee et al., 2007; Balabin et al., 2009). The main advantage of Neural Network is its ability to solve complex equations with a large amount of input parameters.

A combination of factorial design and response surface methodology is a straightforward optimization technique. It is suitable for any data collected from the experiments (Kalil et al., 2000).

Finally, Monte Carlo is a stochastic approach in which a set of input parameters is randomly generated based on a given probability distribution. This random-based technique requires a large number of repeated calculations until the optimal point is reached (Sanpasertparnich, 2007). The Monte Carlo approach is suitable for complicated models with uncertainty in the parameters, and it compatible with MS Excel. Therefore, it was selected for this thesis work. More detail is presented in Chapter 3.

2.4 Limitations of Previous Studies

This study aims to improve the efficiency of ultra supercritical steam conditions of power plants, which is the most advance steam power generation available for coal-fired power plants. This technology is relatively new. Thus, pilot-scale steam conditions needed to be adopted from research studies before simulation could be designed for optimization results. Table 2.4 summarizes a number of research studies presenting various objectives and methodologies for ultra supercritical coal fired-based technology (Romanosky et al., 2007; Wright et al.,2004; Rawls et al., 2007; Viswanathan, 2002; Holcomb , 2003; Viswanathan et al.,2006; Viswanathan and Bakker, 2000; Shimogori,; Holcomb et al., 2005; McDonald, 1997; Goidich et al., 2005; Ashmore, 2006; Mandal, 2006; Hack et al., 2007; Goidich et al., 2006; Okura et al; Sanpasertparnich, 2007; Beér, 2007; Marius et al., 1998; Bergerson and Lave, 2007; Sarunac et al., 2007).

The areas of development of interest include advanced material technology, components improvement, process improvement, coal preparation, and operating steam conditions as presented in Table 2.4. From this table, it can be seen that nickel-based alloys named CCA 617, Inconel 740, and Haynes 230 have been introduced for operation at temperatures up to 760˚C and 34.5 MPa due to the limitations of ferritic alloys.

Moreover, integrating the two high desuperheating feedwater heaters with feedwater trains allow an improvement of net plant efficiency up to 42.3%. There is a design for the turbine to operate at steam pressure of 30.0 MPa with a temperature of 600˚C with at a HP turbine and a temperature of up to 620˚C at an IP turbine. As a result,

the nickel- and cobalt-based super-alloy is a perfect material to build components to withstand high creep strength at high temperature.

Furthermore, the double reheat cycle is used to increase the efficiency and reduce the erosion in a LP turbine since the average temperature of steam is increased. A reduction in moisture content in coal by 8.5% also helps to improve the efficiency of the boiler by about 2.3% and raises the net heat rate by 3%.

It should be noted that most of the research studies only provide individual effects corresponding to a single or a pair of significant operating and process design parameters for USC technology. The study of the net efficiency improvement for the ultra-supercritical power generation can be challenged since there is no research that takes all parametric effects simultaneously into account. One of the reasons is that most operating steam conditions of this new technology are governed by an available advance material used for construction of components for the boiler and steam turbines of the power plants. Thus, it was taken to consideration for the main operating conditions of this study. Elements of this study were initially developed in a previous work, a thesis titled "Monte Carlo Simulation of Pulverized Coal-Fired Power Plants Efficiency Improvement and CO_2 Capture Options" by Teerawat Sanpasertparnich (2007). This study follows up on the concept initially developed by Sanpasertparnich concerning how to achieve the improvement of net plant efficiency, but in this study the operating steam conditions and a design used for ultra-supercritical power plants are examined. Table 2.5 presents a summary of literature that provided the main data on ultra-supercritical power plants.

Table 2.4: Research studies on the ultra-supercritical power generation.

Research Development	Reference	Objective	Methodology	Result represent	Conclusion and new finding	Note
Material Development	Romanosky et al., 2007 **"Steam Turbine Material for Ultra Supercritical Coal Power Plants"**	• Develop materials for USC turbine that can be used and shaped into a finished product under steam conditions of 760˚C and 34.5 MPa.	• Evaluate and select the alloys based on published research and industrial experience by considering creep, fatigue, and oxidation resistance.			• This is the first step of a five-year project aimd at developing high potential material for USC turbines that also match the USC boiler.
	Wright et al.,2005 **"Materials Issues for Turbines for Operation in Ultra-Supercritical Steam"**	• Study of the material of specific components of USC turbines operating under steam conditions of 620˚C and 34 MPa and attempts to increase temperature to 700˚C and 760˚C with 34 MPa steam pressure.	• Apply modeling method to predict material performance and life prediction.	• Creep rupture strength	• Inconel 617 and 740 (Ni-base alloys) can be used at temperatures up to 760˚C. • Casing/shell is large size with complex structure, so Ni-base alloys are introduced as promising material for operation at 760˚C. • 12 Cr alloys and Cr-Mo-V are steel able to produce rotors and discs at temperatures up to 620˚C. • Ni-base alloys can be	

Table 2.4: Research studies on the ultra-supercritical power generation (continued).

Research Development	Reference	Objective	Methodology	Result represent	Conclusion and new finding	Note
					used as HP turbine.	
Material Development	Rawls et al., 2007 **"Advanced Research Materials Program"**	• Develop new alloys focusing on improving the corrosion and erosion resistance.	• Gather information and study of the major areas including structural ceramics, new alloys, and coating.			
	Viswanathan, 2002 **"Boiler Materials for Ultra Supercritical Coal Power Plants"**	• Develop advanced materials for USC boilers operating with 760˚C and 35 MPa.	• Do the design and economic analysis from the published research.		• Inconel 740 and Nimonic 230 are the candidate materials for SH outlet headers and finishing SH tubes. • The plant efficiency was estimated at about 47%.	• This project is the first of nine tasks expected to reach the research goal.
	Holcomb , 2003 **"Ultra-Supercritical Steam Cmorrosion"**	• Study the materials technology for the high temperature and pressure at the turbine for USC plants.	• Do three oxidation experiments in supercritical steam conditions at temperatures up to 650˚C and various pressures up to 34.5 MPa on	• Creep rupture strength	• Ferritic alloys (SAVE12 and NF12) have 10^5 creep rupture strength of 180 MPa at 600˚C. • Austentic alloys maintain their strength at higher temperature than ferritic alloy.	

Table 2.4: Research studies on the ultra-supercritical power generation (continued).

Research Development	Reference	Objective	Methodology	Result represent	Conclusion and new finding	Note
Material Development			six candidate alloys including ferritic alloy SAVE12, austentic alloy SUPER 304H, the high Cr high Ni alloy HR6W, and the three nickel-based superalloys Inconel 617, Haynes 230, and Inconel 740		• To economize the cost at USC turbines considers only high temperature for selecting the materials.	
	Romanosky et al., 2007 **" Advanced Materials for UltraSupercritical Boiler Systems"**	• Identify the advanced materials for use in USC boilers operating at temperatures up to 760˚C.	• Do the mechanical testing on six selected alloys.	• Strength and efficiency.	• Increasing the efficiency by at least 8 to 10% affects the reduction in CO_2 emissions and other pollutant flue gases by nearly 30%. • Nickel-base alloys contain the highest level of Cr that controls the corrosion.	

Table 2.4: Research studies on the ultra-supercritical power generation (continued).

Research Development	Reference	Objective	Methodology	Result represent	Conclusion and new finding	Note
					• Inconel 740, Haynes 230 and CCA 617 can operate at the temperature up to 760˚C.	
Material Development	Viswanathan et al., 2006 **" Materials for ultra-supercritical coal-fired power plant boilers"**	• Improve the materials technology for use in ultra-supercritical (USC) boiler.	• Do the experiment and simulation under steam conditions of 760˚C and 34.5 MPa.	• Present results in terms of net efficiency (η_{net}).	• Using the advanced materials results in the improvement of the efficiency to nearly 52% LHV. • Chromium content of the alloy (austentic alloy) predominantly controls the oxidation resistance. • A new alloy called CCA 617 (nickel-base alloy) withstands the excepted creep strength running overtime with 760˚C and 35 MPa.	
	Viswanathan and Bakker, 2000 **"Materials for Boilers in Ultra Supercritical Power Plants"**	• Report the results of the development of material technology for USC boiler.	• Review the literature of advanced material about the development of ferritic	• Creep rupture strength, fire-side corrosion and steam-side oxidation	• For heavy sections including pipes and headers, the combination of 9-12% Cr content in ferritic steels and C, Nb, Mo, V, and	

Table 2.4: Research studies on the ultra-supercritical power generation (continued).

Research Development	Reference	Objective	Methodology	Result represent	Conclusion and new finding	Note
Material Development			steel and austentic steel for use in three parts of boilers such as heavy sections, SH/RH, and waterwalls .		substitution of W for Nb, which are HCM 12A, NF616 and E911, are introduced as the materials operating up to 620˚C/34 MPa while 12% Cr alloy (NF 12 and SAVE12) is used for the temperature beyond 650˚C. • Ferritic steel is able to be applied in the final stage of SH/RH, where steamside oxidation and fireside corrosion are the main problems at temperatures above 565˚C but Inconel 617, NF709 above 650˚C. • For upper waterwall sections, 12% Cr named HCM2(T23) and HCM12 are	

Table 2.4: Research studies on the ultra-supercritical power generation (continued).

Research Development	Reference	Objective	Methodology	Result represent	Conclusion and new finding	Note
					promising materials in terms of creep strength for use in steam conditions of 595-650˚C.	
Material Development	Shimogori, **"Ultra Super Critical Pressure Coal Fired Boiler State of the Art Technology Application"** (can be seen in steam development)	• Study the current USC technology in Hitachi-Naka Thermal Power Station's No.1 Unit, Japan with steam condition of 24.5 MPa and 600˚C/600˚C (start operation in December 2003) to develop for the 700˚C USC boiler.	• Report the new technology applied for materials improvement in the boiler.	• Development Steam condition in Japan; material strength and steam oxidation scale.	• Improving the creep rupture strength in ferritic steel, Mo (molybdenum) is used instead of W (tungsten) • To combine Mo, B (boron) and N (nitrogen) improves creep strength. • To develop the steam oxidation scale, 9-11% Cr thick pipe welding was applied to the boiler. • Austentic steel called NF709 and Alloy617 is the solution for use in high temperature strength at temperatures up to 700˚C for large diameter pipe and 750˚C for boiler tube.	

Table 2.4: Research studies on the ultra-supercritical power generation (continued).

Research Development	Reference	Objective	Methodology	Result represent	Conclusion and new finding	Note
	Holcomb et al., 2005 **"Ultra Supercritical Steamside Oxidation"**	• Study the currently USC technology in Hitachi-Naka Thermal Power Station's No.1 Unit, Japan, with steam conditions of 24.5 MPa and 600˚C/600˚C (start operation in December 2003) developed for the 700˚C USC boiler.	• Do the material experiments (cyclic oxidation in moist air and TGA) at temperatures in the range 700˚-800˚C in the testing of alloys for an USC turbine including SAVE 12 (ferritic alloy), SUPER 304 H (austentic alloy), HR6W (high Ni alloy), and the three nickel-based superalloys, which are Alloy 617, Alloy 230, and Alloy 740	• Oxidation result in mass change unit (mg/cm^2)	• Ferritic steel has the limitation of operating at steam conditions of about 620-630˚C, so nickel-based super alloy is the solution for temperatures above 630˚C. • The best aspect material based on oxidation testing is the high Cr nickel alloys (alloy 617, alloy 230, alloy 740 and HR6W).	
Component Improvement	McDonald, 1997 **"Status of B&W's Low-Emission Boiler system Development Program**	• Develop an advanced steam cycle and boiler.	• Review and apply the experience of integrated operation of the combustion	• Present in term of net efficiency (η_{net}) and the cost-of-electricity (COE).	• Low-Emission Boiler system Development Program meets net plant efficiency greater than 42% and the cost-of-electricity (COE)	

Table 2.4: Research studies on the ultra-supercritical power generation (continued).

Research Development	Reference	Objective	Methodology	Result represent	Conclusion and new finding	Note
Component Improvement			system.		slightly decreases. • The combination of two high desuperheating feedwater heaters and feedwater train at steam condition 593˚C and 31 MPa achieves net efficiency up to 42.27%.	
	Goidich et al., 2005 **" Design Aspects of the Ultra-Supercritical CFB Boiler"**	• Design the conceptual materials for use in a 400 MW_s Ultra-supercritical CFB boiler.	• Do the simulation and analysis for various performance parameters.	• The features of the 400 MW_s Ultra-supercritical CFB boiler design.	• Austentic steel Super 304H and TP347 HFG are the aspect materials required for the final superheater and the other superheaters and reheaters.	
	Ashmore, 2006 **"Steam turbine technology goes ultra-supercritical"**	• Study the evolutionary technology of advanced steam turbines resisting high temperatures of 600˚C/620˚C and pressure of about 31 MPa.	• Review the typical design applied in turbine operation.	• Show the detail of mechanical design for each type of turbine series.	• HP turbine using a four-cylinder arrangement with a single cross over pipe is a single-flow type with full arc admission and design for use in steam conditions up to 30 MPa/600˚C.	

Table 2.4: Research studies on the ultra-supercritical power generation (continued).

Research Development	Reference	Objective	Methodology	Result represent	Conclusion and new finding	Note
Component Improvement					• IP turbine withstanding temperatures up to 620˚C is a double-flow and double-shell design. • LP turbine of which the blade length is 45 inches for steel and 56 inches for titanium utilizes a double-flow, double-shell design and inner casing. • The temperature limit of 9-11% Cr content in chromium steel alloy is 620˚C • Nickel and cobalt-based super-alloys resist high creep strength at temperatures up to 700˚C.	
	Mandal, 2006 **"Efficiency Improvement in Pulverized Coal Based Power Station"**	• Study the main parameters resulting in improvement of advanced pulverized coal-fired technology.	• Report status of advanced technology at present.	• Creep rupture stress (MPa) and net efficiency (η_{net}).	• Ni-based alloy has high strength resistance to temperatures up to 700˚C. • Washed coal offers ash reduction by 4-5% • A single reheat cycle cooled by a wet cooling	

Table 2.4: Research studies on the ultra-supercritical power generation (continued).

Research Development	Reference	Objective	Methodology	Result represent	Conclusion and new finding	Note
					results in net efficiency of 50-51% while a double reheat cycle cooled by water reaches 53-54%.	
Component Improvement	Hack et al., 2007 **"Design Considerations for Advanced Materials in Oxygen-Fired Supercritical and Ultra-Supercritical Pulverized Coal Boiler"**	• Study the promising materials in term of the concentration of oxygen and sulfur compound for SC and USC pulverized coal-fired power plant integrated oxycombustion.	• Use CFD simulation for material selection and 1000 hours of laboratory experiments.	• Corrosion penetration depth and wastage rate.	• The oxycombustion offers zero CO_2 emissions. • Alloy 622 and FGD is utilized to reduce the corrosion in the design of oxygen-retrofit boiler. • Increasing heat flux in the oxygen-fired Greenfield design; T2 and T92 are required as materials.	
	Goidich et al., 2006 **" Integration of Ultra-supercritical OUT and CFB Boiler Technologies"**	• Study the technology development for ultra supercritical boiler under steam condition 31.5 MPa /604˚C	• Study the features of 800 MW_e ultra supercritical CFB OUT boiler design and the effect of increasing steam condition.	• The relationship between temperature and furnace height.	• The full reheat steam for the 800 MW_e OUT CFB increases temperature by about 717˚C from 621˚C after modification of the design by reducing furnace height to 6.5 ft and increasing the surface of the heat exchanger.	

Table 2.4: Research studies on the ultra-supercritical power generation (continued).

Research Development	Reference	Objective	Methodology	Result represent	Conclusion and new finding	Note
Component Improvement	Okura et al., **"Complete of High-efficiency Coal-fired Power Plant"**	• Review the performance of turbine technology with steam condition 25 MPa and 600˚C/600˚C in the Tamatoh-Atsuma Power Station No.4 unit of Hokkaido Electric Power Co., Inc. (HEPCO) with 700 MW turbine generator (1,735 MW of output capacity and start operation in June 2002).	• Report the specification of the main components including turbine, generator, and condenser being used in Japan.	• Describe the performance details of turbine technology.	• The operation under steam condition 25 MPa and 600˚C/600˚C increases the efficiency in turbine by about 2.8%. • 9% Cr forged steel utilized for turbine components such as main stop valve, adjustable valve combined reheat valve and the main steam and reheat steam inlet pipes can resist temperatures up to 600˚C. • 12% Cr is adopted for the HP-IP rotor, the HP-IP casing, the nozzle box and the HP-IP diaphragm. • SBDF (super-balanced downflow) is the new technology for the condenser to monitor the steam inflow.	

Table 2.4: Research studies on the ultra-supercritical power generation (continued).

Research Development	Reference	Objective	Methodology	Result represent	Conclusion and new finding	Note
Process Improvement	Sanpasertparnich, 2007 **"Monte Carlo Simulation of Pulverized Coal-Fired Power Plant: Efficiency Improvement and CO_2 Capture Options"**	• Identify the effect of operating and design conditions that give maximum power generation efficiency focusing on the subcritical and supercritical pulverized coal-fired power plants.	• Simulate the developed model with various scenarios for a sensitivity analysis by using rank coefficient and Monte Carlo approaches.	• Present in terms of net efficiency (η_{net}) and a rate of CO_2 emission.	• The significant conditions are moisture content in coal, steam pressures throughout a turbine system, boiler efficiency, temperature of preheated air, and temperature of both main steam and reheated steam.	
	Beér, 2007 **" High efficiency electric power generation: The environmental role"**	• Analyze the power plant system development effect on the efficiency and CO_2 emissions including coal-fired Rankine cycle steam plants with advanced steam parameters, natural gas-fired gas turbine-steam, and coal gasification combined cycle plants.	• Review the CCS technology affecting the efficiency improvement.	• Present in terms of net efficiency (η_{net}), CO2 emissions and the cost-of-electricity (COE).	• The plant efficiency increases while the COE is slightly reduced both with and without CCS.	

Table 2.4: Research studies on the ultra-supercritical power generation (continued).

Research Development	Reference	Objective	Methodology	Result represent	Conclusion and new finding	Note
Process Improvement	Marius et al., 1998 **"Development of Ultra Super Critical PF Power Plant in Denmark"**	• Discuss the real experience with the supercritical unit and review the evolution of ultra supercritical power plants in Denmark and identify material utilizaion with temperatures up to 700˚C.	• Review the operation parameters of supercritical and ultra supercritical plants including steam condition, net efficiency, and coal specification.	• Present table of performance parameters and illustrate the configuration of water/steam development.	• The double reheat cycle is utilized to improve the efficiency and reduce the erosion of the LP turbine. • The water walls, superheaters, and thick walled outlet headers are extremely important areas for the boiler, and there is need to develop new material (new austenitic steel). • Nickel-based super alloy is introduced for boilers operating up to 37.5MPa/700˚C.	
Coal Preparation	Bergerson and Lave, 2007 **"The Long-term life cycle private and external costs of high coal usage in the US"**	• Analyze and economize the electricity generation cost by using either coal or natural gas.	• Use IECM software to determine the cost and the possible environmental impacts for each individual scenario.	• Present in terms of net efficiency (η_{net}) and the cost-of-electricity (COE).	• Carbon capture and storage (CCS) combination in an ultra-supercritical PC plant and IGCC plant reduces the efficiency from 40-43% to 31-34% and from 32-38% to 27-33%, respectively.	

Table 2.4: Research studies on the ultra-supercritical power generation (continued).

Research Development	Reference	Objective	Methodology	Result represent	Conclusion and new finding	Note
Coal Preparation	Sarunac et al., 2007 **" One Year of Operating Experience with a Prototype Fluidized Bed Coal Dryer at Coal Creek Generating Station"**	• Study effect of reduction of moisture content in coal.	• Design a prototype coal drying system and its installation.	• Net efficiency (η_{net}) and emission reduction rate (%).	• The integrated coal drying steam designed for new sub-bituminous coal-fired supercritical and ultra-supercritical results in an increase in efficiency. • Reduction by 8.5% of moisture content in coal increases the efficiency in the boiler by about 2.13% and improves the net unit heat rate by 3%. • A fluidized bed dryer (FBD) decreases NO_x and SO_2 by 10% and 10-15%, respectively.	
Steam condition	Shimogori, **"Ultra Super Critical Pressure Coal Fired Boiler State of the Art Technology**	• Study the current USC technology in Hitachi-Naka Thermal Power Station's No.1 Unit, Japan, with steam	• Report the new technology applied for materials improvement in	• Development of steam condition in Japan, material strength, and steam oxidation scale.	• The latest USC power plant in Japan is Hitachinaka No1. (1000 MW) operating under steam condition of 25	

Table 2.4: Research studies on the ultra-supercritical power generation (continued).

Research Development	Reference	Objective	Methodology	Result represent	Conclusion and new finding	Note
Steam condition	**Application"** (can be seen in material development)	condition of 24.5 MPa and 600˚C/600˚C (start operation in December 2003) developed for a 700˚C USC boiler.	the boiler.		MPa/600˚C/600˚C.	

Table 2.5: Summarization of main input for ultra-supercritical pulverized coal-fired power plants according to research studies[1].

Units	Main pressure (MPa)	Main temperature (°C)	1st reheated temperature (°C)	2nd reheated temperature (°C)	Backpressure (kPa)	References
1.USC PC	26.25	600	600			Cao et al., 2007
2. USC PC	34.5	649	593	593		Cao et al., 2007
3. Sub. PC	13.0	535	535			Asthana and Panigrahi, 2008
4. Sup. PC	24.6	600	600			Asthana and Panigrahi, 2008
5. USC PC	14.2	600	600		3.8	Asthana and Panigrahi, 2008
6. USC PC	14.2	600	600		1.5	Asthana and Panigrahi, 2008
7. USC PC	26.25	600	600		4.19	Feng, 2008
8. USC PC	31.0	621	566	566		Wright et al., 2004
9. USC PC	34.0	649	566	566		Wright et al., 2004
10. USC PC	25.0	600-700				Viswanathan et al., 2006
11. USC PC	25.5	598	596			Bugge et al., 2006
12. USC PC	25.9	604	602			Bugge et al., 2006
13. USC PC	29.0	580	580			Bugge et al., 2006
14. USC PC	25.5	597	595			Bugge et al., 2006
15. USC PC	25.9	604	602			Bugge et al., 2006
16. USC PC	25.5	597	595			Bugge et al., 2006
17. USC PC	26.4	605	613			Bugge et al., 2006
18. USC PC	28.0	605	613			Bugge et al., 2006
19. Sub. PC	24.1	538	566			Cao et al., 2007
20. USC PC	31.0	566	566	566		Cao et al., 2007
21. USC PC	31.0	593	593	593		Cao et al., 2007

[1] Note

1. USC steam conditions defined as temperature of main and/or reheat steam exceeding or equal to 593°C and pressure greater than 24.1 MPa (Otsuka and Kaneko, 2007).
2. Materials for USC technology available for operating temperatures up to 650°C (Otsuka and Kaneko, 2007; Wright et al., 2004 and Maziasz et al., 2004).
3. AD 700 project is the best USC technology for future offering of high performance efficiency, which is under development.

Table 2.5: Summarization of main input for ultra-supercritical pulverized coal-fired power plants (continued).

Units	Main pressure (MPa)	Main temperature (°C)	1st reheated temperature (°C)	2nd reheated temperature (°C)	Backpressure (kPa)	References
22. USC PC	34.5	649	593	593		Cao et al., 2007
23. USC PC	30.0	600	620			Maziasz et al., 2004
*24. USC PC	35.0	700	720			Maziasz et al., 2004
25. Sub. PC	24.1	538	566			Otsuka and Kaneko, 2007
26. USC PC	31.4	593	593	593		Otsuka and Kaneko, 2007
27. USC PC	34.3	649	593	593		Otsuka and Kaneko, 2007
28. USC PC	30.0	630	630			Otsuka and Kaneko, 2007
29. USC PC	31.13	593	593	593		U.S.DOE, 1999
*30. USC PC	34.0	700-760	700-760			Asthana and Panigrahi, 2008

Chapter 3

Development of Ultra-Supercritical Coal-Fired Power Plant Model

This chapter provides details of a process-based computer model that was developed for simulating the operation of an ultra-supercritical coal-fired power plant. The model was built on the basis of coal combustion, heat transfer, material and energy balances, and thermodynamics of the steam cycle. The model was written in a Microsoft® Excel spreadsheet using a Crystal Ball® software add-in to perform a sensitivity analysis. A series of empirical equations for thermodynamic properties of working fluid was first regressed using MATLAB® and then integrated into the Excel-spreadsheet model. The following sections present the development of the model, thermodynamic properties, and sensitivity analysis strategies.

3.1 Process Components

The simulation model was constructed according to the conventional configuration of the ultra supercritical pulverized coal-fired power plant shown in Figure 3.1. To build the system of power generation, individual process components were formulated and put together to form the entire power plant. Basic principles applied to form the model (i.e., furnace/boiler, turbine/pump, and feedwater heaters) are detailed below.

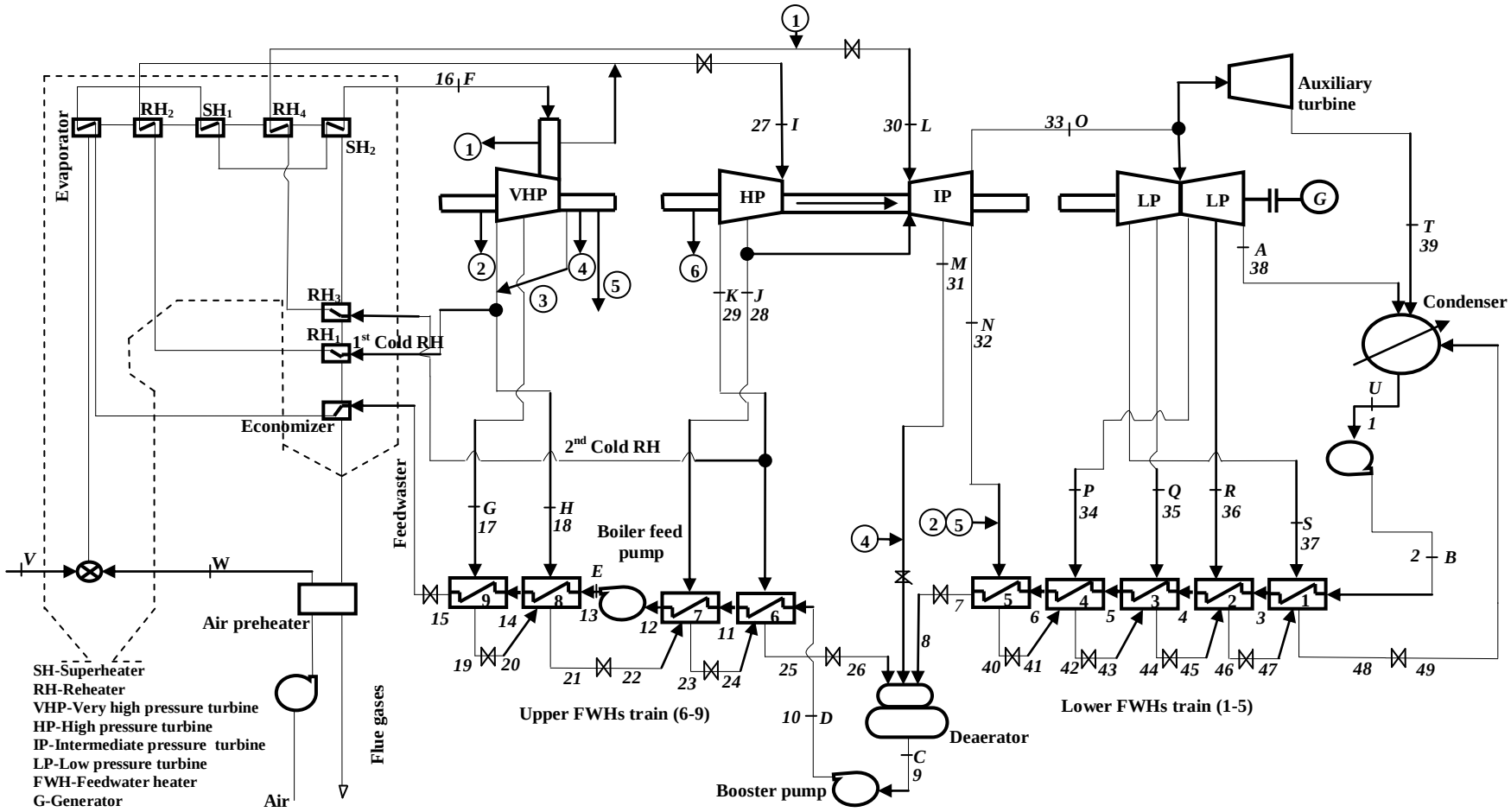

Figure 3.1: Process flow diagram of ultra-supercritical pulverized coal-fired power plant. (Modified from Singer, 1991; Drbal et al., 1996; U.S.DOE, 1999 and Sanpasertparnich, 2007)

3.1.1 Furnace

In the furnace, energy from coal combustion is the primary source of heat input into the boiler for converting liquid water into high pressure steam. Such energy can be determined from a combination of LHV-based combustion heat after vapourization of moisture in coal ($\dot{Q}_l = \dot{m}_{coal} \, . \, q_l$) and waste heat recovered from exhausted flue gas via an air preheater ($\dot{Q}_{Pre\,heater}$). $\dot{Q}_L$ can be derived from Equations (2.1) through (2.3) presented in the previous chapter where coal compositions and moisture content are known. The furnace heat can be written as (Sanpasertpanich, 2007):

$$\dot{Q}_{furnace} = \dot{Q}_l + \dot{Q}_{pre\,heater} \tag{3.1}$$

With a known composition of flue gas, the furnace heat can be transformed into the sum of enthalpy change for each combustion product ($\Delta\dot{H}_i$) (Sanpasertpanich, 2007) as given below:

$$\dot{Q}_{furnace} = \sum_{i=1}^{m} \Delta\dot{H}_i \tag{3.2}$$

The enthalpy change ($\Delta\dot{H}_i$) in this case is referred to as the sensible heat that causes an increase in the flue gas temperature (T) as follows:

$$\Delta\dot{H}_i = \int \dot{m}_i C_{p,i} dT \tag{3.3}$$

where $\dot{m}_i$ represents mass flow rate of the combustion product i which can be determined through material balances of Equations (2.4) through (2.7). $C_{p,i}$ is heat capacity of the corresponding combustion product *i*. Temperature of the flue gas leaving the furnace (combustion zone) and entering the boiler can be obtained by combining Equations (3.2) and (3.3).

3.1.2 Once-through Boiler

The hot flue gas leaving from the furnace (combustion zone) will transfer its energy to the boiler so as to produce high quality steam for driving turbines. For a given value of boiler efficiency (η_{boiler}), the heat absorbed by the boiler ($\dot{Q}_{boiler}$) can be determined as:

$$\dot{Q}_{boiler} = \eta_{boiler} \cdot \dot{Q}_{furnace} \tag{3.4}$$

It can be seen from Figure 3.1 that the one-through boiler is composed of eight heat-transfer components (i.e., one economizer, one evapourator, two superheaters, and four reheaters). Based on this boiler configuration, the heat input for the boiler can be written as:

$$\dot{Q}_{Boiler} = \dot{Q}_{econ} + \dot{Q}_{evap} + \sum_{i=1}^{2} \dot{Q}_{SH,i} + \sum_{i=1}^{4} \dot{Q}_{RH,i} \tag{3.5}$$

where $\dot{Q}_{econ}$, $\dot{Q}_{evap}$, $\dot{Q}_{SH,i}$, and $\dot{Q}_{RH,i}$ represents heat-transfer rates for the economizer, evapourator, superheaters and reheaters, respectively. The individual heat-transfer rates ($\dot{Q}$) can be calculated from the change in enthalpy of working fluid (water) passing through the corresponding heat-transfer components. The general heat-transfer equation then can be given as:

$$\dot{Q} = \dot{m}_{H_2O} \cdot (h_{H_2O,out} - h_{H_2O,in}) \tag{3.6}$$

where $\dot{m}_{H_2O}$ is mass flow rate of working fluid and $h_{H_2O,out}$ and $h_{H_2O,in}$,represent enthalpy of working fluid leaving and entering the heat-transfer components.

3.1.3 Turbines and Pumps

In the steam cycle, power extracted from each turbine can be determined from the change in enthalpy of working fluid or steam passing through the unit. Knowing the

specific entropy of steam (s_i) helps identify the enthalpy of steam leaving the turbine (h_{out}). It should be mentioned that the visual basic application (VBA) add-in to the Microsoft® Excel spreadsheet was also used to construct auxiliary functions in the Excel spreadsheet to determine such enthalpy values. To estimate actual enthalpy extracted from the turbine ($h_{out,actual}$), the correlation of isentropic enthalpy ($h_{out,isen}$) and turbine efficiency (η_T) is as follows:

$$\eta_T = \frac{h_{in} - h_{out,\ actual}}{h_{in} - h_{out,\ isen}} \tag{3.7}$$

Once the actual enthalpy extracted from the turbine is obtained, the power can be easily determined as:

$$\dot{W}_T = \dot{m}_i \cdot (\dot{h}_{in} - \dot{h}_{out,actual}) \tag{3.8}$$

where $\dot{m}_i$ represents mass flow rate of steam passing through each turbine portion.

According to the configuration of the power plant in Figure 3.1, electricity is generated from a series of turbines, starting from VHP, HP, IP, and LP. Because several portions of steam are extracted from individual turbines and used in the feed water heaters, there is a variation in mass flow rate of steam traveling through each turbine section. Gross electricity produced from a steam cycle ($\dot{W}_{T,total}$), therefore, can be determined by combining the power generated from individual turbines as follows:

$$\dot{W}_{T,\ total} = \sum_{i=1}^{m} \dot{W}_{VHP,i} \sum_{i}^{n} \dot{W}_{HP,\ i} + \sum_{i}^{o} \dot{W}_{IP,\ i} + \sum_{i}^{p} \dot{W}_{LP,\ i} \tag{3.9}$$

where $\dot{W}_{VHP,i}$, $\dot{W}_{HP,i}$, $\dot{W}_{IP,i}$ and $\dot{W}_{LP,i}$ represent the power output produced from portion i of the VHP, HP, IP and LP turbine, respectively.

Similar to the power extracted from the turbines, the power required for the pump ($\dot{W}_P$) can be determined from:

$$\dot{W}_P = \frac{\dot{W}_{P,isen}}{\eta_P} \tag{3.10}$$

where η_P and $\dot{W}_{P,isen}$ denote pump efficiency and isentropic power of the pump, respectively. Total power required for the pump can be calculated from those for the individual pumps ($\dot{W}_{P,i}$) as:

$$\dot{W}_{P,total} = \sum_{i}^{p} \dot{W}_{P,i} \tag{3.11}$$

Net power of steam cycle then can be calculated as:

$$\dot{W}_{output} = \dot{W}_{T,total} - \dot{W}_{P,total} \tag{3.12}$$

3.1.4 Feedwater Heaters

The principle of energy conservation was adopted to determine heat transfer for each feedwater heater. The calculation lies on the principle that energy loss of hot stream is equal to energy gain of cold stream as shown below:

$$\sum_{i=1}^{m} (\dot{m}_i . h_i)_{in} = \sum_{i=1}^{n} (\dot{m}_i . h_i)_{out} \tag{3.13}$$

where $\dot{m}_i$ and h_i are mass flow rate and specific enthalpy of the stream i entering or leaving the heater.

3.1.5 Computational Step

It should be noted that this project follows the computational algorithm from the master's thesis "Monte Carlo simulation of pulverized coal-fired power plant: efficiency improvement and CO_2 capture options" (Sanpasertparnich, 2007). The developed model was calculated through the computational steps as illustrated in Figure 3.2.

The simulation started with the input of operating conditions and design parameters of the cycle including coal compositions, percent excess air, net power output, temperature and pressure of operating components (boiler, turbines, air preheater, condenser, and FWHs), pressure drop across the boiler and FWHs, and efficiency of process components (boiler, turbines, and feedwater pumps). After the input step, the calculation was done simultaneously in parallel for the coal combustion and the steam cycle. For the coal combustion, the compositions of flue gas were calculated on the basis of chemical reactions as mentioned in the previous chapter. Then, the heat of combustion was calculated as along with the temperature of hot flue gas. For the steam cycle, the enthalpies of each stream corresponding to the identified operating conditions were first calculated by using the developed thermodynamic property equations. At this point, the work associated with the series of turbines and pumps can be estimated by using mass flow rate and the enthalpy of each section of stream. Such works can be determined by applying Equations (2.4) through (2.7). The net efficiency of the power station is the final result from the previous calculation, which is from the coal combustion and the steam cycle combining together. After this point, the simulation keeps repeating calculation until it reaches a specified iterations (10,000 runs).

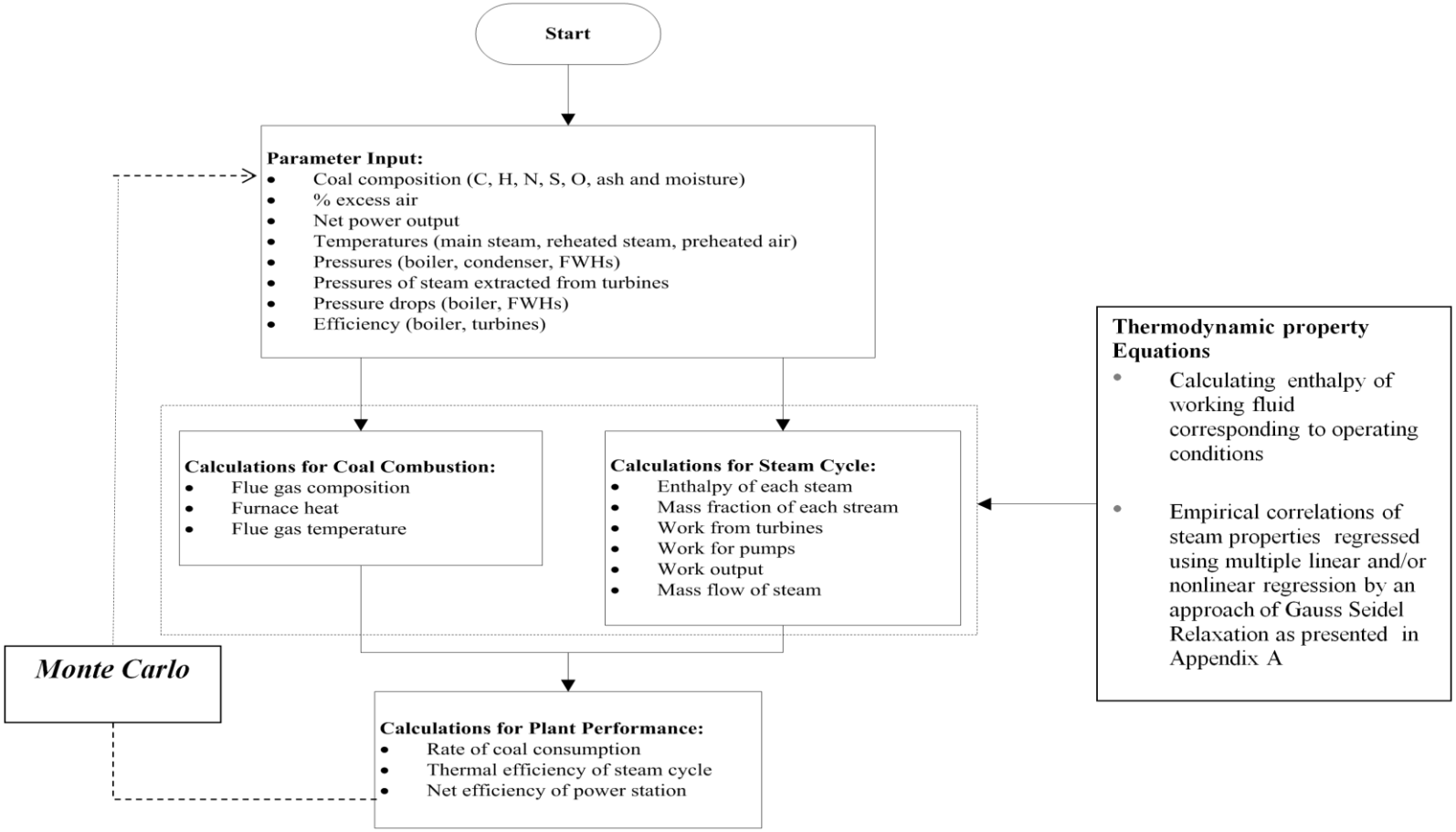

Figure 3.2: Computational algorithm of developed power plant model.

3.2 Thermodynamic Properties

As mentioned in the previous section, calculating performance of individual process components requires information on thermodynamic properties of working fluid including enthalpy (*h*), entropy (*s*), and specific volume (*v*). In this study, a series of empirical equations was developed for thermodynamic properties of steam presented as a function of temperature and pressure. The general thermodynamic equations can be written as:

$$h = f(T, P) = (a_1 + a_2 T^{-1} + a_3 T + a_4 T^2 + a_5 T^3 + a_6 T^4 + a_7 T^5 + a_8 T^6 + a_9 \ln T + a_{10} e^T) + (b_1 + b_2 P^{-1} + b_3 P + b_4 P^2 + b_5 P^3 + b_6 P^4 + b_7 P^5 + b_8 P^6 + b_9 \ln P + b_{10} e^P) \quad (3.14)$$

$$s = f(T, P) = (a_1 + a_2 T^{-1} + a_3 T + a_4 T^2 + a_5 T^3 + a_6 T^4 + a_7 T^5 + a_8 T^6 + a_9 \ln T + a_{10} e^T) + (b_1 + b_2 P^{-1} + b_3 P + b_4 P^2 + b_5 P^3 + b_6 P^4 + b_7 P^5 + b_8 P^6 + b_9 \ln P + b_{10} e^P) \quad (3.15)$$

$$v = f(T, P) = (a_1 + a_2 T^{-1} + a_3 T + a_4 T^2 + a_5 T^3 + a_6 T^4 + a_7 T^5 + a_8 T^6 + a_9 \ln T + a_{10} e^T) + (b_1 + b_2 P^{-1} + b_3 P + b_4 P^2 + b_5 P^3 + b_6 P^4 + b_7 P^5 + b_8 P^6 + b_9 \ln P + b_{10} e^P) \quad (3.16)$$

where *T*, *P*, *h*, *s*, and *v* denote temperature, pressure, enthalpy, entropy, and specific volume, respectively. The coefficients a_1, a_2, a_3, ..., a_{10} and b_1, b_2, b_3, ..., b_{10} are the exact values obtained from multiple linear/non-linear regression.

To obtain such coefficients, the multiple regression was carried out by using MATLAB® incorporated with Gauss Seidel Relaxation technique.

3.2.1 Development of Steam Properties Equations

The related numerical technique adopted in this research is called Gauss Seidel Relaxation. The Gauss Seidel Relaxation approach is a widely used iterative method in which problems obtain simultaneously values satisfying a set of equations (Chapra and Canale, 2007). This iterative method is used to improve a speed of convergence rate and offers round-of-errors control. It is also capable of solving a problem system of multiple linear and/or non-linear equations with several hundred variables involved. To explain the general concept of this method, assume, for example, that a set of *n* equations is given as below:

$$Ax = b \tag{3.17}$$

For simplification, a 3x3 matrix is used as a set of example equations. Assume that the diagonal elements are all nonzero; then, this equation can be rewritten for each unknown. The following three equations can be solved for x_1, x_2, and x_3, respectively:

$$x_1 = \frac{b_1 - a_{12}x_2 - a_{13}x_3}{a_{11}} \tag{3.18}$$

$$x_2 = \frac{b_2 - a_{21}x_1 - a_{23}x_3}{a_{22}} \tag{3.19}$$

$$x_3 = \frac{b_3 - a_{31}x_1 - a_{32}x_2}{a_{33}} \tag{3.20}$$

An initial guess is chosen for x_i to start the calculation of the iterative method. The initial guesses of x_1, x_2, and x_3 are set to zero. These initial values can be substituted into Equation (3.18), which can be used to calculate a new value for $x_1 = b_1 / a_{11}$. Then, immediately substituting this new value of x_1 along with the previous guess of zero for x_3 into Equation (3.19) can compute a new value for x_2. Finally, inserting the new values of x_1 and x_2 into Equation (3.20) is used to calculate a new estimate for x_3. Then, the entire procedure is repeated with the most recent values until the solution converges on the exact values. The following equation is used as a criterion to check convergence and stop the iteration:

$$\left|\varepsilon_{a,i}\right| = \left|\frac{x_i^{it} - x_i^{it-1}}{x_i^{it}}\right| 100\% < \varepsilon_s \tag{3.21}$$

for all $i = 1,\ldots,n$ where n is number of equations, it and $it-1$ are the current and previous iterations, $\left|\varepsilon_{a,i}\right|$ is the absolute relative error at each iteration, and ε_s is the specified tolerance for each unknown (Chapra and Canale, 2007). The approach of Gauss Seidel Relaxation was written in MATLAB® script to calculate the coefficients of the equation system for steam properties presented in the thermodynamics tables. The pseudo code of Gauss Seidel Relaxation is expressed in Appendix A.

a. Enthalpy function for table of saturated water-temperature (Table B1)

The empirical representation of enthalpy of liquid water and enthalpy of saturated steam (h_f and h_g respectively) are derived from temperature (T) as an independent parameter as presented in Appendix B. It should be noted that the developed properties equations representing individual states of working fluid offers error of less than 0.5% in this study. It was found that only one equation representing properties of individual states of working fluid is insufficient due to a large error since one equation cannot cover all possible values. Hence, to improve the accuracy of the steam properties function, each property needs to divide the possible range into sub-intervals. For instance, there are 6 sub-intervals representing the enthalpy of water (h_f) presented in Table B1, which are $0.01 \leq T \leq 200$, $205 \leq T \leq 230$, $235 \leq T \leq 280$, $285 \leq T \leq 330$, $340 \leq T \leq 370$, and $T = 374.14$, respectively. The following two equations are examples of equations at some interval of interest.

Example: if T = 275°C,

$$h_f = 1.37462 \cdot T + 0.00689755 \cdot T^2 + 310.625; \quad 235 \leq T \leq 280$$

$$h_g = -0.444752 \cdot T - 0.00211279 \cdot T^2 - (5.88515 \cdot 10^{-133}) \cdot e^T + 3072.59; \quad 275 \leq T \leq 305$$

where

h_f is enthalpy of water (kJ/kg)

h_g is enthalpy of saturated steam (kJ/kg)

T is Temperature (˚C)

Note

1. The figures represent the comparison between the results obtained from Gauss Seidel Relaxation and the actual values from the thermodynamic tables as given in Appendix B.

2. The equations representing h_f and h_g of Table B1 offer average errors of approximately 0.06% and 0.02%, respectively.

3. As shown in the figures of enthalpy in Appendix B (both h_f and h_g), most calculated values fit perfectly to the actual values except for a few. Thus, the equations obtained from Gauss Seidel Relaxation are well represented.

b. Enthalpy function for table of saturated water-pressure (Table B2)

The equations representing enthalpy of water and enthalpy of saturated steam (h_f and h_g respectively) are derived from pressure (P) as an independent parameter. There are 10 sub-intervals representing for the enthalpy of water (h_f) and 6 sub-intervals representing for the enthalpy of saturated steam (h_g) presented in Table A2 in Appendix B. The following two equations are example of equations at some interval of interest.

Example, if P = 0.75 MPa

$$h_f = -143.75+3923.04 \cdot P-7327.5 \cdot P^2+6295.25 \cdot P^3-1974.24 \cdot P^4;\ 0.375 \leq P \leq 0.85$$

$$h_g = 2715.31+68.8396 \cdot P;\ 0.35 \leq P \leq 0.9$$

where

h_f is enthalpy of water (kJ/kg)

h_g is enthalpy of saturated steam (kJ/kg)

P is pressure (MPa)

Note

1. The figures represent the comparison between the result obtained from Gauss Seidel Relaxation and the actual values from the Thermodynamics textbook are given in Appendix B.

2. Equations representing stream properties corresponding to pressure on Table B2 giving error of 0.5% or lesser are acceptable.

3. The equations representing h_f and h_g of Table B2 offers average error of 0.58% and 0.42% respectively. This means that, this table (Table B2) probably needs improvement or other approach to reduce error coming with the developed equations.

A correlative function of pressure (MPa) and temperature (˚C) is introduced to estimate enthalpy saturated water (both h_f and h_g). It helps reducing error from the developed equations representing enthalpy on Table B3. The calculation of enthalpy where only pressure is known follows these steps. Firstly, convert pressure value to temperature by using the correlative function. Then, calculate the enthalpy by using the equation obtained from table A4 where temperature is independent variable. The figure and equations represent the comparison between the result obtained from Gauss Seidel Relaxation and the actual values from the Thermodynamics handbook are given in Appendix B under Table B3: A correlative function of pressure (MPa) and temperature (˚C). This correlation approach gives average relative error of 0.19%.

c. Enthalpy function for table of superheated water (Table B4)

There are two independent variables which are pressure and temperature (*P* and *T* respectively). Each pressure has its own equation to represent stream properties by various temperatures. To make it convenient for user, the idea of grouping generic pressure is applied by trial error. During a simulation, pressures of 0.01 to 35.00 MPa were selected in this study to formulate equations presented in Table B4 as shown in Appendix B. These equations representing enthalpy on Table B4 offers an average error of 0.32%. However, some pressure such as 6.0, 12.5, 15.0, 17.5, 20.0, 25.0, 30.0 and 35.0 MPa cannot be grouped with others pressure since those pressures have different distributions of properties.

Example, if P = 2.1 MPa and T can be any

$$h = ((0.0222183 \cdot P - 0.0197727 \cdot P^2 + 0.00670717 \cdot P^3 + 0.0000350044 \cdot P^4 + 1.87467) \cdot T) + ((0.000619653 \cdot P - 0.0002618 \cdot P^2 + 0.0000346639 \cdot P^3 - 0.000170446) \cdot T^2) + (-14.8665 \cdot P - 3.30784 \cdot P^2 + 2490.39); \; 1.8 \leq P \leq 2.5$$

Where

h is enthalpy of water (kJ/kg)

P is pressure (MPa)

T is temperature (˚C)

3.3 Sensitivity Analysis and Performance Optimization

Since a model used in this study is composed of the uncertainty of input parameters e.g., main steam temperature and pressure, 1st reheating temperature, VHP inlet pressure, pressure extracted at different stage of individual turbine, turbine efficiency, boiler efficiency, coal moisture content, booster pump outlet pressure, percentage of excess air, pressure at deaerator, preheated air temperature, condensate temperature and pressure drop across boiler and FWHs. Sensitivity analysis is introduced to identify how individual input parameters impact to simulation result particularly on the net plant efficiency by parametric study approach. The operating parameters for the parametric study were selected from the sensitivity chart which was carried out by Monte Carlo simulation. It helps identifying the most significant input parameters and screening out the unimportant before using them for further analysis. Thus, accurate result and less time consuming in simulation. The simulation result was carried out by applying Monte Carlo simulation in which its concept is to construct set of parameters which is used to simulate the model output by randomly selecting values for all input parameters following their given probability distributions. Note that this random-approach simulation was repeated calculation for a number of trials (10,000 in this study). This number of runs was chosen due to capability to provide the optimum output of the pulverized coal-fired power plant (Risso et al., 2011; Srikanta, 1998). The following subsections are denoted for the general description of the Monte Carlo simulation and the parametric study.

3.3.1 Monte Carlo Simulation

The Monte Carlo simulation is a stochastic method based on a basis of risk analysis. Its general idea is to randomly generate sample of input parameters from underlying probability functions to perform simulation. Typically, this randomized method is used for a complex model involving many inherent uncertainties in input variables in order to examine the behaviour of output values under various scenarios or the uncertainty of input parameters. The Monte Carlo simulation then performs after the values were selected from the various probability distributions as shown as Table 3.1 and recalculate the spreadsheet for 10,000 runs. The Crystal Ball® software is incorporated to the Microsoft® Excel spreadsheet to calculate the probability distribution functions and it is used to carry out the Monte Carlo simulation result. This work also provides the sensitivity analysis result obtained from the Monte Carlo simulation where this result is then used for parametric study as shown in Figure 3.3.

3.3.2 Rank Correlation Coefficient

The Crystal Ball® software is selected to perform sensitivity analysis by using an approach of rank correlation coefficient. This approach is a statistical method that is widely used to assess the significance of correlation of paired variables (Cohen, 1988). The advantage of this method is its capability to apply to any types of the input distributions (e.g. beta distribution). The correlation coefficients are ranked in values between -1 to 1. The following equation is used to calculate rank coefficient (r) for individual input parameter.

$$r = \frac{n\sum_{i=1}^{n} x_i y_i - \sum_{i=1}^{n} x_i \sum_{i=1}^{n} y_i}{\sqrt{n\sum_{i=1}^{n} x_i^2 - \left(\sum_{i=1}^{n} x_i\right)^2}.\sqrt{n\sum_{i=1}^{n} y_i^2 - \left(\sum_{i=1}^{n} y_i\right)^2}} \quad (3.22)$$

where x_i and y_i denote a pair of input and output parameters, and n represents the number of paired rank in a sample.

3.3.3 Parametric study

To gain insight into the nature of the model, the results obtained from the sensitivity analysis were used for a parametric study. This helped investigate how each input variable impacts net efficiency. A Monte Carlo simulation package that generates output by selecting the values randomly for all input parameters was performed to carry out a sensitivity chart. The result given by the sensitivity chart represents how individual parameters react toward the model output. The simulation not only provides the sensitivity chart but also generates the range of minimum-maximum output, which can be used to identify the optimal solution for operating and process parameters. In order to perform the parametric study, a number of trials were required for simulating the result to be considered significant. This study applied a total of 10,000 runs to generate the output representing sufficient stability (Srikanta, 1998), thereby providing more accuracy.

It should be noted that this work was simulated under ultra-supercritical conditions with 30.7 MPa/600°C/600°C/600°C (double reheating system). The results obtained from the sensitivity analysis were obtained using an approach of rank coefficient from the Monte Carlo simulation package. Figure 3.3 presents the most significant operating input parameters from the sensitivity analysis in terms of impact on the net

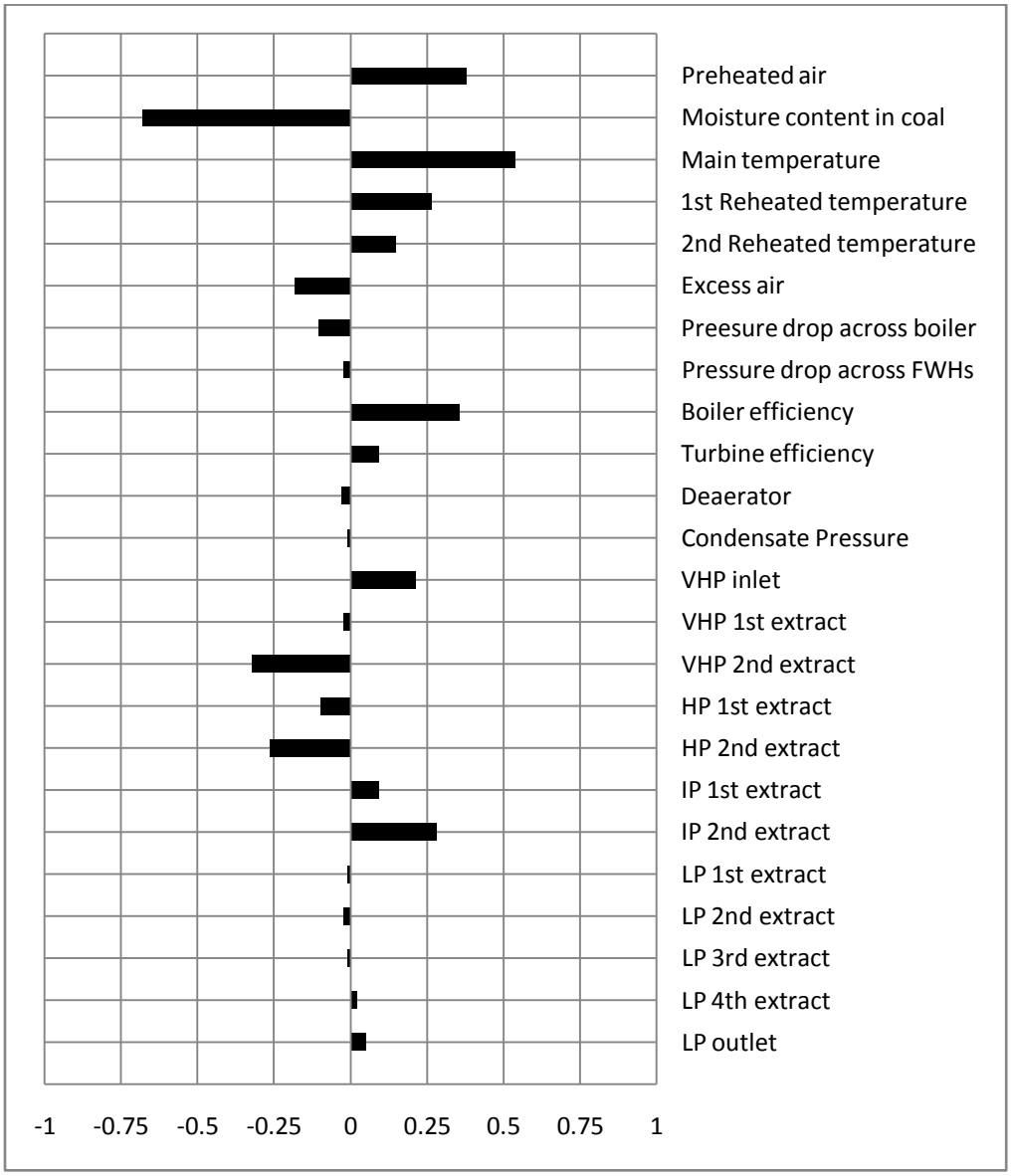

Figure 3.3: Results from sensitivity analysis using the approach of rank correlation coefficient.

efficiency. It was found that the sensitivity chart was ranked between -1 to 1. The value of the rank correlation coefficient shows how the operating parameter has a significant impact on the net efficiency. The higher the correlation coefficient, the greater the sensitivity of the input parameter. A positive coefficient indicates that an increase in the operating parameter influenced an improvement of net efficiency while a negative coefficient implies the opposite effect.

The results obtained from this section only give an idea of the most influential parameters that provide the largest contributions to the model output, particularly the net efficiency. It is then used in further analysis presented in the following chapter.

3.3.4 Simulation Scenario

The range of input parameters to simulate the scenarios is considerably significant. The steam cycle of the power plant is operated under ultra-supercritical conditions. The range of input parameters used for the sensitivity analysis is provided in Table 3.1. The range of process parameters is highlighted as follow:

- Pressure of main steam controlled by pressure of the boiler feed pump was varied in a range of 30.7-33.6 MPa (U.S.DOE, 1999; Feng, 2008 and Asthana and Panigrahi, 2008).

- The range of temperature of main steam and reheat steam is about 566 - 650˚C according to the material available for such new technology (U.S.DOE, 1999; Feng, 2008 and Asthana and Panigrahi, 2008).

- The different temperatures of components in the boiler are in the range of 5-10˚C (Chattopadhyay 2000 and VGB Powertech and Evonik Energy Services, 2008).
- Backpressure in the condenser is within the range of 5-8 kPa. (U.S.DOE, 1999; Booras and Holt, 2004; and Feng, 2008)
- Pressure drop across the boiler is identified in the range of 7 – 10% (IEA, 2007).
- Pressure drop across the feedwater heaters is varied in the range of 3-6% (Drbal et al., 1996)
- Moisture content in coal is identified in the range of 11.1-17.6 % by weight (U.S.DOE, 1999)

Note that the distributions for input parameters are required during Monte Carlo Simulation. This study follows the assumptions for the distribution of individual parameters as reported in Sanpasertparnich (2007). Table 3.1 also presents the type of distribution for this study used during the simulation. The ranges of significant input parameters were obtained from published research studies (i.e., boiler pressure, main steam temperature, 1^{st} reheated steam temperature, 2^{nd} reheated steam temperature). (Refer to Appendix C).

Table 3.1: Main input for ultra-supercritical power plant.

Point	Pressure (Mpa)		Temperature (°C)		Distribution	References
	Min	Max	Min	Max		
For ultra-supercritical PC shown in Figure 1						
A	0.006	0.008	37.59	41.15	Uniform Distribution	[1], [2], [3], [4], [5]
B	1.83	2.321	33.34	42.83	Uniform Distribution	[1], [2], [6]
C	1.05	1.27	190.44	190.55	Uniform Distribution	[1], [2], [6]
D	6.21	8.58	195.01	195.12	Uniform Distribution	[1], [2], [6]
E	33.47	35.00	266.7	277.36	Uniform Distribution	[2], [3], [4], [7], [8], [9]
F	30.12	31.39	566.0	650.0	Uniform Distribution for pressure, and Beta Distribution for temperature (minimum, maximum, alpha, beta) = (566.0, 650.0, 2.0, 3.0)	[2], [3], [4], [7], [8], [9]
G	11.52	12.43	443.45	480.80	Uniform Distribution	[2], [3], [4], [8], [9], [10]
H	8.37	8.93	349.28	429.79	Uniform Distribution	[2], [3], [4], [8], [9], [10]
I	8.21	8.66	566.0	600.0	Beta Distribution (minimum, maximum, alpha, beta) = (566.0, 600.0, 2.0, 3.0)	[2], [3], [7], [9]
J	3.86	6.32	483.33	541.82	Uniform Distribution	[2], [3], [4], [10]
K	3.11	4.29	374.83	453.42	Uniform Distribution	[2], [3], [4], [10]

Table 3.1: Main input for ultra-supercritical power plant**.** (continued).

Point	Pressure (Mpa)		Temperature (°C)		Distribution	References
	Min	Max	Min	Max		
For ultra-supercritical PC shown in Figure 1						
L	2.78	3.07	566.0	600.0	Beta Distribution (minimum, maximum, alpha, beta) = (566.0, 600.0, 2.0, 3.0)	[2], [3], [7], [9]
M	1.23	1.37	454.67	486.95	Uniform Distribution	[2], [3], [4], [10]
N,O	0.52	0.65	330.46	371.83	Uniform Distribution	[2], [3], [4], [10]
P	0.305	0.411	257.15	263.07	Uniform Distribution	[2], [3], [4], [10]
Q	0.092	0.128	126.77	131.48	Uniform Distribution	[2], [3], [4], [10]
R	0.041	0.074	79.38	93.57	Uniform Distribution	[2], [3], [4], [10]
S	0.026	0.039	68.81	78.01	Uniform Distribution	[2], [3], [4], [10]
T	0.006	0.008	37.59	41.15	Uniform Distribution	[1], [2], [3], [4], [5]
U	0.006	0.008	37.59	41.15	Uniform Distribution	[1], [2], [3], [4], [5]
V	0.103	-	25.0	25.0	Fixed	[6], [7]
W	0.103	-	250.0	350.0	Beta Distribution (minimum, maximum, alpha, beta) = (250.0, 350.0, 3.0, 3.0)	[1], [2], [6]
1	30.7	33.6	593.0	650.0	Uniform Distribution	[2]
2	8.3	8.8	392.8	402.2	Uniform Distribution	[2]
3,4,5	20.66	24.31	554.22	574.96	Uniform Distribution	[2]
6	2.83	3.56	566.0	600.0	Uniform Distribution	[2]

Table 3.1: Main input for ultra-supercritical power plant**.** (continued).

Miscellaneous significant parameters				
Description	**Min**	**Max**	**Distribution**	**References**
Coal consumption (ton/hr)	113.076	180.396	Uniform Distribution	[2]
Pressure drop across FWHs	3.0	6.0	Normal Distribution (4.5±1.5%)	[6], [11]
Pressure drop across boiler	7.0	10.0	Normal Distribution (8.5±1.5%)	[4], [6]
Excess air (%)	15.0	20.0	Beta Distribution (minimum, maximum, alpha, beta) = (15.0, 20.0, 3.0, 3.0)	[6]
Boiler efficiency (%)	90.0	94.0	Uniform Distribution	[3]
Turbine efficiency (%)	90.0	99.0	Uniform Distribution	[3], [5]
Free moisture in coal (%)	11.1	17.6	Beta Distribution (minimum, maximum, alpha, beta) = (11.12, 17.6, 3.0, 3.0)	[2], [6]

[1] Singer (1991)
[2] U.S.DOE (1999)
[3] Cao et al. (2007)
[4] Feng (2008)
[5] Asthana and Panigrahi (2008)
[6] Sanpasertparnich (2007)
[7] Chattopadhyay (2000)
[8] Wright et al. (2004)
[9] Kaneko (2004)
[10] Booras and Holt (2004)
[11] IEA (2007)

Chapter 4

Simulation Results and Discussion

This chapter contains the model validation as well as a discussion of a set of simulation results obtained from a pulverized coal-fired power generation plant operating under ultra-supercritical conditions. The maximum-minimum ranges of plant performance including thermal efficiency, net plant efficiency, power output, temperature at combustion zone, and temperature of exhausted flue gas are also provided in this chapter. Sensitivity analysis and parametric studies of individual process parameters are also discussed in detail through this chapter.

4.1 Model Validation

The model reported by the U.S.DOE (1999) was used as a prototype to construct a model of this study. It should be noted that this model was built for running an operation under ultra-supercritical conditions. To ensure this model is acceptable and could work properly, the models reported by the U.S.DOE (1999) and Sanpasertparnich (2007) were also used as references to validate the system by comparing the simulation results. The comparisons were made under the same process conditions including main steam and reheated steam temperature, extracted pressure at the series of turbines, type of coal used for combustion, pressure drop across the boiler and FWHs, preheating air temperature, and boiler and turbine efficiency. It should be noted that the U.S. DOE (1999) did not provide some significant operating parameters including preheating air temperature,

Table 4.1: Comparison of the simulation results between this study and published research (U.S. DOE, 1999 and Sanpasertparnich, 2007).

Description	**Case1 Ultra-supercritical conditions (This study -U.S. DOE, 1999)**		**Case2 Subcritical conditions (This study-Sanpasertparnich, 2007)**	
Coal type	Illinois #6		Illinois #6	
Net power output	397.5		336.0	
Boiler temperature (°C)	593		545	
1st Reheat temperature (°C)	593		545	
2nd Reheat temperature (°C)	593		-	
VHP turbine				
1st extracting pressure (MPa)	12.09		-	
2nd extracting pressure (MPa)	9.35		-	
HP turbine				
1st extracting pressure (MPa)	4.28		3.74	
2nd extracting pressure (MPa)	2.61		-	
IP turbine				
1st extracting pressure (MPa)	1.25		1.27	
2nd extracting pressure (MPa)	0.6		0.9	
LP turbine				
1st extracting pressure (MPa)	0.32		0.22	
2nd extracting pressure (MPa)	0.12		0.07	
3st extracting pressure (MPa)	0.070		0.031	
4nd extracting pressure (MPa)	0.034		0.006	
5st extracting pressure (MPa)	0.0069		-	
Discharge pressure of boiler feed pump (MPa)	34.96		20.57	
Discharge pressure of condensate pump (MPa)	2.32		1.83	
Preheating air temperature (°C)[2]	(250.0-350.0)		(250.0-350.0)	
% excess air[2]	(15.0-20.0)		(15.0-20.0)	
Pressure drop in FWHs (%)[2]	(3.0-6.0)		(3.0-6.0)	
Pressure drop in boiler (%)[2]	(9.0-10.0)		(9.0-10.0)	
Boiler efficiency (%)[2]	(90.0-94.0)		(90.0-92.0)	
Turbine efficiency (%)[2]	(90-99.0)		(90.0-92.0)	
Performance	U.S. DOE, 1999	This study	Sanpasertparnich, 2007	This study
Net efficiency (%)	39.8	39.0-42.9	34.6-38.1	34.1-38.3

[2] Values were assigned for simulation.

percentage of excess air, and efficiency of the boiler and turbine. However, this study assigned those parameters as a range to cover all possibilities. Therefore, the performance presented in Table 4.1 is shown as a range as well. The model validation was done on 2 cases as follows:

1. Compare the simulation results with U.S.DOE. (1999) under ultra-supercritical operating condition.
2. Compare the simulation results with Sanpasertparnich (2007) under subcritical operating condition.

According to Table 4.1, the error after comparison with those two cases were fallen in between a range of 1.9-7.8% with U.S.DOE.(1999) and 0.5-1.3% with Sanpasertparnich (2007). It is clear that the newly developed model is well representative of the system since the simulation results obtained from this study agree well with the two comparison cases.

4.2 Pilot Simulation Results

The validated model was used to compare only the tendencies of the simulation results with the published research (Sanpasertparnich, 2007). This section is intended to double check if the results obtained from this study showed similar trends as in the reported literature. The developed model operated at 25.34 MPa with 600°C/600°C and a back pressure of 5kPa. The highlights of the pilot simulation results are described as follows:

- The net efficiency can be improved by increasing either the temperature of the main steam or the reheating temperature as shown in Figure 4.1. Increasing the temperature of the main steam by 30°C results in an increase in net efficiency of 0.54% whereas net efficiency increases by about 0.50% in the literature, and the net efficiency can be improved by the same magnitude of about 0.53% by raising the temperature of the reheating steam by 48°C. This shows that this model offers the same magnitude and tendency of results as reported in the literature.
- The effect of turbine and boiler efficiency is illustrated in Figure 4.2. Apparently, this model offers an increase in turbine efficiency by 2% (from 90 to 92%) leading to enhancement of the net efficiency by 0.08% while the literature offers an improvement in net efficiency of 0.10% . Moreover, raising boiler efficiency by the same increment from 90 to 92% contributes to increases in net efficiency of 0.71% whereas net efficiency increased by 0.8% presented in the literature.
- The effect of excess air, shown in Figure 4.3can be ignored since increasing 3% in the excess air from 16 to 19% offers a slightly decrease in net efficiency by 0.03% which is exactly the same as 0.03% reported in the literature.
- The impact of preheating air temperature on net plant performance is demonstrated in Figure 4.4. To rise preheated air temperature by 80°C leads to an increase in net efficiency by 1% obtained from both this study and the literature.

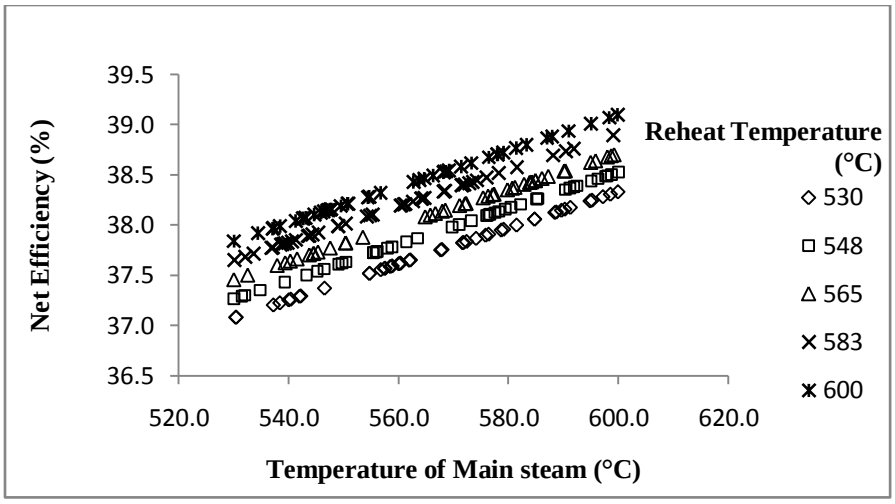

Figure 4.1: Effect of main steam temperature and reheat temperature[3].

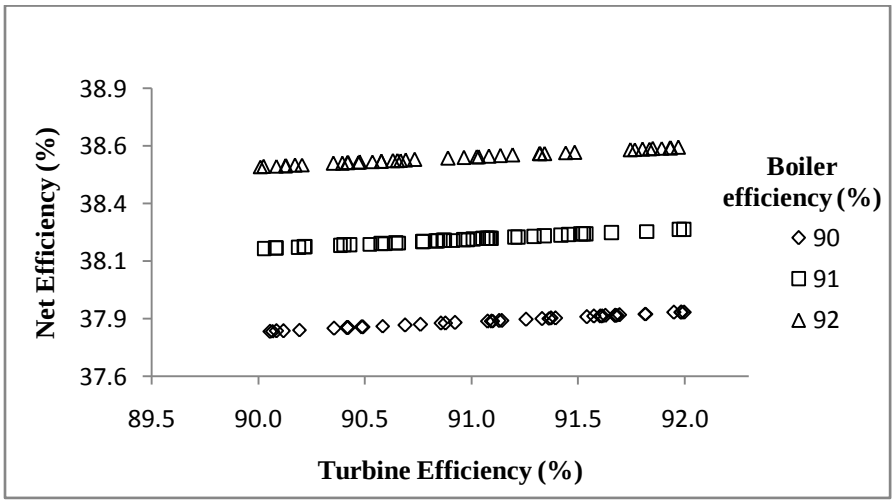

Figure 4.2: Effect of turbine and boiler efficiency[3].

[3] (Operating Condition: 600°C Main steam temperature, 600°C 1st Reheated steam temperature, 600°C 2nd Reheated steam temperature, 25.34 MPa HP inlet pressure, 5.5 MPa HP outlet pressure at 1st stage, 4.31 MPa HP outlet pressure at 2nd stage, 1.27 MPa IP outlet pressure at 1st stage, 0.9 MPa IP outlet pressure at 2nd stage, 0.223 MPa LP outlet pressure at 1st stage, 0.074 MPa LP outlet pressure at 2nd stage, 0.031 MPa LP outlet pressure at 3rd stage and 5 kPa backpressure)

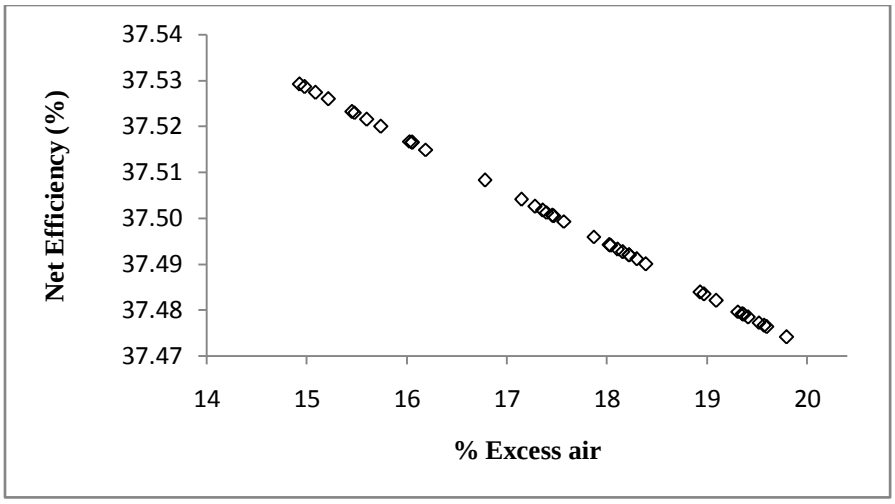

Figure 4.3: Effect of excess air[4]

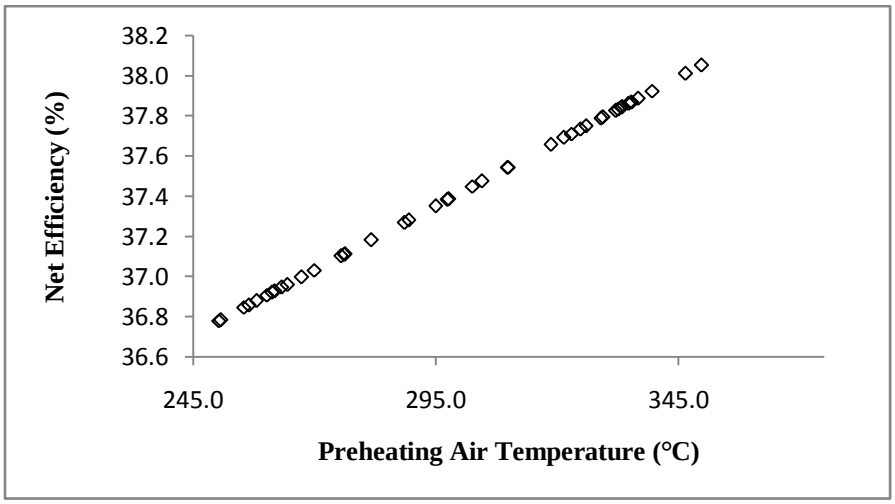

Figure 4.4: Effect of preheating air temperature[4]

[4] (Operating Condition: 600°C Main steam temperature, 600°C 1st Reheated steam temperature, 600°C 2nd Reheated steam temperature, 25.34 MPa HP inlet pressure, 5.5 MPa HP outlet pressure at 1st stage, 4.31 MPa HP outlet pressure at 2nd stage, 1.27 MPa IP outlet pressure at 1st stage, 0.9 MPa IP outlet pressure at 2nd stage, 0.223 MPa LP outlet pressure at 1st stage, 0.074 MPa LP outlet pressure at 2nd stage, 0.031 MPa LP outlet pressure at 3rd stage and 5 kPa backpressure)

According to the pilot study, the results obtained gave small variance compared to the results reported in the literature when all operating and process parameters are fixed with the same values. Thus, the simulation results obtained from this study offer the same trend and magnitude as presented in the literature (Sanpasertparnich, 2007). Therefore, the model is well validated.

4.3 Maximum-Minimum Ranges of Plant Performance

A summary of the maximum-minimum ranges of plant performance is illustrated in Table 4.2. All results in this subsection were generated through the Monte Carlo simulation in which all operating and process parameters including steam pressure and temperature, excess air, and coal moisture, etc., were randomly selected for each run of the simulation. The operating and process parameters were given in Table 2.5. It should be noted that the characteristics of Illinois #6 bituminous coal that were presented in Table 2.1 were selected for this process parameter in this study.

4.4 Parametric Studies on Plant Performance

This section reports the simulation results for individual parameters' affects on plant performance, which is the net plant efficiency in this case. The process parameters of interest in this section were obtained from the previous section. This study was conducted for only the parameters with the most significant effects on net plant efficiency as discussed above. These selected parameters include moisture content in coal,

Table 4.2: Maximum-minimum performance of ultra-supercritical pulverized coal-fired power plant.

Parameters	Range	
	Min.	**Max.**
Thermal efficiency (%)	46.33	56.60
Net efficiency (%HHV)	37.1	47.3
Net heat rate (kJ/kWh HHV)	812660	1081968
Coal consumption (kg/s)	26.39	42.27
Combustion zone temperature (°C)	1736	1917
% Flue gas composition CO_2; mole %	13.88	14.50
H_2O; mole %	6.97	7.12
N_2; mole %	74.99	75.42
O_2; mole %	2.67	3.21
SO_2, NO and others; mole %	0.49	0.52

preheated air temperature, main and reheated temperature, turbine and boiler efficiency, excess air and pressure drop across boiler and feedwater heaters, and pressure at different stages in a turbine series. For the purpose of parametric study, only one parameter of interest was changed each time and the rest were kept unchanged in order to examine the individual effects on the plant performance.

4.4.1 Effect of Moisture Content in Coal

Coal moisture content has a significant impact on plant performance. Figure 4.5 illustrates how reducing free moisture content in coal enhances net efficiency. Supplying high moisture content in coal apparently leads to the reverse effect on net efficiency. It was shown that the net plant efficiency increases by about 2.5% with a decrease in moisture content in coal from 17.72 to 11.24% regardless of the temperature of preheated air. It is obvious that the lower the moisture content in coal, the higher the net plant efficiency. This is because part of the heat released during the combustion process is withdrawn to vapourize the moisture content in wet supplied coal, resulting in a reduction in temperature of flue gas supplied to the steam cycle. This process leads to less energy available to generate steam in a boiler.

4.4.2 Effect of Preheating Air Temperature

Preheating incoming air prior to entering the furnace also helps improve the net efficiency of power generation due to an increase in the temperature of the air. There is some energy loss at the furnace from the exhausted flue gas, which is called the waste heat. This waste heat is recovered in an air preheater by transferring heat from the flue gas leaving the boiler to supplied air, reflecting an increase in air temperature for coal combustion. Hence, this rise in air temperature allows the combustion to proceed at a higher temperature, resulting in generation of higher quality steam. The relationship between net plant efficiency and preheating supplied air temperature is illustrated in Figure 4.5. The net efficiency increases in a linear manner due to an increase in supplied air corresponding to its preheating temperature regardless of coal moisture content. For every 100°C rise in preheated air temperature, an increase of net plant efficiency of about 1.3% occurs. However, the preheated air temperature must not exceed the limitations of the material used for air preheaters, which is not beyond 350°C (Singer, 1991; Chattopadhyay, 2000; Woodruff et al., 2005; Sanpasertpanich, 2007).

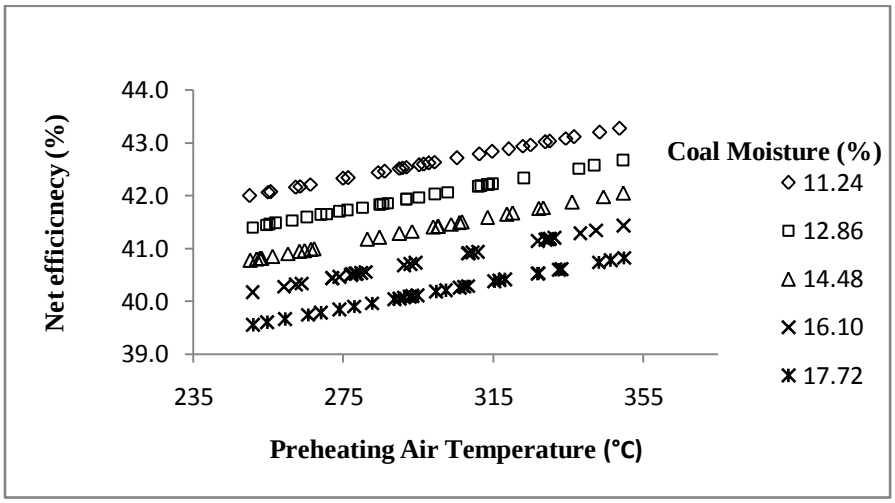

Figure 4.5: Effect of coal moisture content and temperature of preheating air[5].

[5] (Operating Condition: 600°C Main steam temperature, 600°C 1st Reheated steam temperature, 600°C 2nd Reheated steam temperature, 30.7 MPa VHP inlet pressure, 12.01 MPa VHP outlet pressure at 1st stage, 8.92 VHP outlet pressure at 2nd stage, 4.35 MPa HP outlet pressure at 1st stage, 2.84 MPa HP outlet pressure at 2nd stage, 1.26 MPa IP outlet pressure at 1st stage, 0.61 MPa IP outlet pressure at 2nd stage, 0.331 MPa LP outlet pressure at 1st stage, 0.121 MPa LP outlet pressure at 2nd stage, 0.072 MPa LP outlet pressure at 3rd stage, 0.036 MPa LP outlet pressure at 4th stage and 8 kPa backpressure)

4.4.3 Effect of Main Steam Temperature and 1st Reheating Temperature

Generally, achieving greater net plant efficiency can be done by an increase in superheated steam conditions before entering the turbine series. From a thermodynamic viewpoint, it is more effective to elevate the main stream pressure as well as the temperature of main and reheated steam. This concept reflects the higher enthalpy change (more energy) and greater electricity production in the generator attached to the series of turbines, respectively. However, pressure of 31.1 MPa was chosen and fixed during the simulation in this study due to its good representation of USC pressure for main steam and the available material used for USC technology (refer to Table 2.4). The improvement of net plant efficiency was obtained when increasing the temperature of either main or reheated steam of the power cycle. The results from this section are clearly illustrated in Figure 4.6. The net efficiency is improved by 0.54% by raising main steam temperature by 30°C whereas the net efficiency is enhanced by 0.27% by increasing the 1st reheating steam temperature by the same increment (30°C). The metallurgical restrictions of higher pressure and temperature of steam condition were taken into consideration since it could lead to significant problems with components such as the boiler and turbines. Hence, the elevated steam conditions of pressure and temperature of main steam and reheated steam have to meet this limitation to ensure that the result is accurate.

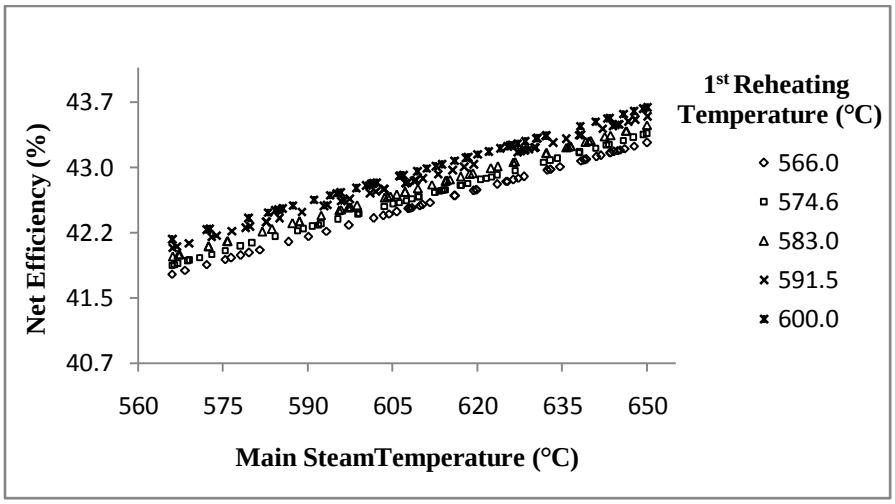

Figure 4.6: Effect of temperature of main steam and 1st reheated steam[6].

[6] (Operating Condition: 600°C Main steam temperature, 600°C 1st Reheated steam temperature, 600°C 2nd Reheated steam temperature, 30.7 MPa VHP inlet pressure, 12.01 MPa VHP outlet pressure at 1st stage, 8.92 VHP outlet pressure at 2nd stage, 4.35 MPa HP outlet pressure at 1st stage, 2.84 MPa HP outlet pressure at 2nd stage, 1.26 MPa IP outlet pressure at 1st stage, 0.61MPa IP outlet pressure at 2nd stage, 0.331 MPa LP outlet pressure at 1st stage, 0.121 MPa LP outlet pressure at 2nd stage, 0.072 MPa LP outlet pressure at 3rd stage, 0.036 MPa LP outlet pressure at 4th stage and 8 kPa backpressure)

4.4.4 Effect of Boiler and Turbine Efficiencies

Figure 4.7 illustrates the effect of turbine and boiler efficiency on the net plant performance. Increasing turbine efficiency from 90 to 94% can be achieve with a small improvement of net plant efficiency of about 0.17% whereas an increase in boiler efficiency of the same magnitude contributes to a rise in net plant efficiency of 1.42%. Thus, the efficiency of the turbine could then be negligible. It is clearly shown that the boiler efficiency has a significant impact on net plant efficiency greater than that of the turbine efficiency.

4.4.5 Effect of Excess Air Supply

A specific amount of excess air is required to ensure that the combustion is complete. The proper amount of supplied air varies by type of fuel. The optimal excess air for coal is in the range of 15-20%, which offers the highest efficiency. However, excess air supplied to coal combustion contributes to a negative impact on boiler efficiency, leading to a decrease in net plant efficiency. The reason for this behaviour is that when the amount of excess air is added to the boiler, the mass of flue gas is increased while traveling through the combustion zone resulting in high heat losses. This also leads to a reduction in temperature of flue gas available for the steam cycle, thereby offering less net plant efficiency. Figure 4.8 demonstrates the effect of the percent of excess air on net efficiency. It was found that a slight decrease in net efficiency by about 0.06% is influenced by an increase in percent excess air from 15 to 20%.

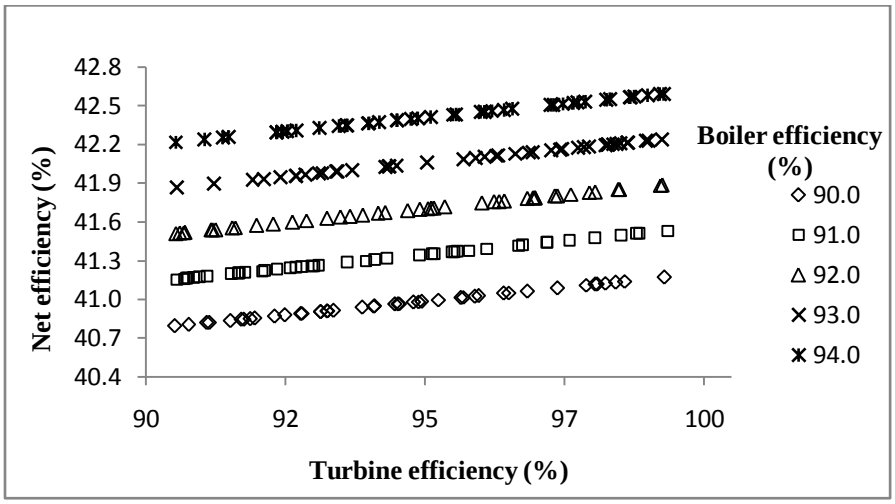

Figure 4.7: Effect of turbine and boiler efficiency[7].

[7] (Operating Condition: 600°C Main steam temperature, 600°C 1st Reheated steam temperature, 600°C 2nd Reheated steam temperature, 30.7 MPa VHP inlet pressure, 12.01 MPa VHP outlet pressure at 1st stage, 8.92 VHP outlet pressure at 2nd stage, 4.35 MPa HP outlet pressure at 1st stage, 2.84 MPa HP outlet pressure at 2nd stage, 1.26 MPa IP outlet pressure at 1st stage, 0.61 MPa IP outlet pressure at 2nd stage, 0.331 MPa LP outlet pressure at 1st stage, 0.121 MPa LP outlet pressure at 2nd stage, 0.072 MPa LP outlet pressure at 3rd stage, 0.036 MPa LP outlet pressure at 4th stage and 8 kPa backpressure)

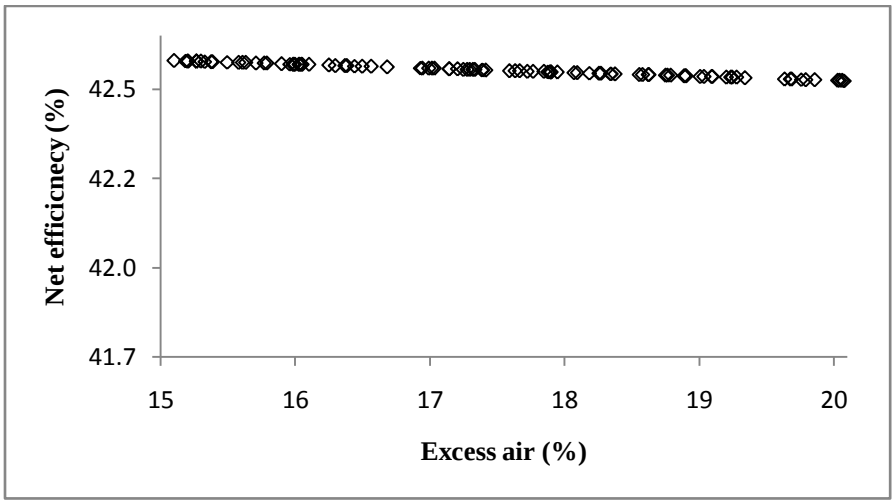

Figure 4.8 Effect of excess air for coal combustion[8].

[8] (Operating Condition: 600°C Main steam temperature, 600°C 1st Reheated steam temperature, 600°C 2nd Reheated steam temperature, 30.7 MPa VHP inlet pressure, 12.01 MPa VHP outlet pressure at 1st stage, 8.92 VHP outlet pressure at 2nd stage, 4.35 MPa HP outlet pressure at 1st stage, 2.84 MPa HP outlet pressure at 2nd stage, 1.26 MPa IP outlet pressure at 1st stage, 0.61 MPa IP outlet pressure at 2nd stage, 0.331 MPa LP outlet pressure at 1st stage, 0.121MPa LP outlet pressure at 2nd stage, 0.072 MPa LP outlet pressure at 3rd stage, 0.036 MPa LP outlet pressure at 4th stage and 8 kPa backpressure)

4.4.6 Effect of Pressure Drop across Boiler and FWH_s

The enthalpy of steam is associated with both temperature and pressure of steam. It is well known that the higher the pressure drop, the greater the loss of quantity of steam. This causes a reduction in plant performance. Figure 4.9 illustrates the effect of pressure drop across the boiler and FWH_s, influencing the net efficiency. As can be seen from the figure, the pressure drop across FWH_s is relatively insignificant since it gives a very small change in net efficiency whereas the pressure drop in the boiler contributes more. Apparently, lowering the pressure drop across the boiler between 10 to 7 % helps improve the net plant efficiency by about 0.34%.

4.4.7 Effect of Pressure Distribution in the Turbine Series

It is widely known that there are two approaches to achieving high performance of a steam cycle, which are either raising turbine inlet pressure or lowing turbine outlet pressure. These two approaches imply that the steam pressure at different stages in the turbine series has potentially significant impacts on power plant performance. The term **Pressure Ratio** is adopted in this section and used as an indicator to represent the differences between two pressure boundaries at individual turbines. It is derived from a ratio of turbine inlet and outlet pressure. The following subsections are dedicated to demonstrating the effect of such pressures at each individual turbine, particularly the outlet pressure at the VHP turbine, the 1^{st} stage extract and the outlet pressure at the HP turbine, the 1^{st} stage extract and the outlet pressure at the IP turbine, and the outlet pressure at the LP turbine, respectively.

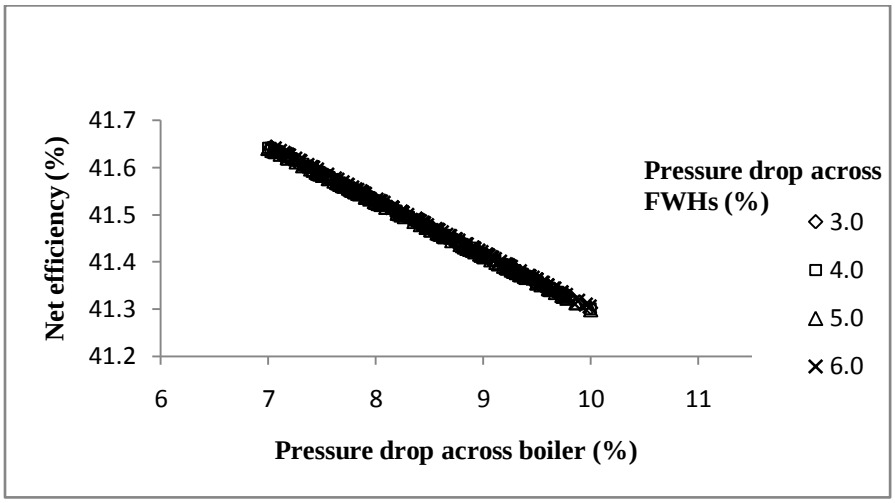

Figure 4.9: Effect of pressure drop across boiler and FWH_s[9].

[9] (Operating Condition: 600°C Main steam temperature, 600°C 1st Reheated steam temperature, 600°C 2nd Reheated steam temperature, 30.7 MPa VHP inlet pressure, 12.01 MPa VHP outlet pressure at 1st stage, 8.92 VHP outlet pressure at 2nd stage, 4.35 MPa HP outlet pressure at 1st stage, 2.84 MPa HP outlet pressure at 2nd stage, 1.26 MPa IP outlet pressure at 1st stage, 0.61 MPa IP outlet pressure at 2nd stage, 0.331 MPa LP outlet pressure at 1st stage, 0.121 MPa LP outlet pressure at 2nd stage, 0.072 MPa LP outlet pressure at 3rd stage, 0.036 MPa LP outlet pressure at 4th stage and 8 kPa backpressure)

a. Pressure of VHP Turbine

Figure 4.10 represents the effect of pressure ratio at the 2nd stage outlet in the VHP turbine on the net plant efficiency. It is shown that a reduction of the VHP outlet pressure reflects an efficiency improvement. According to Figure 4.10, reducing the outlet pressure from 8.93 to 8.51 MPa helps enhance the efficiency by about 0.20%. Regardless of its positive impact, however, lowering the outlet pressure below a specific point (8.51 MPa) could lead to a decrease in net efficiency. According to the power plant model shown in Figure 3.1, an amount of steam extracted at different stages in the turbine is used to transfer heat to the feedwater heaters. Reducing the pressure by extracting steam beyond the optimal point causes a decreased temperature of the feedwater heater. Consequently, the efficiency of the power plant declines.

Moreover, raising the pressure ratio or inlet pressure apparently causes the efficiency to slightly increase. This is because there is a greater amount of enthalpy change for power generation at the higher inlet pressure. Thus, offering an increase in net plant efficiency. It should be noted that this subsection examines the impact of the change in VHP inlet and outlet pressure on net efficiency. Therefore, only VHP inlet and outlet pressure are considered as main parameters, and all of the operating and process parameters were fixed constant. Increasing the inlet pressure from 30.12 to 31.39 MPa by raising the pressure ratio from 3.50 to 3.65 with the VHP outlet pressure constant at 8.65 MPa contributes to a slight reduction in the net efficiency by about 0.05%. This is because more workload is added to the boiler feed pump.

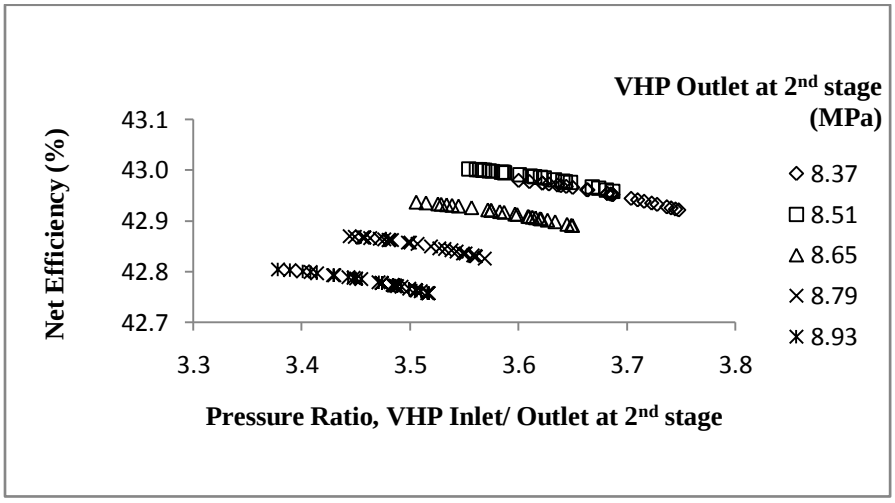

Figure 4.10: Effect of extract pressure at the 2nd stage of VHP turbine [10].

[10] (Operating Condition: 600°C Main steam temperature, 600°C 1st Reheated steam temperature, 600°C 2nd Reheated steam temperature, 30.7 MPa VHP inlet pressure, 12.01 MPa VHP outlet pressure at 1st stage, varying VHP outlet pressure at 2nd stage, 4.35 MPa HP outlet pressure at 1st stage, 2.84 MPa HP outlet pressure at 2nd stage, 1.26 MPa IP outlet pressure at 1st stage, 0.61 MPa IP outlet pressure at 2nd stage, 0.331 MPa LP outlet pressure at 1st stage, 0.121 MPa LP outlet pressure at 2nd stage, 0.072 MPa LP outlet pressure at 3rd stage, 0.036 MPa LP outlet pressure at 4th stage and 8 kPa backpressure)

b. Pressure of HP Turbine

Figure 4.11 and Figure 4.12 illustrate the effect of steam pressure extracted at the 1st and 2nd stages in the HP turbine. Both figures indicate that increasing pressure ratio leads to increased efficiency. According to Figure 4.11, increasing the pressure ratio of the HP turbine or raising the HP inlet pressure from 1.29 to 1.93 MPa leads to an improvement of net efficiency. This is because at a high inlet pressure, there is more energy available for operating high quality steam, thereby offering an increase in net plant efficiency. Similarly, increasing pressure ratio from 1.90 to 2.54, as shown in Figure 4.12, causes an increase in the net efficiency that gradually reduces at certain level. However, at a constant outlet pressure, increasing the pressure ratio in the HP turbine offers the reverse contribution to the net efficiency due to the increased work load added to the booster pump. Figure 4.11 shows that fixing the HP outlet pressure at 5.09 MPa and raising the HP inlet pressure from 8.21 to 8.66 MPa by increasing in pressure ratio from 1.60 to 1.70 leads to a reduction in net efficiency by about 0.04%.

Moreover, to achieve higher efficiency, the HP outlet pressure needs to be reduced. Figure 4.11 shows that lowering the outlet pressure from 6.32 to 4.48 MPa causes an improvement in the net efficiency of up to 0.53% whereas reducing the outlet pressure from 4.30 to 3.40 MPa, as in Figure 4.12, results in an improvement of the net efficiency by about 0.2%. Regardless of its positive effect, however, decreasing the 2nd outlet pressure at the HP turbine to a value lower than 3.40 MPa (optimum) leads to a reduction in the net efficiency due to the drop in temperature of the feedwater heater as discussion in the previous subsection (refer to **a**).

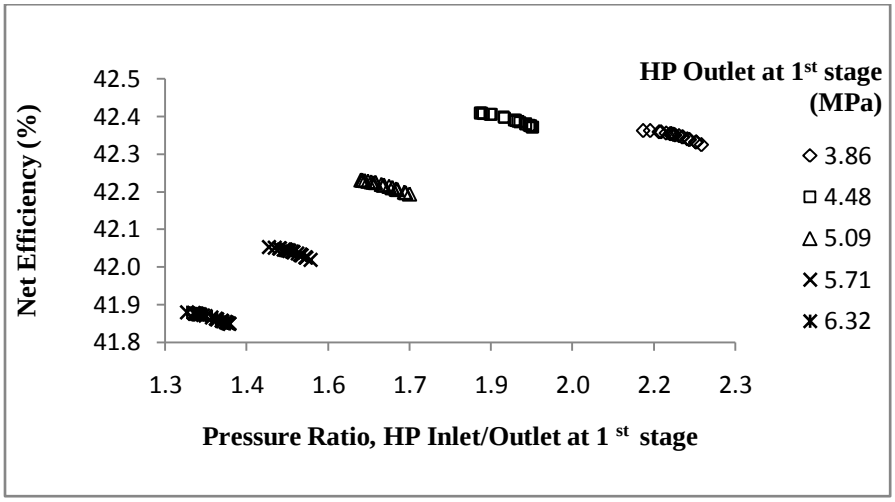

Figure 4.11: Effect of extract pressure at the 1st stage of HP turbine[11].

[11] (Operating Condition: 600°C Main steam temperature, 600°C 1st Reheated steam temperature, 600°C 2nd Reheated steam temperature, 30.7 MPa VHP inlet pressure, 12.01 MPa VHP outlet pressure at 1st stage, 8.92 MPa VHP outlet pressure at 2nd stage, varying HP outlet pressure at 1st stage, 2.84 MPa HP outlet pressure at 2nd stage, 1.26 MPa IP outlet pressure at 1st stage, 0.61 MPa IP outlet pressure at 2nd stage, 0.331 MPa LP outlet pressure at 1st stage, 0.121 MPa LP outlet pressure at 2nd stage, 0.072 MPa LP outlet pressure at 3rd stage , 0.036 MPa LP outlet pressure at 4th stage and 8 kPa backpressure)

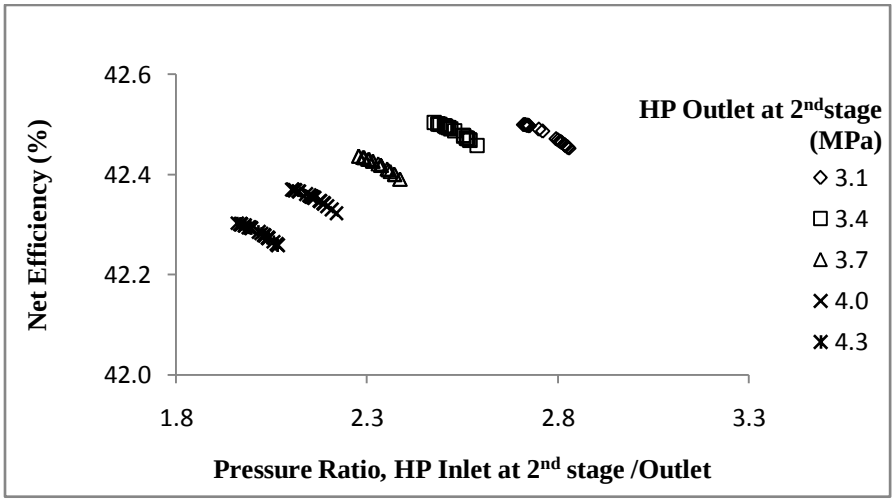

Figure 4.12: Effect of extract pressure at the 2nd stage of HP turbine[12].

[12](Operating Condition: 600°C Main steam temperature, 600°C 1st Reheated steam temperature, 600°C 2nd Reheated steam temperature, 30.7 MPa VHP inlet pressure, 12.01 MPa VHP outlet pressure at 1st stage, 8.92 MPa VHP outlet pressure at 2nd stage, 4.35 MPa HP outlet pressure at 1st stage, varying HP outlet pressure at 2nd stage, 1.26 MPa IP outlet pressure at 1st stage, 0.61 MPa IP outlet pressure at 2nd stage, 0.331 MPa LP outlet pressure at 1st stage, 0.121 MPa LP outlet pressure at 2nd stage, 0.072 MPa LP outlet pressure at 3rd stage , 0.036 MPa LP outlet pressure at 4th stage and 8 kPa backpressure)

c. Pressure of IP Turbine

The effect of steam pressure extracted at different stages of IP turbines is also presented in Figure 4.13 and Figure 4.14. Note that reducing the pressure ratio can be achieved by either decreasing the inlet pressure or increasing the outlet pressure. From Figure 4.13, it is clearly seen that a reduction in the pressure ratio contributes to an improvement of the net efficiency. For instance, at a constant outlet pressure of 1.23 MPa, the net efficiency is increased by about 0.66% by decreasing the pressure ratio from 2.48 to 2.29. This could happen since a connection between IP inlet pressure and HP outlet pressure. Based on the configuration of the power plant shown in Figure 2.4, the HP outlet pressure is extracted to drive the IP turbine, meaning that the higher IP inlet pressure, the greater HP exhausting pressure, resulting in a reduction in the net efficiency. However, lowering the pressure ratio below an optimum point results in a slight reduction in the net efficiency. This can be seen from Figure 4.13; by keeping the HP outlet pressure fixed at 1.23 MPa, increasing the IP inlet pressure influences a slight reduction in the net efficiency due to more work load (refer to **b**).

Furthermore, increasing the pressure ratio by decreasing the outlet pressure leaving the IP turbine leads to a negative impact on the net efficiency. From Figure 4.13, decreasing IP outlet pressure at the 1^{st} stage from 1.37 to 1.23 MPa leads to a reduction in net efficiency by 1.08%. Similarly, Figure 4.14 shows that the net efficiency drops about 2.15% by reducing the IP outlet pressure at the 2^{nd} stage from 0.63 to 0.52 MPa.

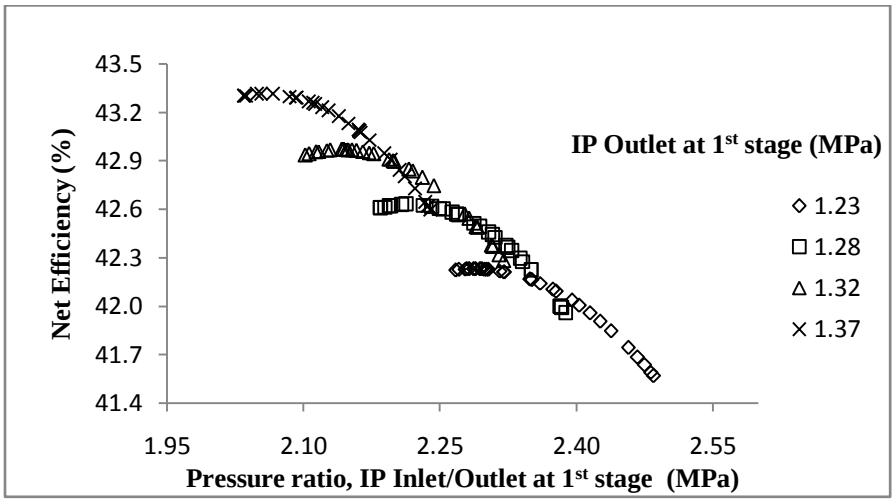

Figure 4.13: Effect of extract pressure at the 1st stage of IP turbine[13].

[13] (Operating Condition: 600°C Main steam temperature, 600°C 1st Reheated steam temperature, 600°C 2nd Reheated steam temperature, 30.7 MPa VHP inlet pressure, 12.01 MPa VHP outlet pressure at 1st stage, 8.92 MPa VHP outlet pressure at 2nd stage, 4.35 MPa HP outlet pressure at 1st stage, 2.84 MPa HP outlet pressure at 2nd stage, varying IP outlet pressure at 1st stage, 0.61 MPa IP outlet pressure at 2nd stage, 0.331 MPa LP outlet pressure at 1st stage, 0.121 MPa LP outlet pressure at 2nd stage, 0.072 MPa LP outlet pressure at 3rd stage, 0.036 MPa LP outlet pressure at 4th stage and 8 kPa backpressure)

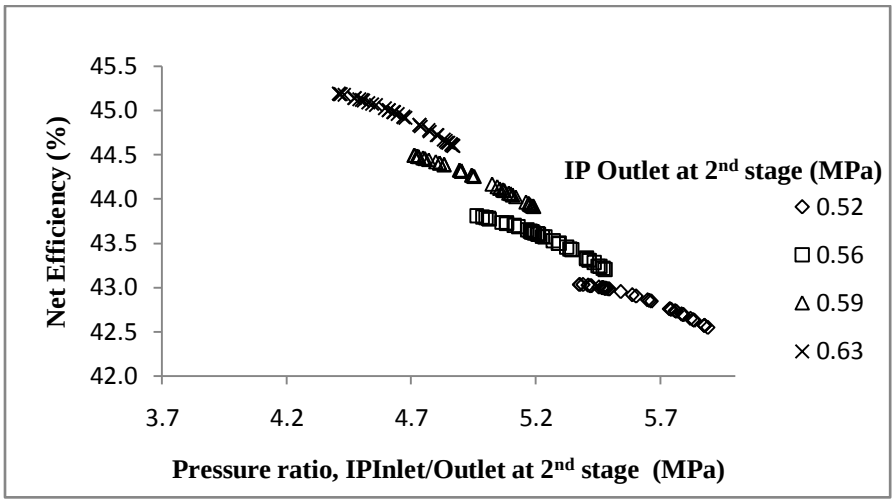

Figure 4.14: Effect of extract pressure at the 2nd stage of IP turbine[14].

[14] (Operating Condition: 600°C Main steam temperature, 600°C 1st Reheated steam temperature, 600°C 2nd Reheated steam temperature, 30.7 MPa VHP inlet pressure, 12.01 MPa VHP outlet pressure at 1st stage, 8.92 MPa VHP outlet pressure at 2nd stage, 4.35 MPa HP outlet pressure at 1st stage, 2.84 MPa HP outlet pressure at 2nd stage, 1.26 MPa IP outlet pressure at 1st stage, varying IP outlet pressure at 2nd stage, 0.331 MPa LP outlet pressure at 1st stage, 0.121 MPa LP outlet pressure at 2nd stage, 0.072 MPa LP outlet pressure at 3rd stage, 0.036 MPa LP outlet pressure at 4th stage and 8 kPa backpressure)

d. Pressure of LP Turbine

Figure 4.15 shows the effect of exhaust pressure in the LP turbine. Decreasing the pressure outlet at the LP turbine contributes to an improvement of the net efficiency even though it produces additional work required by the condensate pump. This low exhaust steam pressure offers more work output derived from the LP turbine, and, thus, achieves an increase of net plant efficiency. According to Figure 4.15, the efficiency increased by about 1.86% with a reduction in the outlet pressure from 8 to 6 kPa. However, the moisture content cannot be greater than 10% in this study due to damage that can occur on the blades of the turbines.

4.5 Efficiency Correlation for Ultra-supercritical Power Plant

This section aims to construct an empirical efficiency correlation for any ultra-supercritical pulverized coal-fired power generation plant that includes all operating and process parameters affecting net efficiency. This could be used to predict the system's net efficiency where the operating and process parameters are all known. Based on the parametric studies presented in previous sections, most parameters affecting the net efficiency behave in a linear manner except pressure in the series of turbines. Steps to develop the empirical efficiency correlation are presented as follows:

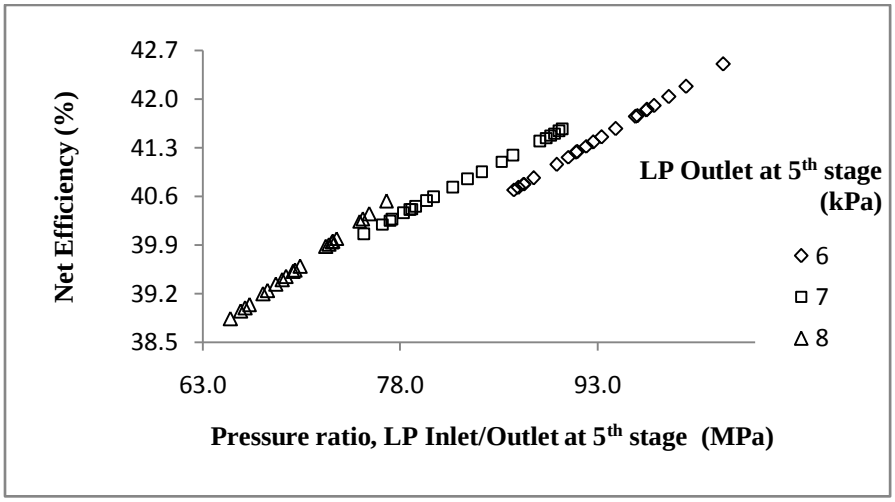

Figure 4.15: Effect of extract pressure at the 5th stage of LP turbine[15].

[15] (Operating Condition: 600°C Main steam temperature, 600°C 1st Reheated steam temperature, 600°C 2nd Reheated steam temperature, 30.7 MPa VHP inlet pressure, 12.01 MPa VHP outlet pressure at 1st stage, 8.92 MPa VHP outlet pressure at 2nd stage, 4.35 MPa HP outlet pressure at 1st stage, 2.84 MPa HP outlet pressure at 2nd stage, 1.26 MPa IP outlet pressure at 1st stage, 0.61 MPa IP outlet pressure at 2nd stage, 0.331 MPa LP outlet pressure at 1st stage, 0.121 MPa LP outlet pressure at 2nd stage, 0.072 MPa LP outlet pressure at 3rd stage, 0.036 MPa LP outlet pressure at 4th stage and varying backpressure)

a. Investigate the variation of net efficiency in the series of turbines

This subsection focuses on the correlation of the turbine series to the system. The model is composed of the series of four turbines including VHP, HP, IP, and LP as presented in Figure 3.1. The correlation equation was investigated in terms of the variation of the system's net efficiency corresponding to the change in the turbine pressure. According to the parametric studies, the pressures extracted at different stages of the turbine including VHP_2, HP_1, HP_2, IP_1, IP_2 and LP_5 have significant effects on the net efficiency of the system in non-linear relations. The efficiency variation equation of each turbine can be obtained by non-linear regression of the collection of its operating conditions – efficiency pairs.

First of all, the net efficiency variation equation of the power plant ($\eta_{sys,turbine}$) in relation to the turbine series can be defined as:

$$\Delta\eta_{sys,turbine} = a\Delta\eta_{VHP2} + b\Delta\eta_{HP1} + c\Delta\eta_{HP2} + d\Delta\eta_{IP1} + e\Delta\eta_{IP2} + f\Delta\eta_{LP5} \quad (4.1)$$

where $\Delta\eta_{sys,turbine}$, $\Delta\eta_{VHP2}$, $\Delta\eta_{HP1}$, $\Delta\eta_{HP2}$, $\Delta\eta_{IP1}$, $\Delta\eta_{IP2}$ and $\Delta\eta_{LP5}$ denote the variation in net efficiency of the system in relation to the turbine series, the variation of the system's net efficiency caused by the 2nd stage VHP turbine pressure, the variation of net efficiency caused by the 1st stage HP turbine pressure, the variation of net efficiency caused by the 2nd stage HP turbine pressure, the variation of net efficiency caused by the 1st stage IP turbine pressure, the variation of net efficiency caused by the 2nd stage IP turbine pressure, and the variation of net efficiency caused by the 5th stage LP turbine pressure, respectively.

Referring to Equation (4.1), considering only one turbine at a time, the equation for individual turbines can be presented as:

$$\Delta\eta_{VHP2} = a_1 \cdot VHP_2^2 + a_2 \cdot VHP_2 + a_3 \quad (4.2)$$

where $\Delta\eta_{VHP2}$ is the variation of net efficiency at the 2nd stage VHP turbine pressure from the base condition, which is equal to $\eta_{base} - \eta_{VHP2}$, where a_1, a_2 and a_3 are the regression coefficients.

It should be noted that the base condition of the power plant was set to operate at 31.1 MPa VHP inlet, 11.73 MPa VHP at the 1st stage, 8.43 MPa VHP at the 2nd stage, 4.28 MPa HP at the 1st stage, 3.06 MPa HP at the 2nd stage, 1.33 MPa IP at the 1st stage, 0.62 MPa IP at the 2nd stage, and 6.4 kPa at the 5th stage (backpressure).

The variation of net efficiency at the 2nd stage *VHP* pressure ($\Delta\eta_{VHP2}$) is obtained by deducting the efficiency of VHP_2 (η_{VHP2}) derived from the model by the efficiency of the base conditions (η_{base} =46.6%). All values of other operating and process parameters except the VHP pressure extracted at the 2nd stage must be set to constant (at base condition), meaning that the variations of net efficiency of the rest of the system is equal to zero. After applying polynomial regression, coefficients a_1, a_2, and a_3 can be obtained. The complete equation of the variation of net efficiency at the 2nd stage of VHP turbine is represented below:

$$\Delta\eta_{VHP2} = 2.7578 \cdot VHP_2^2 - 46.4374 \cdot VHP_2 + 195.6627 \quad (4.3)$$

Repeat this step for other extraction pressures at different turbines including $HP_{1,}$ $HP_{2,}$ $IP_{1,}$ IP_{2}, and $LP_{4.}$ The variation in net efficiency of individual turbines can be represented as:

$$\Delta\eta_{HP1} = 0.206 \cdot HP_1^2 - 1.7417 \cdot HP_1 + 3.8619 \quad (4.4)$$

$$\Delta\eta_{HP2} = 1.7525 \cdot HP_2^2 - 11.3601 \cdot HP_2 + 18.3758 \quad (4.5)$$

$$\Delta\eta_{IP1} = 6.8111 \cdot IP_1^2 - 21.9734 \cdot IP_1 + 17.17 \quad (4.6)$$

$$\Delta\eta_{IP2} = 14.2321 \cdot IP_2^2 - 36.8283 \cdot IP_2 + 17.5439 \quad (4.7)$$

$$\Delta\eta_{LP5} = -2.202 \cdot 10^5 \cdot LP_5^2 + 4.0728 \cdot 10^5 \cdot LP_5 - 16.4994 \quad (4.8)$$

where $VHP_{2,}$ $HP_{1,}$ $HP_{2,}$ $IP_{1,}$ IP_{2}, and LP_4 represent the pressure extracted at 2nd stage VHP turbine (MPa), the pressure extracted at 1st stage HP turbine (MPa), the pressure extracted at 2nd stage HP turbine (MPa), the pressure extracted at 1st stage IP turbine (MPa), the pressure extracted at 2nd stage IP turbine (MPa), and the pressure extracted at 5th stage LP turbine (MPa).

b. Investigate the variation of net efficiency for process parameters.

From the parametric study results, the most influential parameters affecting net efficiency include excess air (E_a), moisture content in coal (F_m), preheated air temperature (T_a), main steam and 1st reheating steam temperature (T_m and T_{r1}), efficiency of the boiler and turbine ($\boldsymbol{\eta}_{\text{boiler}}$ and $\boldsymbol{\eta}_{\text{turbine}}$), and pressure drop in the boiler and FWHs (P_{boiler} and P_{FWHs}). By applying the same concept as with the operating parameters in the turbine series, the variation of net efficiency influenced by process parameters can be defined as Equation (4.9).

$$\Delta\eta_{sys,proces} = g\Delta\eta_{Ea} + h\Delta\eta_{Fm} + i\Delta\eta_{Ta} + j\Delta\eta_{Tm} + k\Delta\eta_{Tr1} + l\Delta\eta_{\eta boiler} + m\Delta\eta_{\eta turbine} + n\Delta\eta_{Pboiler} + o\Delta\eta_{PFWHs} \quad (4.9)$$

Since these process parameters have linear relation to the system's efficiency, linear regression is used. After regression, the variations of efficiency of individual process parameters are shown in Equation (4.10) to Equation (4.18).

$$\Delta\eta_{Ea} = 0.0113 \cdot E_a - 0.9134 \quad (4.10)$$

$$\Delta\eta_{Fm} = 0.3729 \cdot F_m - 4.0328 \quad (4.11)$$

$$\Delta\eta_{Ta} = -0.0128 \cdot T_a + 5.0259 \quad (4.12)$$

$$\Delta\eta_{Tm} = -0.0131 \cdot T_m + 8.7772 \quad (4.13)$$

$$\Delta\eta_{Tr1} = -0.0126 \cdot T_{r1} + 8.3332 \quad (4.14)$$

$$\Delta\eta_{boiler} = -0.3618 \cdot \eta_{boiler} + 34.0171 \quad (4.15)$$

$$\Delta\eta_{turbine} = -0.0429 \cdot \eta_{turbine} + 4.2492 \quad (4.16)$$

$$\Delta P_{boiler} = 0.1143 \cdot P_{boiler} + 0.1602 \quad (4.17)$$

$$\Delta P_{FWHs} = 0.0008 \cdot P_{FWHs} + 0.9582 \quad (4.18)$$

c. Empirical net efficiency correlation for a pulverized coal-fired power plant.

This section examines the combined parametric effects of both operating and process parameters on the system's net efficiency, which can be defined as Equation (4.19) and Equation (4.20). By substituting Equation (4.3) through Equation (4.8) together with Equation (4.10) through Equation (4.18) into Equation (4.20) and applying multivariable regression, the efficiency correlation equation for an USC-PC power plant

that includes operating and process parametric effects can be presented as Equation (4.21).

$$\eta_{net,sys} = \eta_{base} - (\Delta\eta_{turbine} + \Delta\eta_{process}) \tag{4.19}$$

$$\begin{aligned}\eta_{net,sys} = \eta_{base} - (&a\Delta\eta_{VHP1} + b\Delta\eta_{HP1} + c\Delta\eta_{HP2} + d\Delta\eta_{IP1} + e\Delta\eta_{IP1} + f\Delta\eta_{LP5} + g\Delta\eta_{Ea} + \\ &h\Delta\eta_{Fm} + i\Delta\eta_{Ta} + j\Delta\eta_{Tm} + k\Delta\eta_{Tr1} + l\Delta\eta_{\eta boiler} + m\Delta\eta_{\eta turbine} + n\Delta\eta_{Pboiler} + \\ &o\Delta\eta_{PFWHs})\end{aligned} \tag{4.20}$$

$$\begin{aligned}\eta_{net,sys} = {} & -1457.4746 - 19.2454 \cdot VHP_2^2 + 324.06447 \cdot VHP_2 + 0.4225 \cdot HP_1^2 - 3.5725 \cdot HP_1 - \\ & 10 \cdot HP_2^2 + 64.8223 \cdot HP_2 - 5.3686 \cdot IP_1^2 + 17.3197 \cdot IP_1 + 4.8612 \cdot IP_2^2 - \\ & 12.5793 \cdot IP_2 + 2.2590 \cdot 10^5 \cdot LP_5^2 - 0.0418 \cdot 10^5 \cdot LP_5 - 0.010 \cdot E_a - \\ & 0.3327 \cdot F_m + 0.0114 \cdot T_a + 0.0117 \cdot T_m + 0.0112 \cdot T_{r1} + 0.3228 \cdot \eta_{boiler} + 0.0383 \cdot \\ & \eta_{turbine} - 0.1020 \cdot P_{boiler} - 0.0007 \cdot P_{FWHs}\end{aligned} \tag{4.21}$$

where $E_a, F_m, T_a, T_m, T_{r1,} \eta_{boiler}, \eta_{turbine\ r,} P_{boiler}$ and P_{FWHs} represent the excess air (%), the free moisture content in coal (%), the preheated air temperature (°C), the main steam temperature (°C), the 1st reheating steam temperature (°C), the boiler efficiency (%), the turbine efficiency (%), the pressure drop across the boiler (%), and the pressure drop across FWHs (%), respectively.

It should be noted that this equation was developed for Illinois#6 bituminous coal and is only valid for the range of operating and process conditions given in Table 3.1. Figure 4.16 illustrates a parity plot of the net efficiency calculated from the empirical correlation and that obtained from the theoretical model. According to the plot, a coefficient of determination (R^2) of 0.97 indicates that the empirical correlation equation offers reliable prediction of the system's net efficiency.

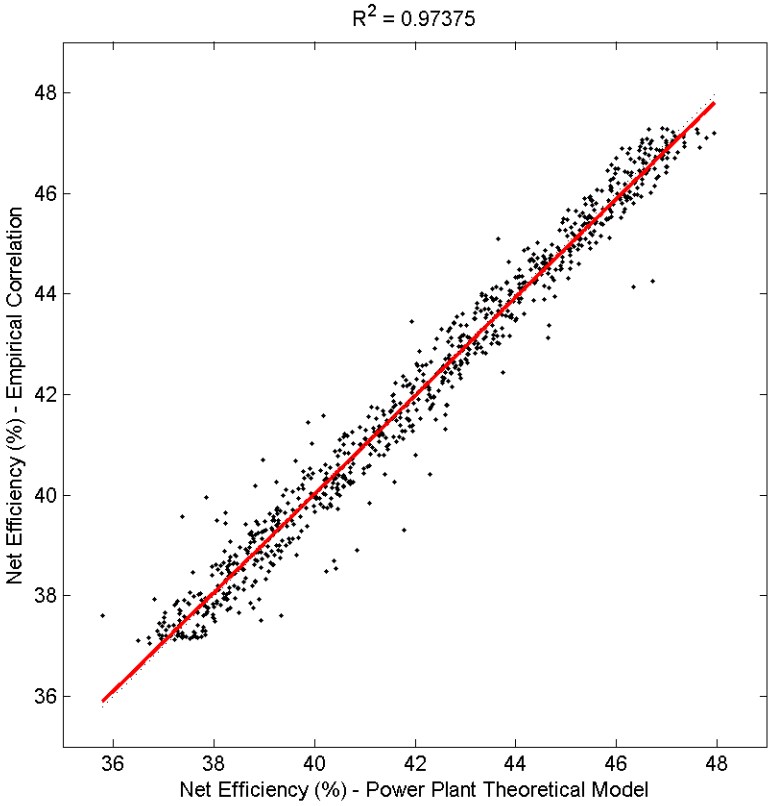

Figure 4.16: Parity plot of net efficiency between empirical correlation and theoretical model.

(Original in color)

Chapter 5

Conclusions and Future Work

5.1 Conclusion

This thesis aimed to identify the optimal conditions offering the maximum net plant efficiency from various ranges of operating and design parameters for an ultra-supercritical coal-fired power plant. The study focuses only on the advanced technology of a pulverized coal-fired power plant operating under ultra-supercritical operating conditions. This was achieved by first constructing the developed model based on thermodynamics associated with steam properties, a steam power cycle, the principle of coal combustion and its chemical reactions, and the principles of pulverized coal-fired technology. The thermodynamic steam properties were carried out by an approach of Gauss Seidel Relaxation written in MATLAB® script to obtain the coefficients of steam properties, including enthalpy (h), entropy (s), and specific volume (v) as given in Appendix B. The developed model was also verified by comparing pilot results with the literature to ensure accuracy of the model. The following are highlights of the conclusions obtained from this study:

- The computer based-model for Pulverized coal-fired power plant operating at ultra-supercritical was developed.
- Thermodynamic properties equation of working fluid was successfully constructed.

- The verification of the computer based-model was carried out by comparing the simulation results with published data. It was found that the simulation results obtained from this study agree well with the literature data in the two cases.
- The main process operating and design parameters are the moisture content in coal, the preheated air temperature, the temperature of main and 1^{st} reheated steam, the inlet pressure of the VHP turbine, the pressure extracted at the 2^{nd} stage of the VHP turbine, the pressure extracted at the 1^{st} stage of the HP turbine, the pressure extracted at the 2^{nd} stage of the HP turbine, the pressure extracted at the 1^{st} stage of IP turbine, the pressure extracted at the 2^{nd} stage of the IP turbine, the backpressure, the efficiency of the boiler and turbine, and the pressure drop across the boiler.
- The empirical correlation equation of net efficiency was successfully developed based on the identified parametric effects. A coefficient of determination (R^2) of 0.97 shows the confidence of the correlation equation that can be used to estimate the reliable net efficiency of USC-PC power plants.

5.2 Recommendations for Future work

To achieve more effective results, future study could incorporate the following improvements:

- Implement optimization based on the obtained parametric effects to achieve at optimal possible efficiency.
- Integrate with CCS technology: CO_2 Capture unit into the developed plant model.
- Investigate other type of coal-fired power plants that operating at USC conditions such as CFB, PFB and IGCC.
- Study the cost of electricity for an ultra-supercritical pulverized coal-fired power plant operating under ultra-supercritical conditions.
- Enhance the speed of simulation; a computer language might be needed to such as C++ since the model used in this study was written in Microsoft® Excel.

References

Armstrong, P.; Sasaki, T.; Abe, T. and Matsuda, J. (2003). *Design and Operating Experience of Supercritical Pressure Coal Fired Plant.* Electric Power, *Hitachi Power Systems America, Ltd., Database.*

Ashmore, C. (2006). Steam Turbine Technology Goes Ultra Supercritical. *Energy Focus*. **(6),** 128-130.

Asthana, V. and Panigrahi, P.K. (2008). *Performance of Power Plants with High Temperature Conditions at Suv-Critical Pressure,* The 5th European Thermal Sciences Conference, May 18-22, Eindhoven, Netherlands

Balabin, R.M.; Safieva, R.Z. and Lomakina, E.I. (2009). Universal Technique for Optimization of Neural Network Training Parameters: Gasoline near Infrared Data Example. *Neural Computing and Applications,* **18(6),** 57–565.

Beér, J.M. (2007). High Efficiency Electric Power Generation: The Environmental Role. *Progress in Energy and Combustion Science*. **33(2),** 107–134.

Bergerson, J. and Lave, L. (2007). The Long-Term Life Cycle Private and External Costs of High Coal Usage in the US. *Energy Policy,* **35(12),** 6225-6234.

Biegler, L.T.; Cervantes, A.M. and Wachter, A. (2002). Advances in Simultaneous Strategies for Dynamic Process Optimization. *Chemical Engineering Science.* **57(4),** 575 – 593.

Bezerraa, M.A.; SantelliR.E.; Oliveiraa, E.P.; Villar, L.S. and Escaleiraa, L.A. (2008). Response Surface Methodology (RSM) as a Tool for Optimization in Analytical Chemistry. *Talanta.* **76(5),** 965–977.

Booras and Holt (2004*). Pulverized Coal and IGCC Plant Cost and Performance Estimates.* Gasification Technologies Conference, October 3-6, Washington, DC.

Boyce, M.P. (2012). Gas *Turbine Engineering Handbook: 4th Edition,* Elsevier Inc., Oxford.

Bugge, J. and Kjaer, S. (2006). High-Efficiency Coal-Fired Power Plants Development and Perspectives. *Energy,* **31(10-11),** 1437-1445.

Cao, Y.; Wei, X.; Wu, J.; Wang, B. and Li, Y. (2007). Development of Ultra-supercritical Power Plant in China. *Challenges of Power Engineering and Environment*. **4**, 231-236.

Chapra, S.C. and Canale, R.P. (2007). *Numerical methods for engineer: 5th Edition*, Tata McGraw-Hill Publishing Company limited, New Delhi.

Chattopadhyay, P. (2000). *Boiler Operation Engineering-Questions and Answer: 2nd Edition*, Mcgraw-Hill, New York.

Cohen, J. (1988). *Statistical power analysis for the behavioral sciences: 2nd Edition*, Lawrence Erlbaum Associates, New York.

Chew P. E. (2003). PF-Fired Supercritical Power Plant. *Proceedings of the Institution of Mechanical Engineers. Part A. Journal of power and energy.* **217(1),** 35-43.

Department of Trade and Industry (United Kingdom) (DTI). (2006). *The Energy Challenge: Energy Review Report 2006*. Norwich.

Drbal, L.F.; Boston, P.G.; Westra, K.L. and Erickson, R.B. (1996). *Power Plant Engineering: 1stEdition*, Black & Veatch, Springer, New York.

Driscoll, M.J. and Hejzlar, P. (2004). 300 MWe Supercritical CO2 Plant Layout and Design. *Center for Advanced Nuclear Energy Systems: MIT Nuclear Engineering Department.* MIT-GFR-014.

Folger, P. (2010). Carbon Capture: A Technology Assessment. *Congressional Research Service Reports: University of Nebraska - Lincoln.* July 19.

Feng, W. (2008). 1000 MW Ultra-Supercritical Turbine Steam Parameter Optimization. *Frontiers of Energy and Power Engineering in China.* **2(2),** 187-193.

Goidich, S.J.; Wu, S.; Fan, Z. and Bose, A.C. (2005). *Design Aspects of the Ultra-Supercritical CFB Boiler.* International Pittsburgh Coal Conference, September 12-15, Pittsburgh, PA.

Goidich, S.J.; Fan, Z.; Sippu, O. and Bose, A.C. (2006). *Integration of Ultra-Supercritical OUT and CFB Boiler Technologies.* The 19th International Fluidized Bed Combustion Conference, May 12, Vienna, Austria.

Hack, H.; Seltzer, A. and Stanko, G. (2007). Design Considerations for Advanced Materials in Oxygen-Fired Supercritical and Ultra-Supercritical Pulverized Coal Boilers. *The 5th International Conference on Advances in Materials Technology for Fossil Power Plants*, October 3-5, Florida, USA.

Holcomb, G.R.; Alman, D.E.; Bullard, S.B.; Covino, B.S.; Cramer, S.D. and Ziomek-Moroz, M. (2003). *Ultra Supercritical Steam Corrosion.* National Energy Technology Laboratory, Pittsburgh, PA.

Holcomb, G.R.; Covino, B.S.; Bullard, S.J.; Cramer, S.D. and Ziomek-Moroz, M. (2005). Ultra Supercritical Steamside Oxidation: Advances in Materials Technology for Fossil Power Plants. *Proceedings of the 4th International Conference* (ASM International). 451-462.

International Energy Agency (IEA). (2006a). Key World Energy Statistics 2006, Paris, France.

International Energy Agency (IEA). (2007). Pulverised Coal Combustion (PCC). Retrieved April 27, 2009, from http://www.ieacoal.org.uk/site/ieacoal_old/databases/ccts/pulverized-coal-combustion-pcc?

Kalil, S.J.; Maugeri, F. and Rodrigues, M.I. (2000). Response Surface Analysis and Simulation as a Tool for Bioprocess Design and Optimization. *Process Biochemistry.* **35(6),** 539–550.

Kaneko, K. and Hashimoto, T. (1996). 1000 MW Coal Fired Supercritical Variable Pressure Operation Boiler with Vertical Furnace. *Mitsubishi Heavy Industries Ltd. Technical Review,* **33(3),** 105-109.

Kimura, H.; Matsuda, J. and Sakai, K. *Latest Experience of Coal Fired Supercritical Sliding Pressure Operation Boiler and Application for Oversea Sutility.* Babcock-Hitachi K.K.

Lee, K.Y.; Heo, J.S.; Hoffman, J.A.; Sung-Ho Kim and Won-Hee Jung. (2007). *Neural Network-Based Modeling for A Large-Scale Power Plant.* Power Engineering Society General Meeting. June 24-28, Tampa, FL.

Mandal, P.K. (2006) Efficiency Improvement in Pulverized Coal Based Power Stations. *Proceedings of the 1st National Conference on Advances in Energy Research (AER).*

McDonald, D.K. (1997). Status of B&W's Low-Emission Boiler System Development Program. *Proceedings of the Advanced Coal-Based and Environmental Systems '97 Conference*.

Messerle, V.E. and Ustimenko, A.B. (2007). The 31st International Technical Conference on Coal Utilization and Fuel Systems. *Challenges of Power Engineering and Environment*. **54(3),** 242-247.

Mukhopadhyay, D.M.; Balitanas, M.O.; A., A.F; Jeon, S. and Bhattacharyya, D. (2009). Genetic Algorithm: A Tutorial Review. *International Journal of of Grid and Distributed Computing*. **2(3),** 25-32.

Okura, R.; Shioshita, S.; Kawasato, Y. and Shimizu J. (2003). Completion of High-efficiency Coal-fired Power Plant. *Hitachi Review,* **52(2),** 79-83.

Pande, M.V.; Director, D. and Nagpur, N. (2008). Latest Technologies – Supercritical (SC) and Ultra-supercritical (USC). *Workshop on Power Plant Performance Monitoring*: *Energy Manager Training Database.* December 24.

Perry, R.H., Green, D.W. and Maloney, J.O. (1997). *Perry's Chemical Engineers' Handbook: 7th Edition,* McGraw-Hill, New York.

Peltier, Robert. (2005). Genesee Phase 3, Edmonton, Alberta, Canada. *Power: Jul/Aug 2005.* **149(6),** 46.

Pe˜na, B.; Teruel, E. and Díez, L.I. (2011). Soft-Computing Models for Soot- Blowing Optimization in Coal-Fired Utility Boilers. *Applied Soft Computing.* **11(2).** 1657–1668.

Risso, F.V.A.; Rissp, V.F. and Schiozer, D.J. (2011). Risk Analysis of Petroleum Fields using Latin Hpercube, Monte Carol and Derivative Tree Techniques. *Journal of Petroleum and Gas Exploration Research.* **1(1),** 14-22.

Romanosky, R.R.; Rawls, P.A. and Purgert, R.M. (2007). Advanced Materials for Ultra-Supercritical Boiler Systems, *Project facts*, August.

Robertson, A. and White, J. (1997). *Topping PCFB Combustion Plant with Supercritical Steam Pressure*. The 10th International Conference and Exhibition for the Power Generating Industries, December 7-11, Dallas, TX.

Sanpasertparnich, T. (2007). *Monte Carlo Simulation of Pulverized Coal-Fired Power Plant: Efficiency Improvement and CO_2 Capture Options : M.A.Sc. Thesis,* University of Regina, Saskatchewan, Canada.

Sarunac, N.; Ness, M. and Bullinger, C. (2007). One Year of Operating Experience with a Prototype Fluidized Bed Coal Dryer at Coal Creek Generating Station. *Prepared for Presentation at the 3rd International Conference on Clean Coal Technologies for our Future*, May 15-17, Sardinia, Italy.

Singer, J.G. (1991). *Combustion Fossil Power: a Reference Book on Fuel Burning and Steam Generation: 4th Edition*, Combustion Engineering Power Systems Group, Winsor, Conecticut.

Srikanta, M. (1998). *Alternatives to Monte-Carlo Simulation for Probabilistic Reserves Estimation and Production Forecasting*. SPE Annual Technical Conference and Exhibition, New Orleans.

Srinivas, N. and Deb, K. (1994). Muiltiobjective Optimization Using Nondominated Sorting in Genetic Algorithms. *Evolution Computation.* **2(3),** 221- 248.

Tsiklauri, G. and Talbert, R. (2005). Supercritical steam cycle for nuclear power plant. *Nuclear Engineering and Design*, **235(15),** 1651-1664.

U.S. Department of Energy (U.S.DOE). (1999). *Market Based Advanced Coal Power System: Section 3 Pulverized Coal-Fired Plants,* Washinton, DC.

Viswanathan, R. and Bakker, W.T. (2000). Materials for Boiler in Ultra-Supercritical Power Plant Boilers. *Proceedings of 2000 International Joint Power Generation Conference*, July 23-26, Miami Beach, Florida.

Viswanathan, R.; Coleman, K. and Rao, U. (2006). Materials for Ultra-Supercritical Coal-Fired Power Plant Boilers. *International Journal of Pressure Vessels and Piping*, **83(11-12),** 778-783.

VGB Powertech and Evonik Energy Services. (2008). Supercritical and Ultra-Supercritical Technology. *Indo German Energy Programme.* Retrieved from http://www.emt-india.net/PowerPlantComponent/Output1.1/14.pdf

Wright, I.G.; Maziasz, P.J.; Ellis, F.V.; Gibbons, T.B.; Woodford, D.A. (2004). Materials Issues for Turbines for Operation in Ultra-Supercritical Steam. *Advanced Research Materials Program.*

Woodruff, E.B; Lammers, H.B. and Lammers, T.F. (2005). *Steam Plant Operation: 8th Edition,* McGraw-Hill, New York.

Zhao, Z. (2004). Co_2 Reductions through Efficiency Improvement to Existing Coal-Fired Power Plant and Deployment of Supercritical Units in China. *Proceedings of APEC Workshop*, February 16, Queensland, Australia.

Appendices

Appendix A
Pseudo code of Gauss Seidel Relaxation.

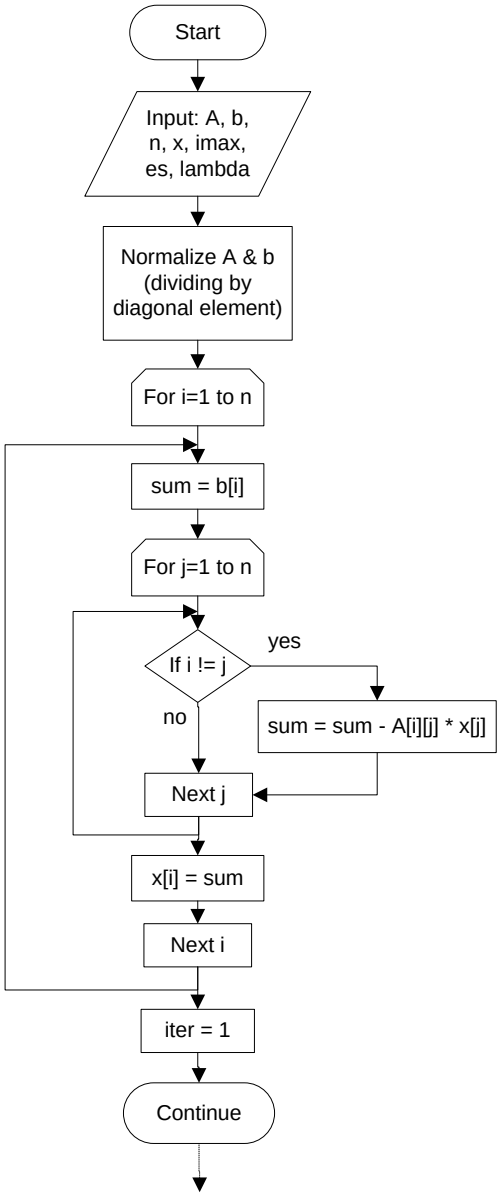

Figure A.1: Pseudo code of Gauss Seidel Relaxation.

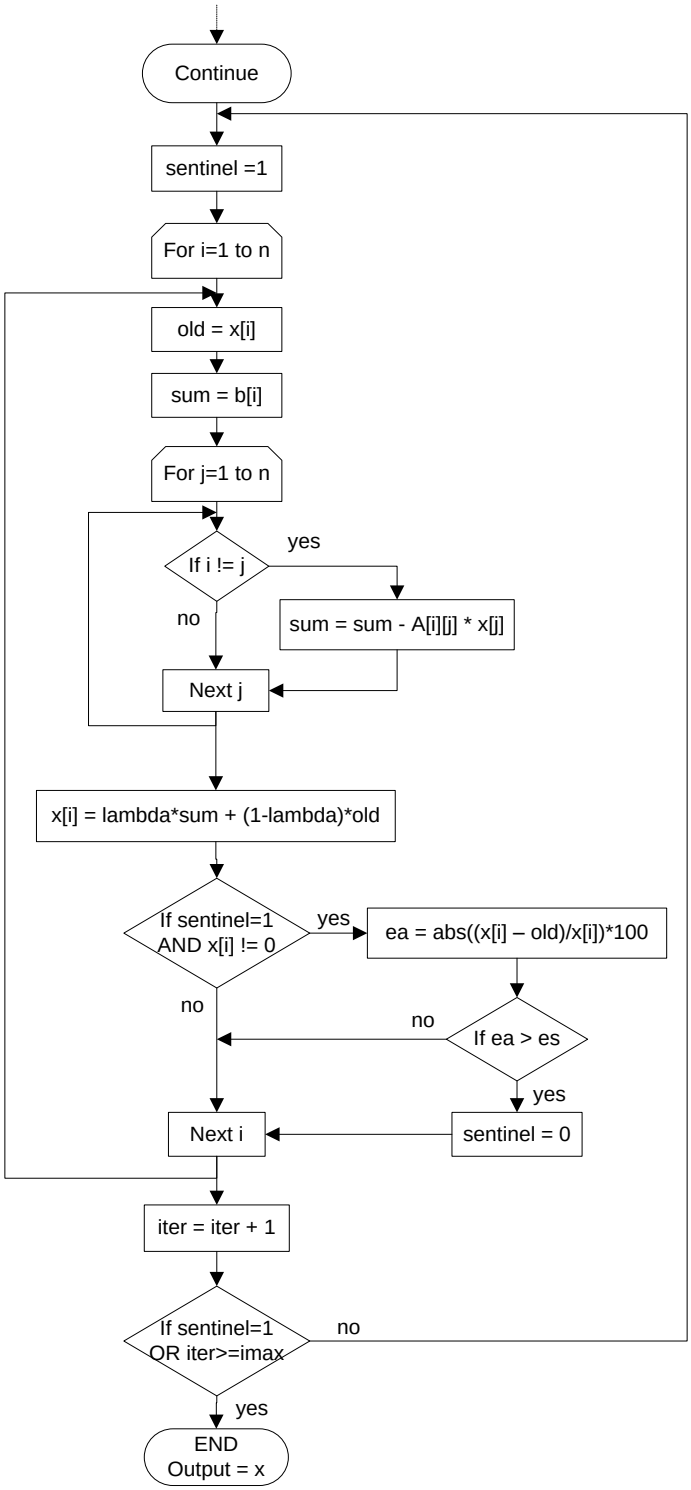

Figure A.1: Pseudo code of Gauss Seidel Relaxation (continued).

Appendix B
Results of the property equations.

Table B1: Saturated water – Temperature table.

h_f (kJ/kg)		h_g (kJ/kg)	
Equations	**Applied ranges (MPa)**	**Equations**	**Applied ranges (MPa)**
$h_f = 4.2136 \cdot T - 0.0008313 \cdot T^2 + 0.0000067488 \cdot T^3 - 0.0000000074243 \cdot T^4 - 0.0321$	$0.01 \leq T \leq 200$	$h_g = 1.8456 \cdot T - 0.00036356 \cdot T^2 - 0.0000045141 \cdot T^3 - 0.000000016972 \cdot T^4 + 2501.4$	$0.01 \leq T \leq 250$
$h_f = 1.8089 \cdot T + 0.0061 \cdot T^2 + 249.7076$	$205 \leq T \leq 230$	$h_g = -0.123433 \cdot T - 0.000778212 \cdot T^2 - (6.6538410 \cdot 10^{-118}) \cdot e^T + 2880.97$	$255 \leq T \leq 270$
$h_f = 1.37462 \cdot T + 0.00689755 \cdot T^2 + 310.625$	$235 \leq T \leq 280$	$h_g = -0.444752 \cdot T - 0.00211279 \cdot T^2 - (5.88515 \cdot 10^{-133}) \cdot e^T + 3072.59$	$275 \leq T \leq 305$
$h_f = 1.74004 \cdot T + 0.00654255 \cdot T^2 + (6.17159 \cdot 10^{-140}) \cdot e^T + 234.15$	$285 \leq T \leq 330$	$h_g = 13.6814 \cdot T + 0.0214101 \cdot T^2 - 0.0000972278 \cdot T^3 - (1.09272 \cdot 10^{-159}) \cdot e^T - 682.795$	$310 \leq T \leq 370$
$h_f = -2.43049 \cdot T + 0.0101028 \cdot T^2 + 0.0000184761 \cdot T^3 + 0.000000148279 \cdot T^4 + (5.14197 \cdot 10^{-161}) \cdot e^T + 2327.23$	$340 \leq T \leq 370$	$h_g = -55.6888 \cdot T + 22934.7$	$T = 374.14$
$h_f = -15.0955 \cdot T - 0.0683882 \cdot T^2 - 0.000175975 \cdot T^3 + 0.000000807913 \cdot T^4 + 10705.7$	$T = 374.14$		

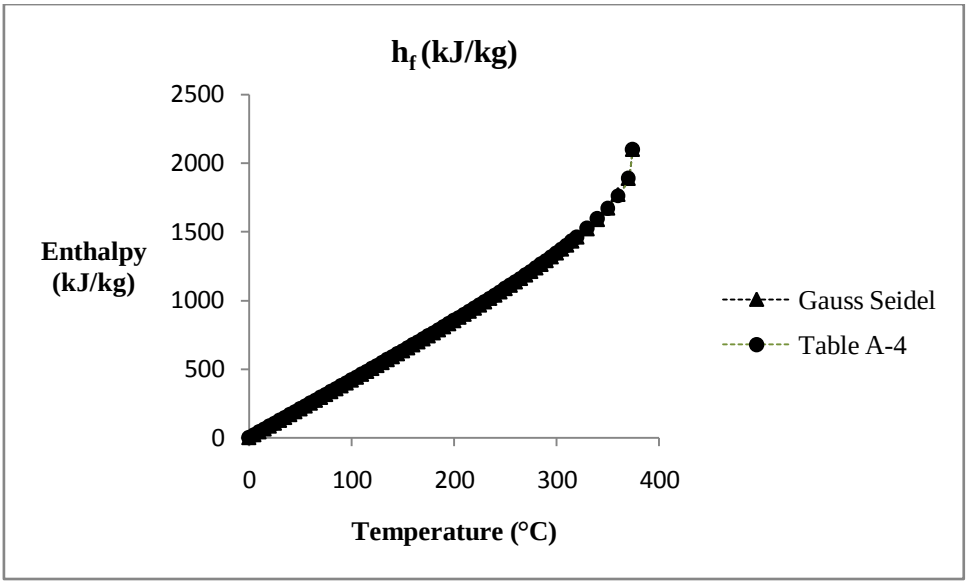

Figure B.1 Present accuracy obtained from Enthalpy function of liquid enthalpy (sensible heat) for table of saturated water-temperature (Table A-4).

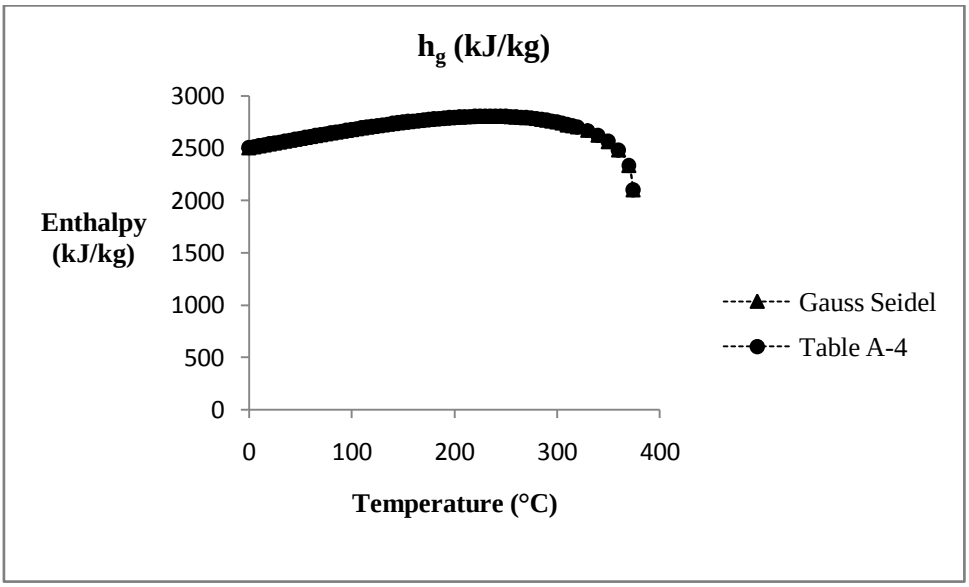

Figure B.2 Present accuracy obtained from Enthalpy function of saturated steam for table of saturated water-temperature (Table A-4).

Table B2: Saturated water – Temperature table.

h_f (kJ/kg)		h_g (kJ/kg)	
Equations	**Applied ranges (MPa)**	**Equations**	**Applied ranges (MPa)**
$h_f = -19.6778+53.352 \cdot P -4.3705 \cdot P^2$	$P= 0.0006113$	$h_g = 2493.51+22.6814 \cdot P-1.81683 \cdot P^2$	$6.11 \cdot 10^{-4} \leq P \leq 0.005$
$h_f = -31.456+69.0573 \cdot P-8.29623 \cdot P^2$	$0.001 \leq P \leq 0.003$	$h_g = 2495.55+38.2895 \cdot ln(P)$	$0.0075 \leq P \leq 0.075$
$h_f = 3.72637+83.3221 \cdot ln (P)$	$0.004 \leq P \leq 0.025$	$h_g = 2657.03+244.766 \cdot P$	$0.1 \leq P \leq 0.325$
$h_f = -51.835+100.287 \cdot ln(P)$	$0.03 \leq P \leq 0.075$	$h_g = 2715.31+68.8396 \cdot P$	$0.35 \leq P \leq 0.9$
$h_f = 289.333+1491.33 \cdot P-1893.49 \cdot P^2-2222.28 \cdot P^3+6793.47 \cdot P^4$	$0.1 \leq P \leq 0.35$	$h_g = 2760.07+20.7585 \cdot P$	$0.95 \leq P \leq 2.25$
$h_f = -143.75+3923.04 \cdot P-7327.5 \cdot P^2+6295.25 \cdot P^3-1974.24 \cdot P^4$	$0.375 \leq P \leq 0.85$	$h_g = 2807.51+2.80974 \cdot P-1.11976 \cdot P^2$	$2.5 \leq P \leq 22.09$
$h_f = 528.896+280.572 \cdot P-46.606 \cdot P^2$	$0.9 \leq P \leq 1.75$		
$h_f =715.422+272.647 \cdot ln(P)$	$2 \leq P \leq 6$		
$h_f =967.478+43.6519 \cdot P$	$7 \leq P \leq 13$		
$=988.323+41.483 \cdot P$	$14 \leq P \leq 22.09$		

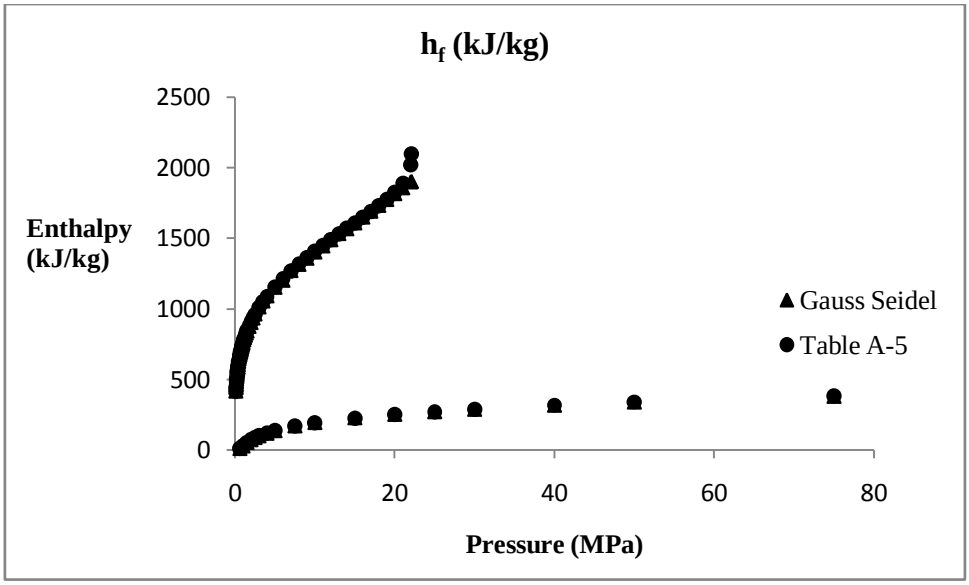

Figure B.3 Present accuracy obtained from Enthalpy function of liquid enthalpy (sensible heat) for table of saturated water-temperature (Table A-5).

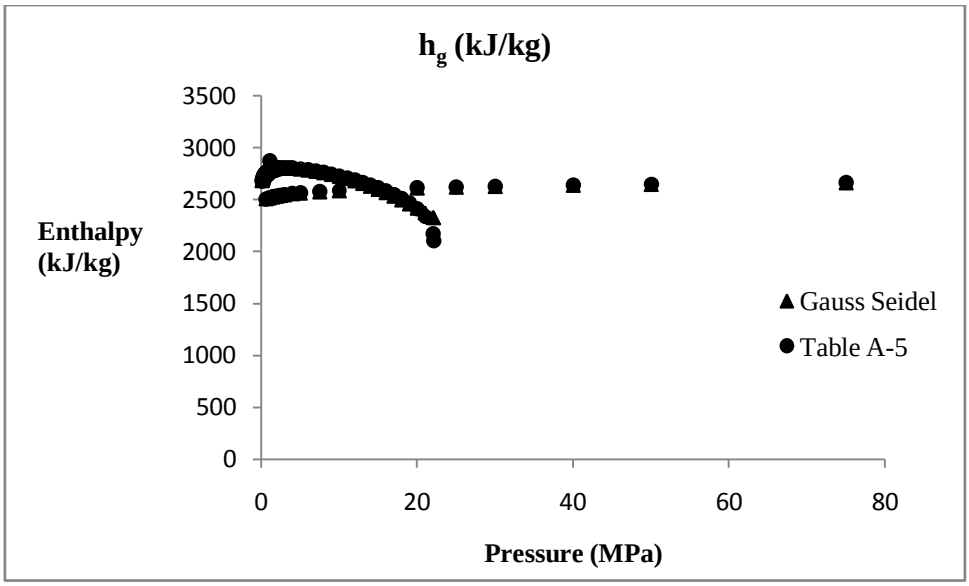

Figure B.4 Present accuracy obtained from Enthalpy function of saturated steam for table of saturated water-temperature (Table A-4).

Table B3: Correlation function of pressure and temperature[16].

Equation $T = fn\ (P);\ (^{\circ}C)$	**Applied range (MPa)**
$T= 28.4829 \cdot P-6.55217 \cdot P^2-14.9519$	$6.11 \cdot 10^{-4} \leq P \leq 0.002$
$T = 17.0217 \cdot \ln(P)+5.48459$	$0.0025 \leq P \leq 0.005$
$T = 20.9056 \cdot \ln(P)-2.32244$	$0.0075 \leq P \leq 0.03$
$T = 24.4303 \cdot \ln(P)-14.2418$	$0.04 \leq P \leq 0.075$
$T = 18870.75 \cdot P-4933.58 \cdot P^2+5572.03 \cdot P^{3+}85.0662 \cdot \ln(P)-241.129$	$0.1 \leq P \leq 0.3$
$T= 11.4236 \cdot P-28.7987 \cdot P^2+29.2658 \cdot P^{3+}27.3916 \cdot \ln(P)+161.942$	$0.325 \leq P \leq 0.7$
$T= 30.1671 \cdot P-23.0629 \cdot P^2-11.0449 \cdot P^3+137.665$	$0.75 \leq P \leq 1.4$
$T= 49.691 \cdot P-7.89091 \cdot P^2+0.595315P^3+139.79$	$1.5 \leq P \leq 5$
$T= 15.0741 \cdot P-0.502709 \cdot P^2+0.00789269P^3+202.62$	$6 \leq P \leq 22.09$

[16] A correlative function of pressure (MPa) and temperature (˚C) is used to estimate enthalpy as per the following steps: Convert pressure value to temperature by using the correlative function. Then, calculate the enthalpy by using the equation obtained from Table A4 where temperature is an independent variable.

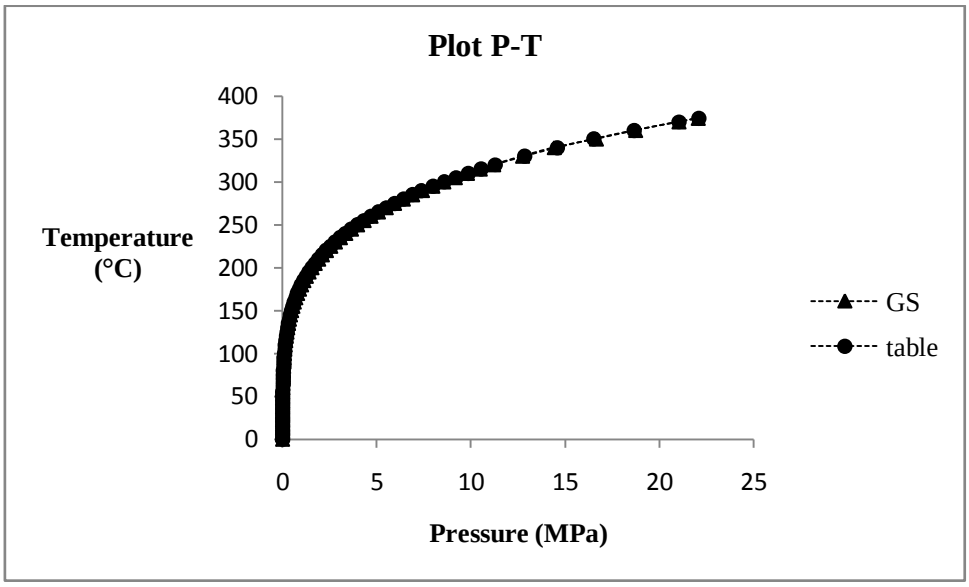

Figure B.5 Present accuracy obtained from a correlative function of pressure and temperature according to Table A-4.

Table B4: Superheated water[17].

Equations $h = \{fn_1(P)\}T + \{fn_2(P)\}T^2 + \ldots$; **(kJ/kg)**	**Applied ranges (MPa)**
$h=((-0.0037\cdot P+0.1535\cdot P^2-0.067\cdot P^3+1.7999)\cdot T)+((0.0000538827\cdot P-0.000176118\cdot P^2+0.0000737209\cdot P^3+0.000330174)\cdot T^2)+(-33.0056\cdot P-16.9765\cdot P^2+9.72939\cdot P^3+2508.98)$	$0.01 \le P \le 1.6$
$h =((0.0222183\cdot P-0.0197727\cdot P^2+0.00670717\cdot P^3+0.0000350044\cdot P^4+1.87467)\cdot T)+((0.000619653\cdot P-0.0002618\cdot P^2+0.0000346639\cdot P^3-0.000170446)\cdot T^2)+(-14.8665\cdot P-3.30784\cdot P^2+2490.39)$	$1.8 \le P \le 2.5$
$h = ((-179.438\cdot P+93.2006\cdot P^2-21.3644\cdot P^3+1.77765\cdot P^4+0.0574932\cdot P^5-0.0116245\cdot P^6+129.4)\cdot T)+((0.0844271\cdot P-0.0427178\cdot P^2+0.00955464\cdot P^3-0.000758969\cdot P^4-0.0000311757\cdot P^5+0.00000547578\cdot P^6-0.0616679)\cdot T^2)+((0.000000913491\cdot P-0.000000268799\cdot P^2+0.0000000256461\cdot P^3-0.00000100429)\cdot T^3)+((102463\cdot P-55120.8\cdot P^2+12999.8\cdot P^3-1119.43\cdot P^4-31.9633\cdot P^5+7.09694\cdot P^6-69495.7)\cdot \log_{10}(T))+(149071-217162\cdot P+117232\cdot P^2-27724.4\cdot P^3+2391.79\cdot P^4+68.6358\cdot P^5-15.2342\cdot P^6)$	$3.0 \le P \le 5.0$
$h = -1091.8 \cdot P + 51.0126 \cdot P^2 + 1.8424 \cdot T - 0.00028925 \cdot T^2 + 0.00000033943 \cdot T^3 + 679.5866 \cdot \log_{10}(T) + 5394.6$	$P = 6.0$
$h = ((16.6017\cdot P-1.15164\cdot P^2-56.3031)\cdot T)+((-0.00200925\cdot P+0.000113818\cdot P^2+0.00824653)\cdot T^2)+((-0.0000041847\cdot P+0.000000296014\cdot P^2+0.0000147897)\cdot T^3)+((-20864\cdot P+1466.27\cdot P^2+73070.2)\cdot \log_{10}(T))+(47993.3\cdot P-3378.08\cdot P^2-165652)$	$7.0 \le P \le 8.0$
$h = ((-72.8168+17.0724\cdot P-0.952319\cdot P^2)\cdot T)+((0.00132808-0.000632337\cdot P+0.0000497975\cdot P^2)\cdot T^2)+((0.0000114233+0.00000241035\cdot P+0.000000126802\cdot P^2)\cdot T^3)+((84645.7-18921.8\cdot P+1042.5\cdot P^2)\cdot \log_{10}(T))+(42782.7\cdot P-2354.55\cdot P^2-189453)$	$9.0 \le P \le 10.0$
$h = -1993.9 \cdot P + 108.429 \cdot P^{22} + 2.6639 \cdot P^3 + 3.3568 \cdot T - 0.0018 \cdot T^2 + 0.00000087471 \cdot T^3 + 608.7492 \cdot \log_{10}(T) + 3134.6$	$P = 12.5$
$h = -7531.8 \cdot P + 304.0181 \cdot P^2 + 5.4628 \cdot T - 0.0037 \cdot T^2 + 0.0000015021 \cdot T^3 + 45882$	$P = 15.0$
$h = -1873.9 \cdot P + 83.2239 \cdot P^2 + 4.6481 \cdot T - 0.0024 \cdot T^2 + 0.00000089222 \cdot T^3 + 8743.6$	$P = 17.5$
$h = -2099.6 \cdot P + 83.5083 \cdot P^2 + 5.2497 \cdot T - 0.003 \cdot T^2 + 0.0000010971 \cdot T3 + 9814.7$	$P = 20.0$
$h = -5150.4 \cdot P + 180.8227 \cdot P^2 + 11.6509 \cdot T - 0.011 \cdot T^2 + 0.0000044055 \cdot T^3 + 15257$	$P = 25.0$
$h = -5599.9 \cdot P + 41.2271 \cdot P^2 + 16.376 \cdot T - 0.0174 \cdot T^2 + 0.0000072511 \cdot T^3 + 129210$	$P = 30.0$
$h = -6528.1 \cdot P + 26.5469 \cdot P^2 + 49.9977 \cdot T - 0.0678 \cdot T^2 + 0.000031902 \cdot T^3 + 186920$	$P = 35.0$

[17] This table is considered only from P = 0.01 to P = 30 MPa. A Gauss Seidel approach was applied to decrease the number of equations and optimize error.

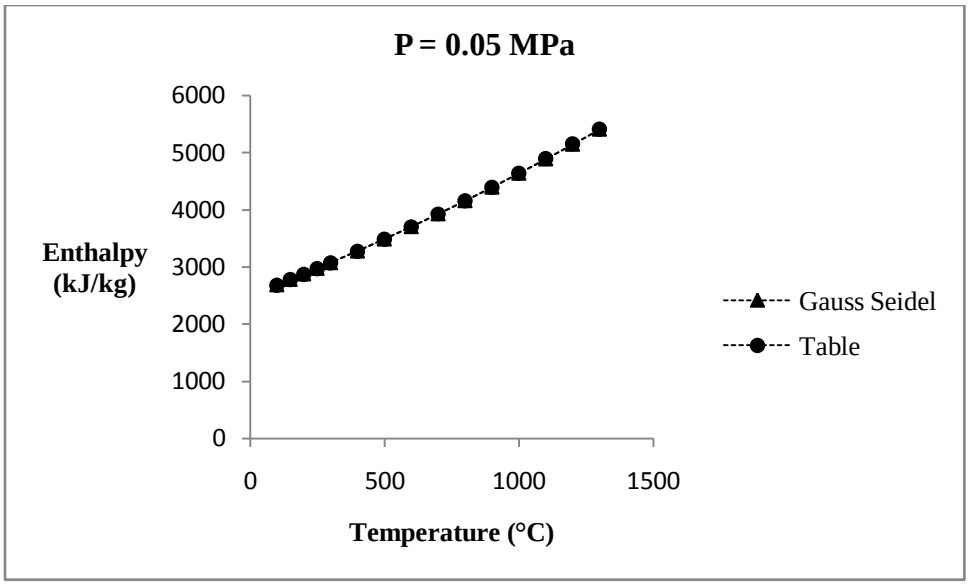

Figure B.6 Present accuracy obtained from Enthalpy function of 0.05 MPa pressure for table of superheated water (Table A-6).

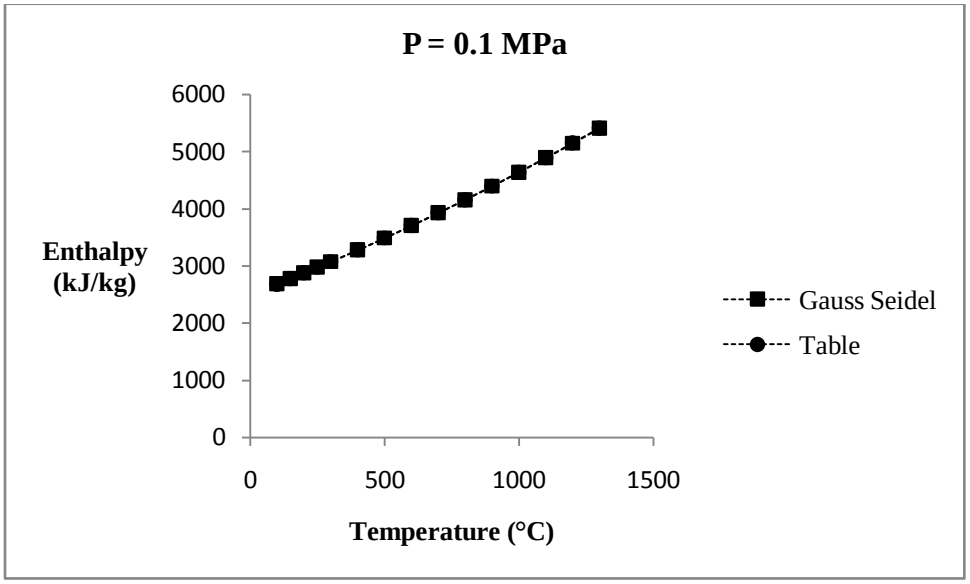

Figure B.7 Present accuracy obtained from Enthalpy function of 0.1 MPa pressure for table of superheated water (Table A-6).

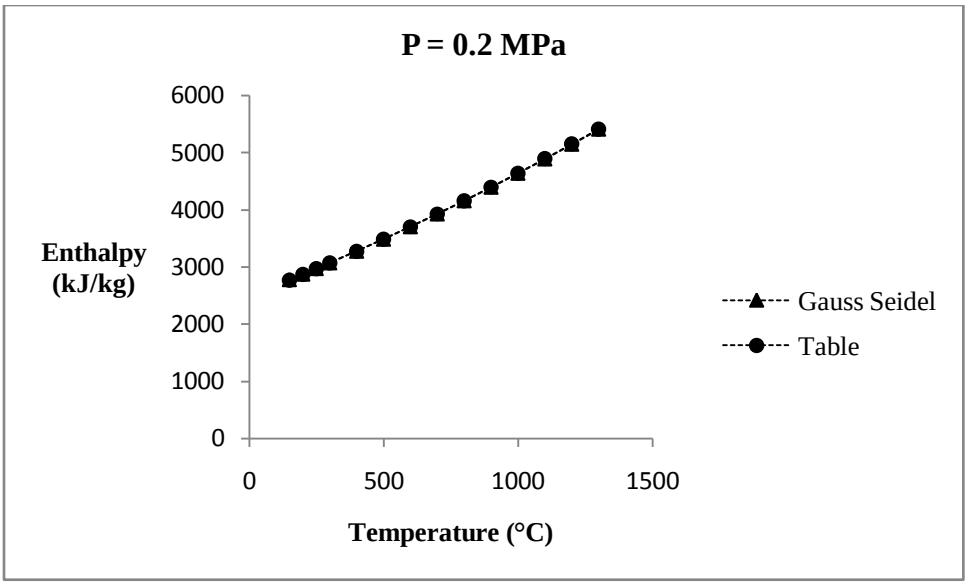

Figure B.8 Present accuracy obtained from Enthalpy function of 0.2 MPa pressure for table of superheated water (Table A-6).

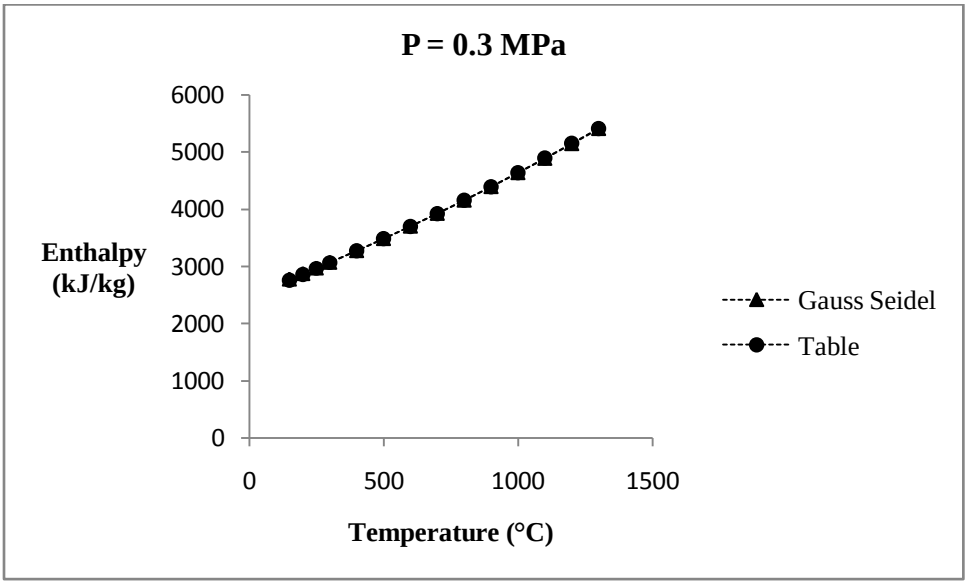

Figure B.9 Present accuracy obtained from Enthalpy function of 0.3 MPa pressure for table of superheated water (Table A-6).

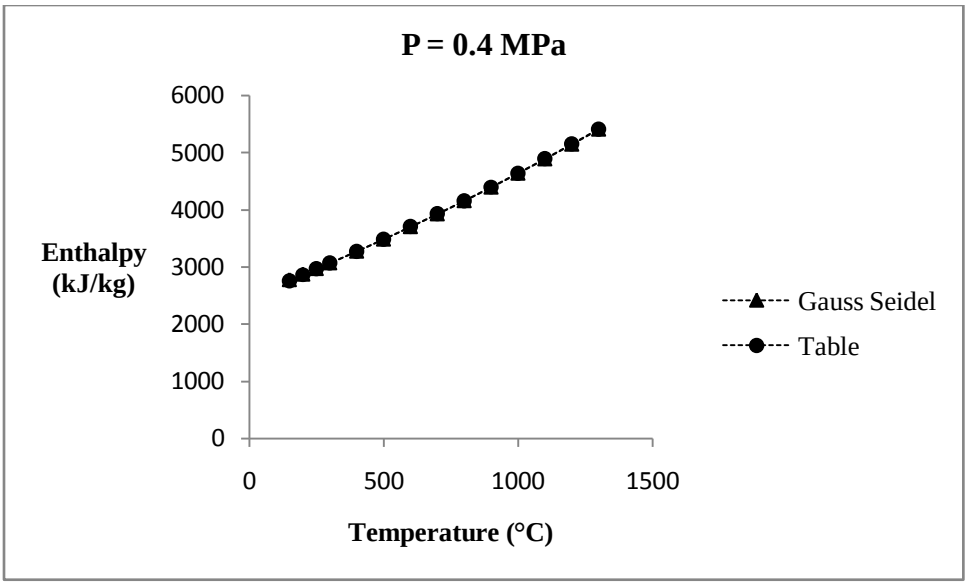

Figure B.10 Present accuracy obtained from Enthalpy function of 0.4 MPa pressure for table of superheated water (Table A-6).

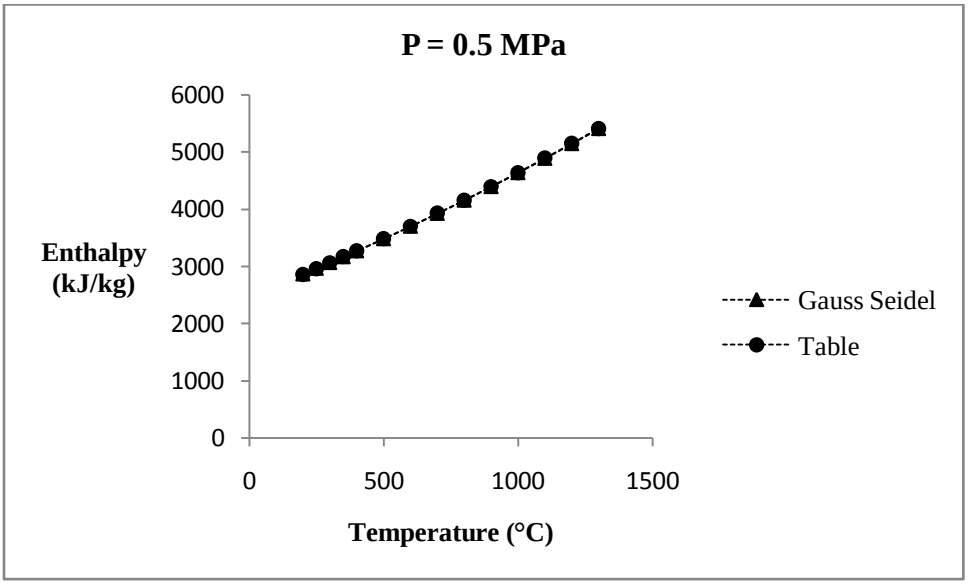

Figure B.11 Present accuracy obtained from Enthalpy function of 0.5 MPa pressure for table of superheated water (Table A-6).

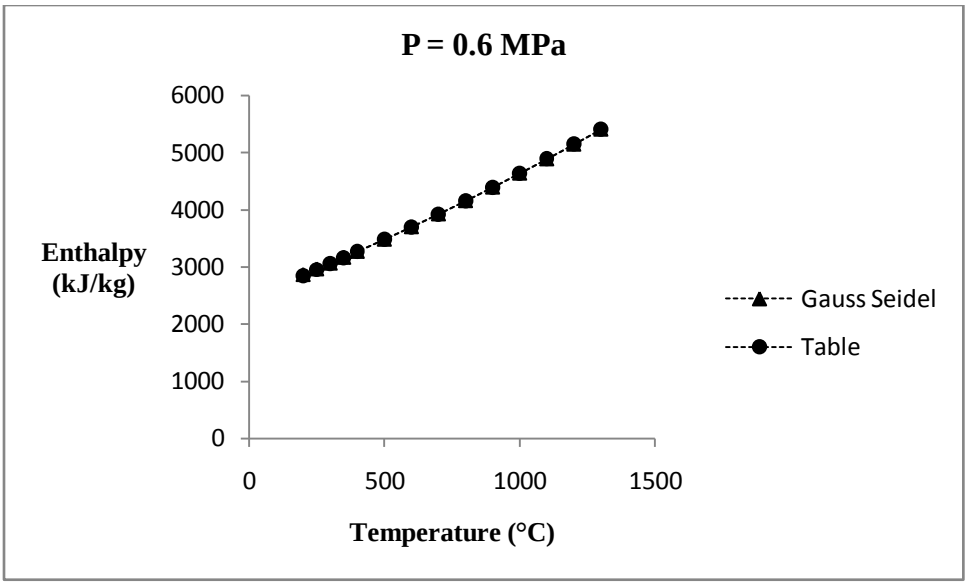

Figure B.12 Present accuracy obtained from Enthalpy function of 0.6 MPa pressure for table of superheated water (Table A-6).

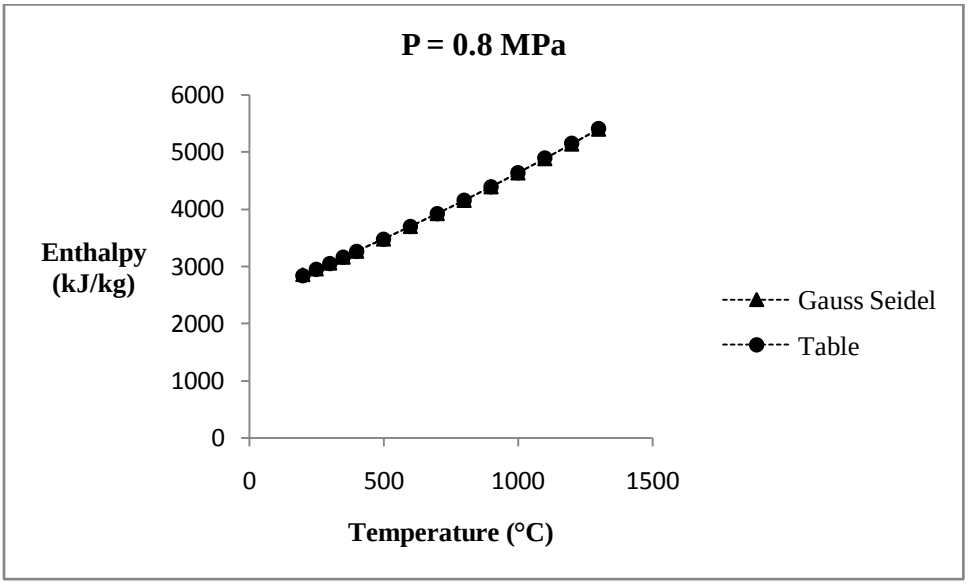

Figure B.13 Present accuracy obtained from Enthalpy function of 0.8 MPa pressure for table of superheated water (Table A-6).

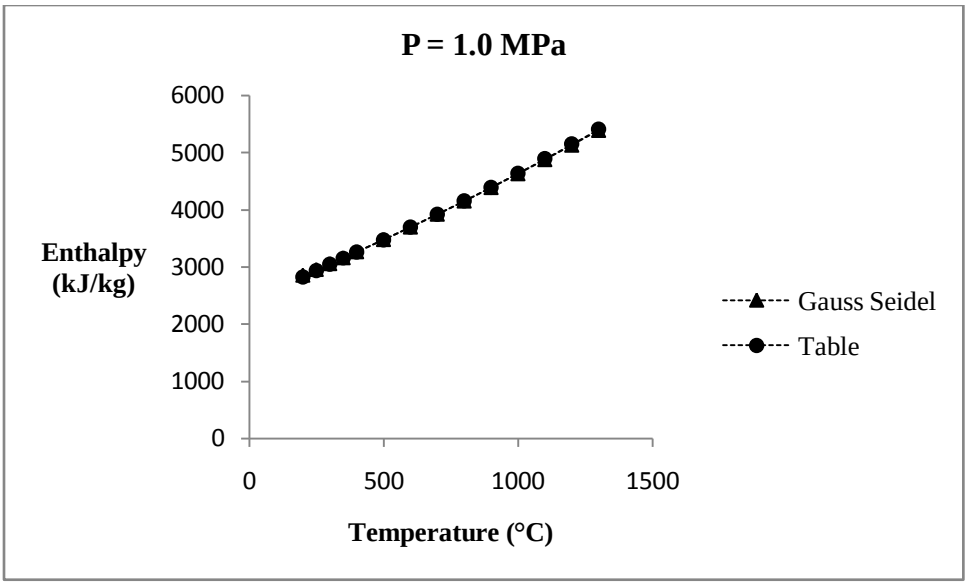

Figure B.14 Present accuracy obtained from Enthalpy function of 1.0 MPa pressure for table of superheated water (Table A-6).

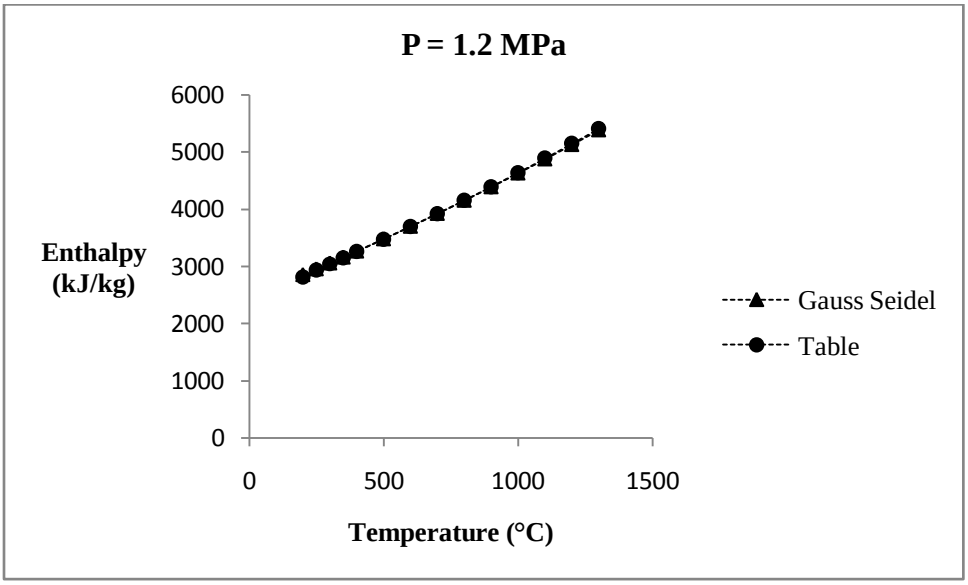

Figure B.15 Present accuracy obtained from Enthalpy function of 1.2 MPa pressure for table of superheated water (Table A-6).

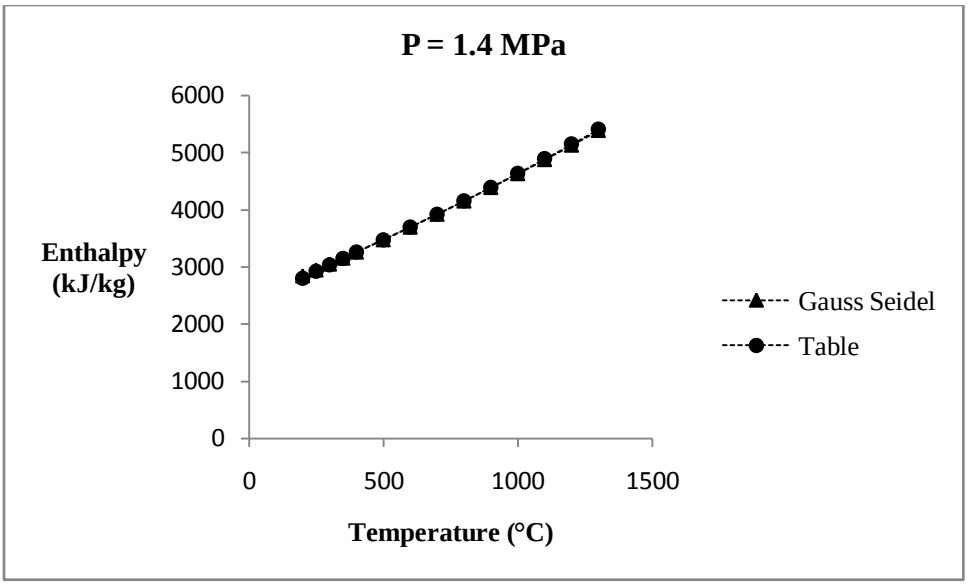

Figure B.16 Present accuracy obtained from Enthalpy function of 1.4 MPa pressure for table of superheated water (Table A-6).

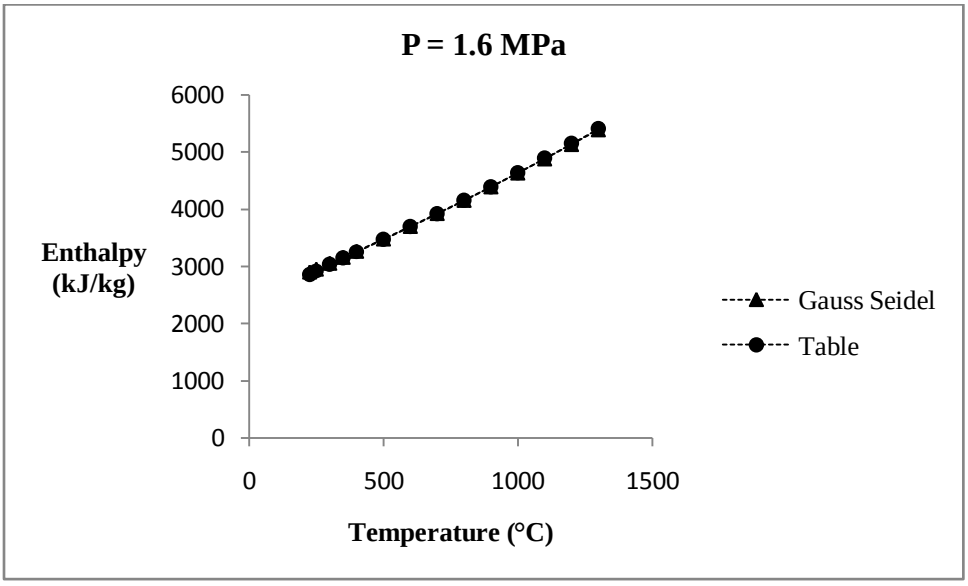

Figure B.17 Present accuracy obtained from Enthalpy function of 1.6 MPa pressure for table of superheated water (Table A-6).

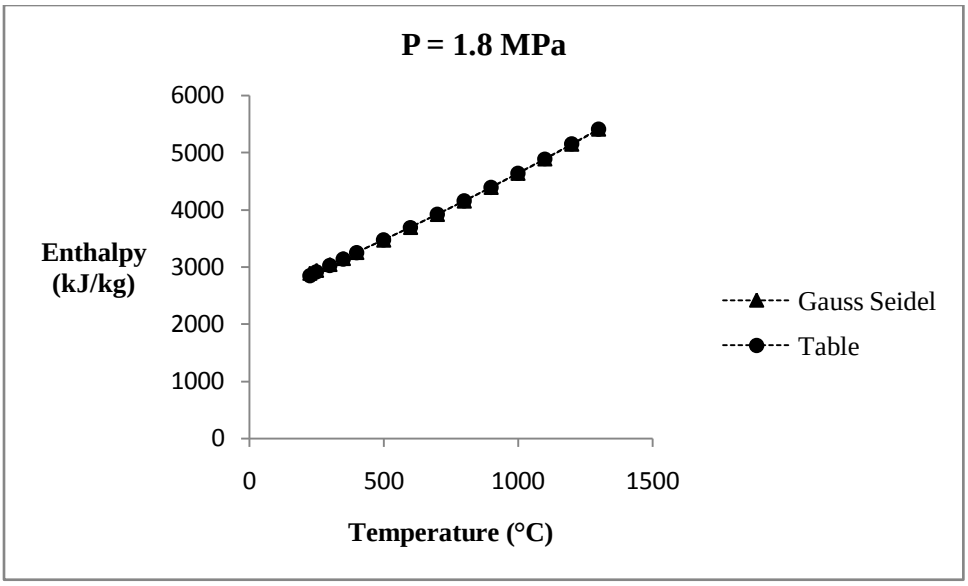

Figure B.18 Present accuracy obtained from Enthalpy function of 1.8 MPa pressure for table of superheated water (Table A-6).

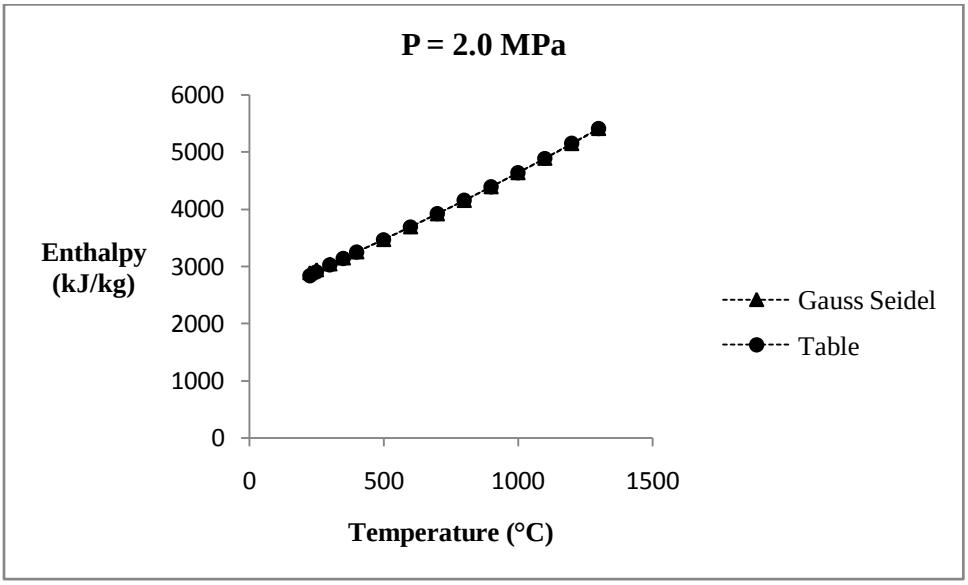

Figure B.19 Present accuracy obtained from Enthalpy function of 2.0 MPa pressure for table of superheated water (Table A-6).

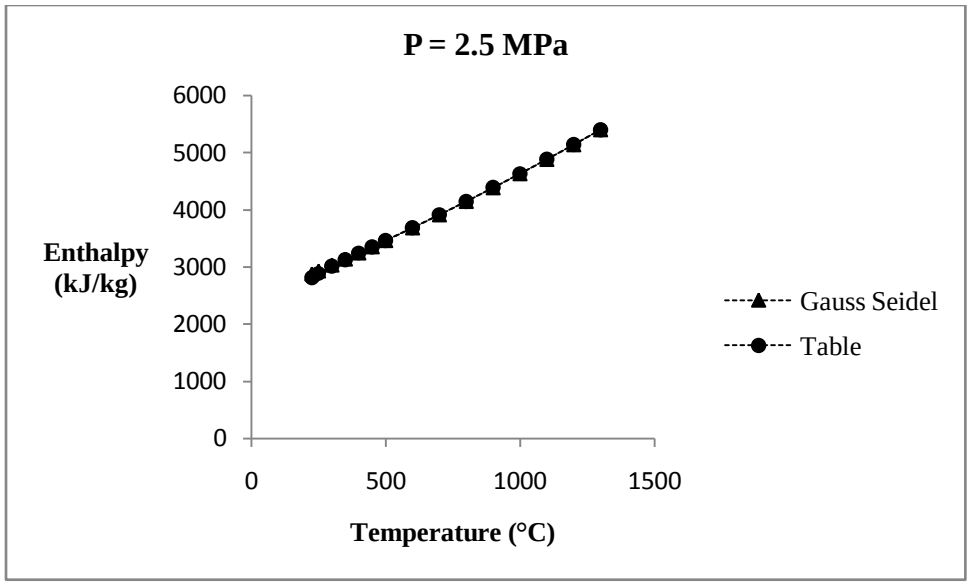

Figure B.20 Present accuracy obtained from Enthalpy function of 2.5 MPa pressure for table of superheated water (Table A-6).

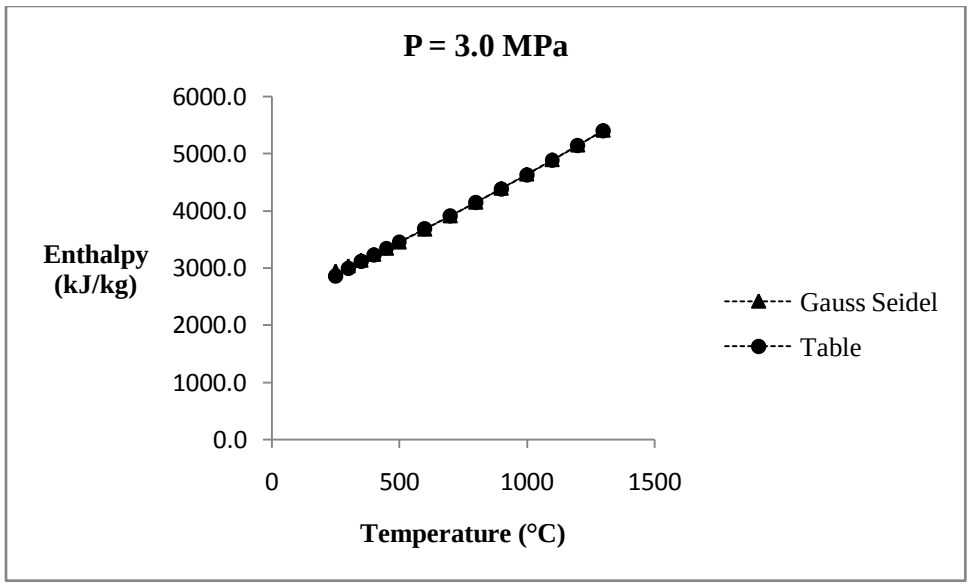

Figure B.21 Present accuracy obtained from Enthalpy function of 3.0 MPa pressure for table of superheated water (Table A-6).

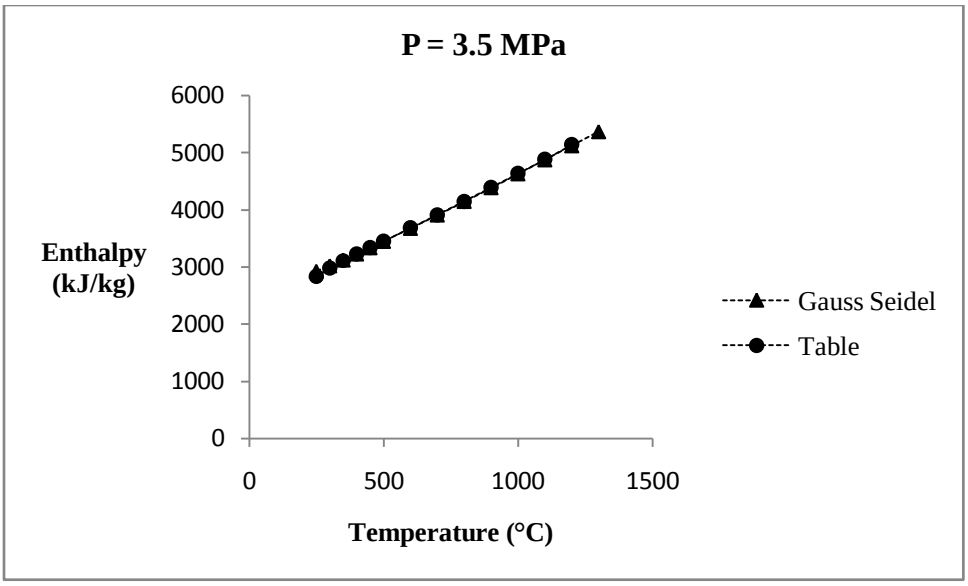

Figure B.22 Present accuracy obtained from Enthalpy function of 3.5 MPa pressure for table of superheated water (Table A-6).

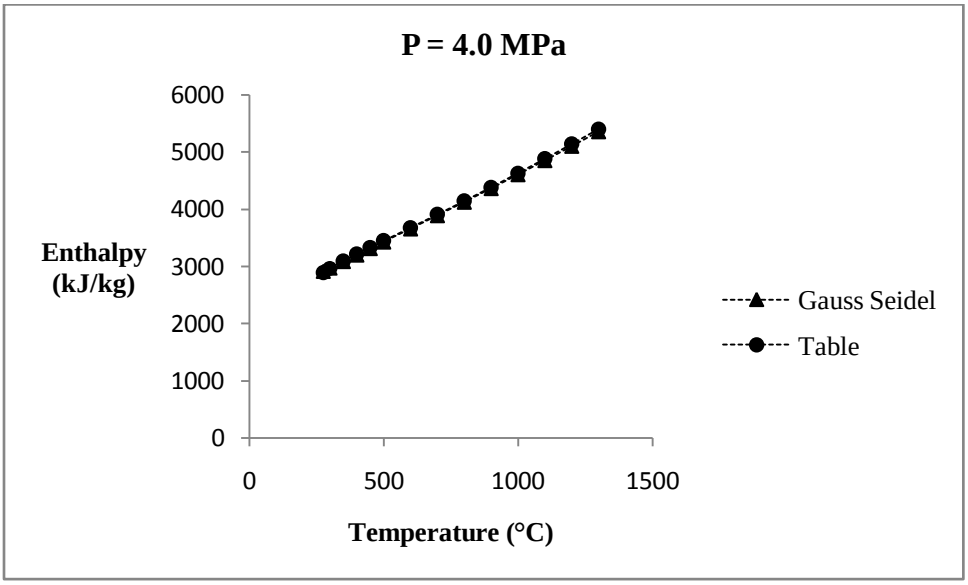

Figure B.23 Present accuracy obtained from Enthalpy function of 4.0 MPa pressure for table of superheated water (Table A-6).

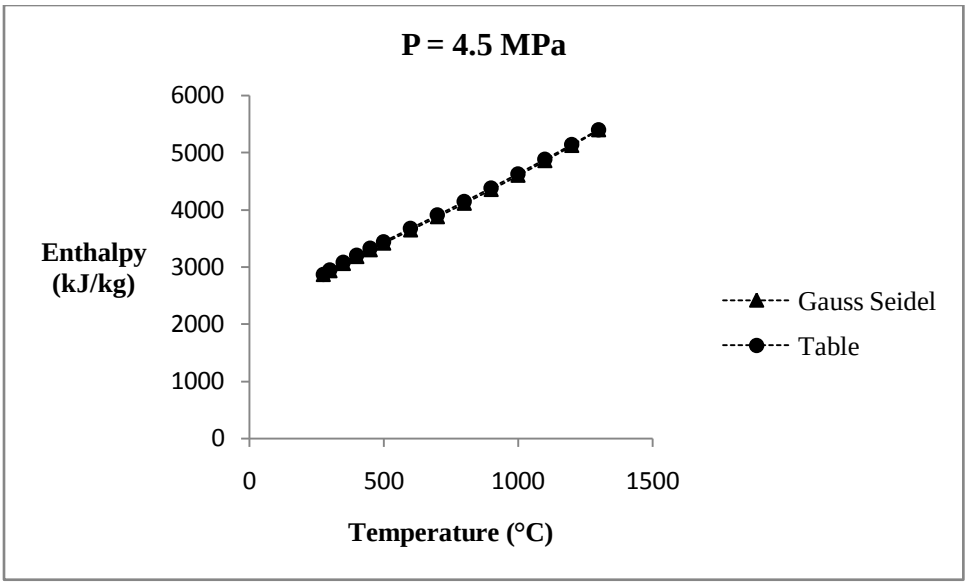

Figure B.24 Present accuracy obtained from Enthalpy function of 4.5 MPa pressure for table of superheated water (Table A-6).

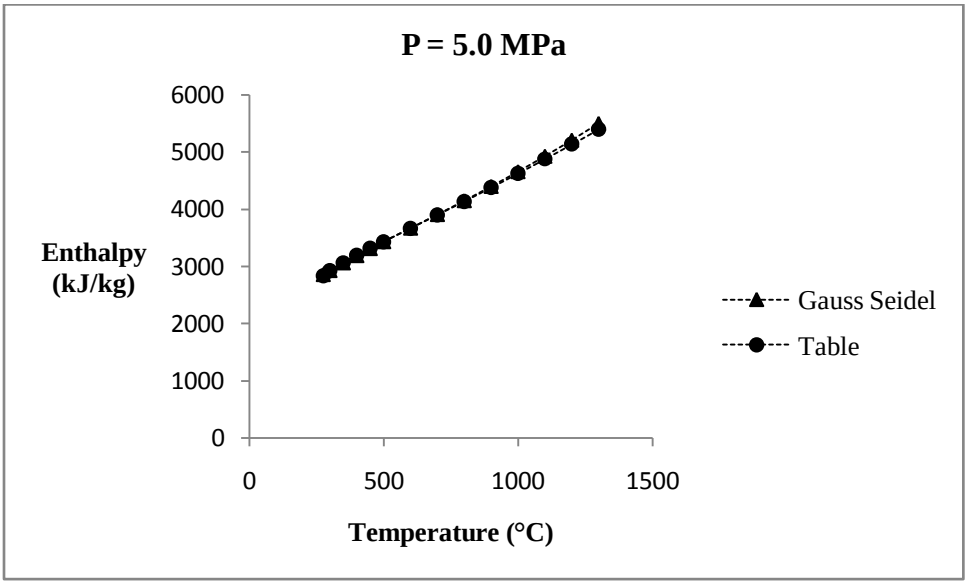

Figure B.25 Present accuracy obtained from Enthalpy function of 5.0 MPa pressure for table of superheated water (Table A-6).

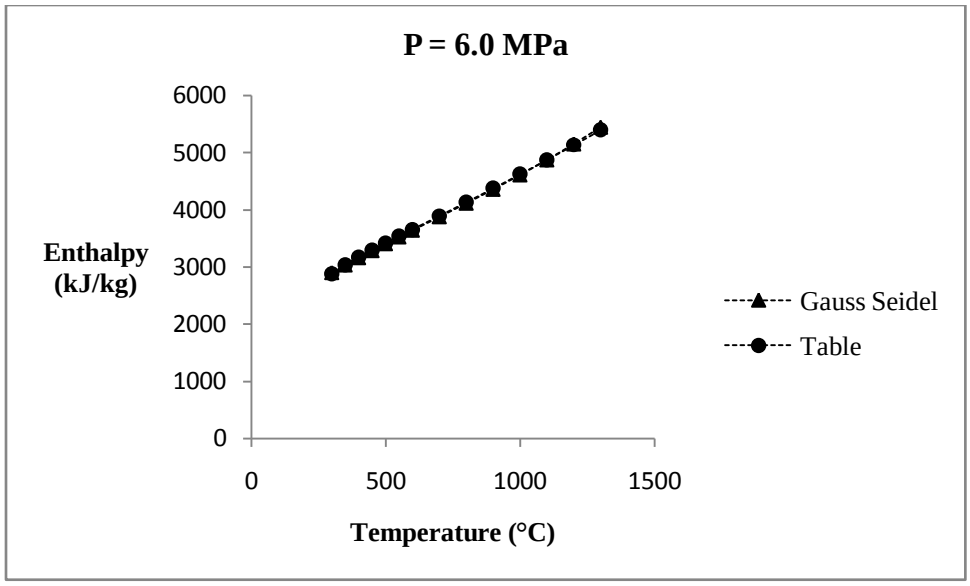

Figure B.26 Present accuracy obtained from Enthalpy function of 6.0 MPa pressure for table of superheated water (Table A-6).

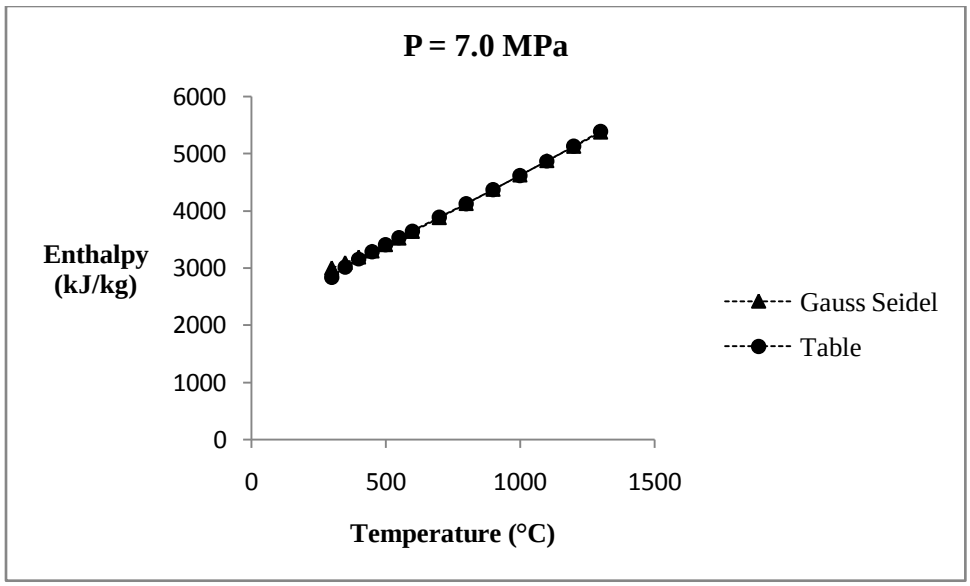

Figure B.27 Present accuracy obtained from Enthalpy function of 7.0 MPa pressure for table of superheated water (Table A-6).

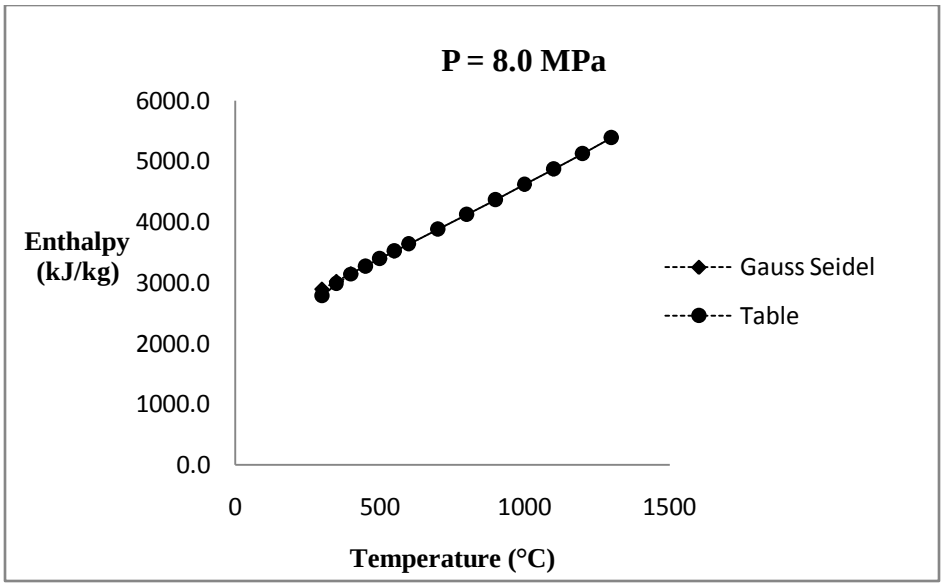

Figure B.28 Present accuracy obtained from Enthalpy function of 8.0 MPa pressure for table of superheated water (Table A-6).

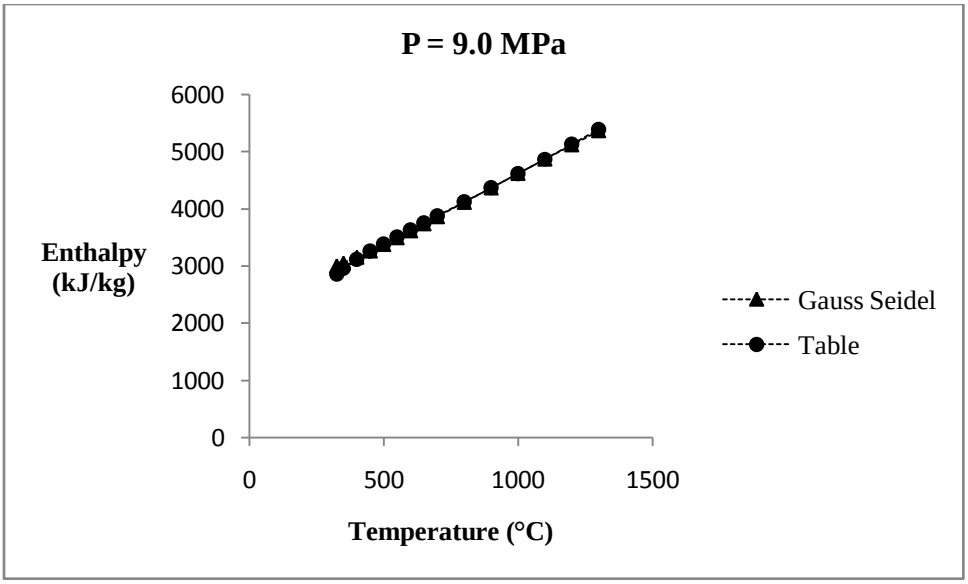

Figure B.29 Present accuracy obtained from Enthalpy function of 9.0 MPa pressure for table of superheated water (Table A-6).

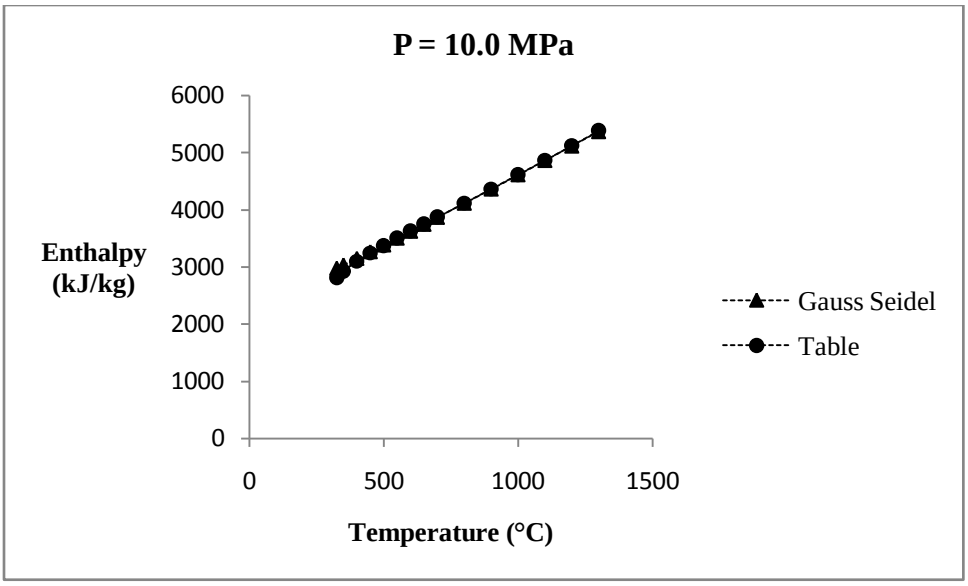

Figure B.30 Present accuracy obtained from Enthalpy function of 10.0 MPa pressure for table of superheated water (Table A-6).

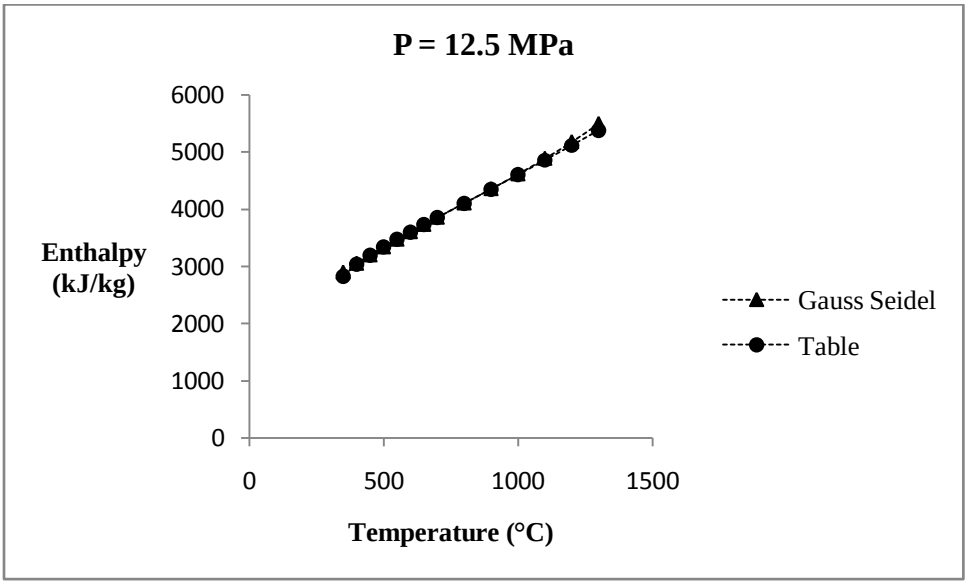

Figure B.31 Present accuracy obtained from Enthalpy function 12.5 MPa pressure for table of superheated water (Table A-6).

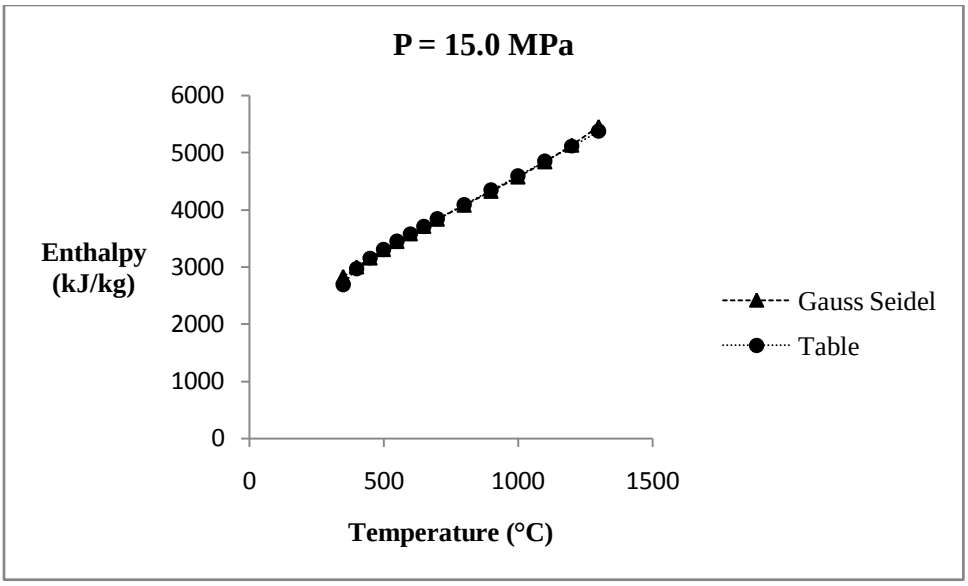

Figure B.32 Present accuracy obtained from Enthalpy function of 15.0MPa pressure for table of superheated water (Table A-6).

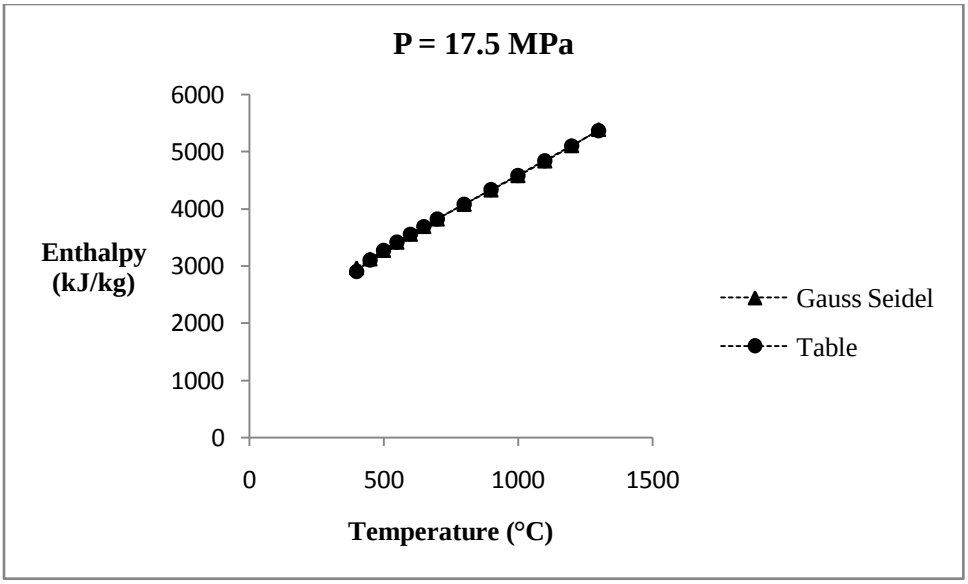

Figure B.33 Present accuracy obtained from Enthalpy function of 17.5MPa pressure for table of superheated water (Table A-6).

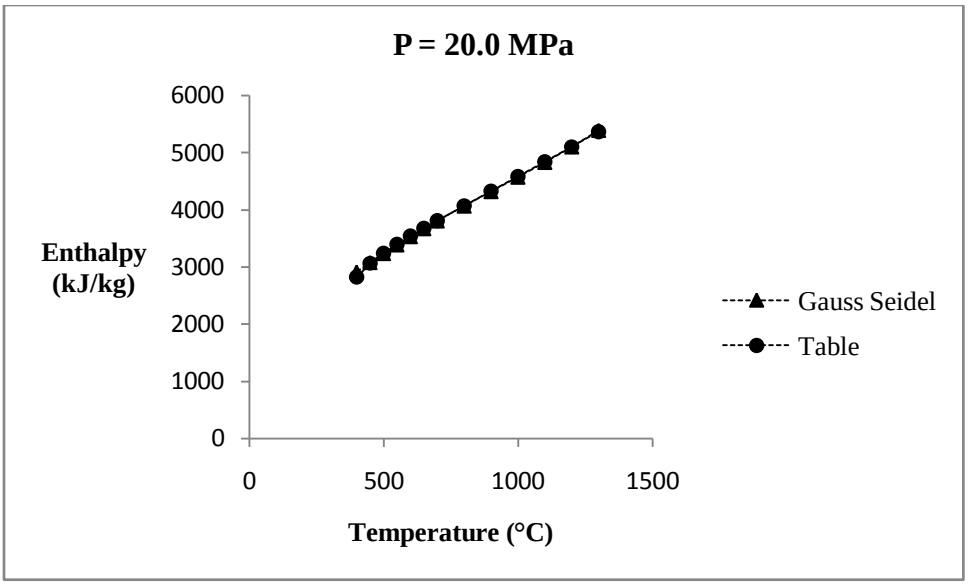

Figure B.34 Present accuracy obtained from Enthalpy function of 20.0 MPa pressure for table of superheated water (Table A-6).

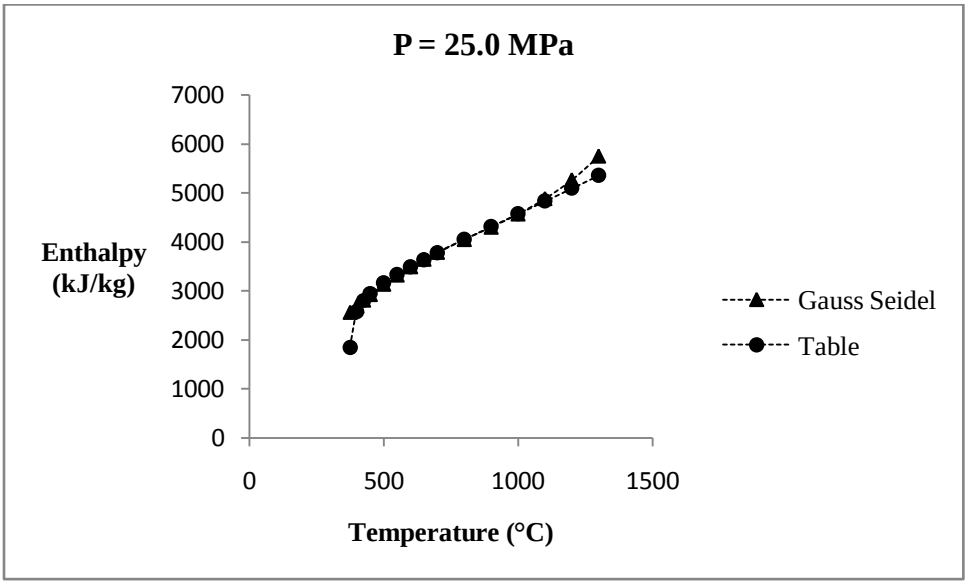

Figure B.35 Present accuracy obtained from Enthalpy function of 25.0 MPa pressure for table of superheated water (Table A-6).

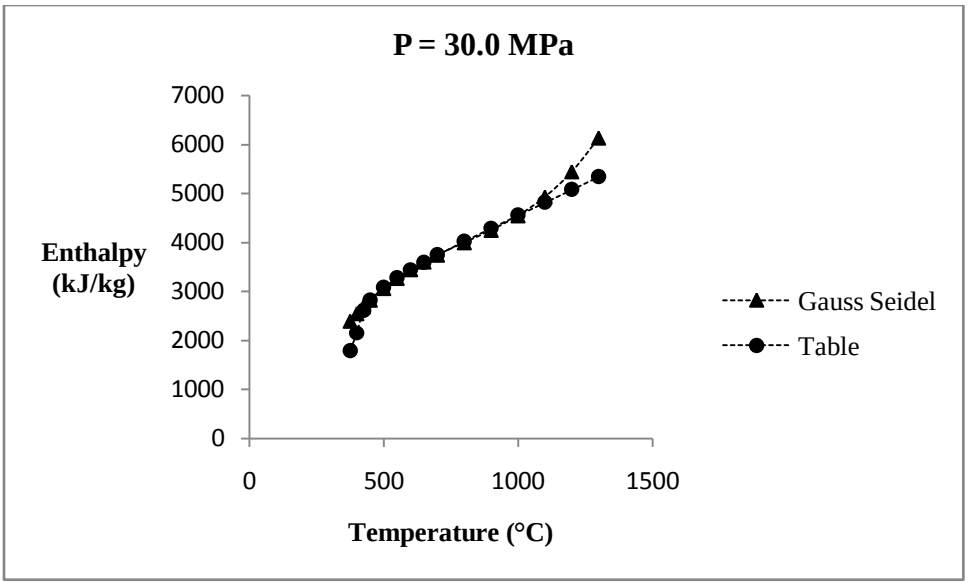

Figure B.36 Present accuracy obtained from Enthalpy function of 30.0 MPa pressure for table of superheated water (Table A-6).

Appendix C
A summary of research studies on ultra supercritical operating conditions.

Table C.1: Define the group of main input for ultra supercritical pulverized coal-fired power plant.

Category	Steam condition	Reference
1.	25.0-26.5 MPa/ 595-605°C/ 593-615 °C	Bugge et al. (2006), Cao et al. (2007), Feng (2008)
2.	28.0-30.0 MPa/ 580-630°C/ 580-630 °C	Bugge et al. (2006), Carbon abatement technologies programme (2006), Otsuka and Kaneko (2007)
3.	31.0-34.5 MPa/ 566-649°C/ 566-593 °C/ 566-593 °C	Cao et al. (2007), Feng (2008), Wright et al.(2004), U.S.DOE, 1999, Kaneko et al. (1996)

Table C.2: The other miscellaneous important operating parameters.

Description	Operating parameters of interest	Unit	Reference
1st reheating pressure	4.0-4.41	MPa	Cao et al. (2007), Kaneko et al.(2007)
Backpressure	3.0-8.0	kPa	Cao et al. (2007), Feng (2008), Asthana and Panigrahi (2008), U.S.DOE (1999)
Condensate pressure	2.32	MPa	U.S.DOE (1999)
Booster pump pressure	6.89	MPa	U.S.DOE (1999)
Pressure drop across boiler	3.0-6.0	%	Feng (2008), Sanpasertparnich (2007)
Pressure drop across FWHs	9.0-10.0	%	Sanpasertparnich (2007) IEA (2007)
Boiler efficiency	93.8	%	Cao et al. (2007),
Turbine efficiency	90,92, 98.9	%	Asthana and Panigrahi (2008), Cao et al. (2007)
% excess air	15.0-20.0	%	Sanpasertparnich (2007)